PhD Thesis

Bexarotene and astaxanthin modulate cholesterol and amyloid-beta metabolism at the blood-brain barrier

submitted by

Elham Fanaee Danesh, Dipl.-Ing.

for the Academic Degree of

Doctor of Philosophy (PhD)

at the

Medical University of Graz, AUSTRIA

Otto Loewi Research Center for Vascular Biology, Immunology and Inflammation, Immunology and Pathophysiology

under the supervision of

Assoz. Prof. Priv.-Doz. Mag. Dr.rer.nat. Ute Panzenboeck

2019

I never dreamed about

the success - I worked for it

Jessica Hardy

DECLARATION

I hereby declare that this thesis is my own original work and that I have fully acknowledged by name all of those individuals and organizations that have contributed to the research for this thesis and agreed to publish the data in this thesis. Due acknowledgement has been made in the text to all other material used. Throughout this thesis and in all related publications I followed the “Standards of Good Scientific Practice and Ombuds Committee at the Medical University of Graz”.

The major part of investigation presented in this thesis has been summarized and published in:

Astaxanthin exerts protective effects similar to bexarotene in Alzheimer's disease by modulating amyloid-beta and cholesterol homeostasis in blood-brain barrier endothelial cells. Fanaee-Danesh E, Gali CC, Tadic J, Zandl-Lang M, Carmen Kober A, Agujetas VR, et al. Biochim Biophys Acta Mol Basis Dis. 2019 Sep 1;1865(9):2224–45 (1).

List of all co-authors to this publication:

- *Division of Immunology and Pathophysiology, Otto Loewi Research Center, Medical University of Graz, Graz, Austria*: Elham Fanaee-Danesh, Chaitanya Chakravarthi Gali, Martina Zandl-Lang, Nicole Maria Albrecher, Carmen Tam-Amersdorfer, Anika Stracke, Anil Paul Chirackal Manavalan, Marielies Reiter, Yidan Sun, Alexandra Kober, Ute Panzenboeck (corresponding author).

- *Institute of Molecular Biosciences, NAWI Graz, University of Graz, Graz, Austria:* Jelena Tadic

- *Institute of Molecular Biosciences, University of Graz, Graz, Austria*: Frank Madeo

- *Department of Cell Death and Proliferation, Institut d'Investigacions Biomèdiques de Barcelona, Consejo Superior de Investigaciones Científicas (CSIC). IDIBAPS. Centro de Investigación Biomédica en Red sobre*

Enfermedades Neurodegenerativas (CIBERNED). Barcelona, Spain: Anna Colell, Vicente Roca Agujetas, Cristina de Dios

- *Department of Biomedicine, Facultat de Medicina, Universitat de Barcelona, Barcelona, Spain*: Cristina de Dios

- *Division of Molecular Biology and Biochemistry, Gottfried Schatz Research Center, Medical University of Graz, Graz, Austria*: Ernst Malle

Graz, August 2019 Elham Fanaee Danesh

ACKNOWLEDGEMENTS

I would like to thank my supervisor Ute Panzenboeck for her constant support and constructive suggestions, which were determinant for the performance of the work presented in this thesis. I greatly appreciate her kind advice throughout my PhD research studies.

I wish to express my gratitude to the Medical University of Graz and DK-MCD in providing financial assistance for me for international activities, fabulous conferences, and research stays to expand my scientific knowledge and to make “brain circulation” accessible.

My sincere appreciation for Karin Osibow for her professional organisation that her assistance made my PhD truly possible.

I acknowledge my thesis committee, Dr. Wolfgang Graier, Gottfried Schatz Research Center (for Cell Signaling, Metabolism and Aging), Division of Molecular Biology and Biochemistry and Dr. Robert Zimmermann (Institute of Molecular Biosciences) for their encouragement and insightful comments.

I also would like to thank Dr. Anna Colell and colleagues Vicente Roca Agujetas and Cristina de Dios for hosting me at the Institut d'Investigacions Biomèdiques de Barcelona, and Dr. Helmut Kubista and Gabriele Gaupmann for hosting me at Institute of Neurophysiology and Neuropharmacology (Medical University of Vienna) and for their extended guidance throughout my project work.

I am grateful to my colleagues, especially Nicole, Martina, Marie, Chaitanya, Carmen, Christina and Anika. With such lovely and engaging people it was a pleasure coming to work every day.

My heartfelt thanks to my husband Farshad Mirzapour who supported and enabled me to do this journey. I dedicate this project to our daughter Awa Mirzapour whom I am proud of.

During my PhD studies I, Elham Fanaee-Danesh, received funding from the Austrian Science Fund (FWF), grants P24783-B19 (to U.P.), and W1226-B18 (to E.F.D., J.T., F.M., and U.P.; Doctoral College of Metabolic and Cardiovascular Disease, DK-MCD, co-funded by the Medical University of Graz). F.M. is also grateful to the Austrian Science Fund for grants P23490-B20, P29262, P24381, P29203, P27893, I1000, and “SFB Lipotox” (F3012), as well as the Bundesministerium für Wissenschaft, Forschung und Wirtschaft, and the Karl-Franzens University of Graz for grant “Unkonventionelle Forschung”. We acknowledge support from NAWI Graz and the BioTechMed-Graz flagship project “EPIAge”. Additional support was provided by Fundació La Marató de TV3 grant 2014-0930 (to A.C.) and an FPU fellowship from Ministerio de Economía y Competitividad (MEC) (to C.dD) and the Austrian National Bank (OeNB, 17600 to E.M.).

TABLE OF CONTENTS

ABBREVIATIONS

ABCA1: ATP binding cassette transporter subfamily A member 1

ABCG1: ATP binding cassette transporter subfamily G member 1

AD: Alzheimer's disease

Aβ: amyloid-beta peptide

APP: amyloid precursor protein

ADAM10: A disintegrin and metalloproteinase domain-containing protein 10

ALS: Amyotrophic Lateral Sclerosis

apoA-I: apolipoprotein A-I

apoE: apolipoprotein E

Asx: astaxanthin

BACE1: β-site of APP cleaving enzyme, beta-secretase

BBB: blood-brain barrier

BCEC: brain capillary endothelial cells

Bex: bexarotene

CD31: cluster of differentiation 31

CD13: aminopeptidase N

CTFs: C-terminal fragments

DEA: diethylamine

FA: formic acid

GFAP: glial fibrillary acidic protein

GW 6471: N-((2S)-2-(((1Z)-1-Methyl-3-oxo-3-(4-(trifluoromethyl)phenyl)prop-1-enyl)amino)-3-(4-(2-(5-methyl-2-phenyl-1,3-oxazol-4-yl)ethoxy)phenyl)propyl)propanamide

HDL_3: high-density lipoprotein subclass 3

IBA1: ionized calcium-binding adaptor molecule 1

LRP-1: low-density lipoprotein receptor-related protein 1

LXR: liver X receptor

mBCEC: murine BCEC

PA 452: 2-[[3-(Hexyloxy)-5,6,7,8-tetrahydro-5,5,8,8-tetramethyl-2 naphthalenyl]methylamino]-5-pyrimidinecarboxylic acid

pBCEC: porcine BCEC

PDGFRβ: beta-type platelet-derived growth factor receptor

PPAR: peroxisome proliferator-activated receptor

PLTP: phospholipid transfer protein

ROS: reactive oxygen species

RXR: retinoid X receptor

sAPPα: soluble amyloid precursor protein-α

SF: serum-free

SMA: smooth muscle actin

SYP: synaptophysin

TEER: transendothelial electrical resistance

vWF: von Willebrand factor

3xTg AD: APP Swe/MAPT P301L/PSEN1 M146V

LIST OF TABLES

LIST OF FIGURES

KURZFASSUNG

Hintergrund: Die Alzheimer Erkrankung (AD) ist die häufigste neurodegenerative Erkrankung des Menschen. Sie wird durch abgelagerte Amyloid-β Peptide (Aβ), die entweder im Übermaß produziert, oder nicht ausreichend abtransportiert werden, ausgelöst. Der Plasmacholesterolspiegel wurde als möglicher Risikofaktor für AD identifiziert, da seine Höhe mit der Neubildung von Aβ korreliert. Da die Blut-Hirn-Schranke (BBB) an den genannten Prozessen beteiligt ist, haben wir die Wirkung von Bexaroten (Bex) und Astaxanthin (Asx) sowohl auf die Regulation des zellulären Cholesterinstoffwechsels, als auch auf die Produktion von Aβ und dessen Transport in zerebromikrovaskulären Endothelzellen (BCEC) untersucht. Bex ist ein Retinoid-X-Rezeptor (RXR) Agonist und Asx ein Agonist des Peroxisome proliferator-activated Rezeptor-α (PPARα) und ein starkes Antioxidans. Für die *in vitro* Zellkulturversuche wurden Endothelzellen aus Hirnen von Schlachtschweinen (pBCEC) gewonnen, für die Tierversuche ein dreifach transgenes Alzheimer-Mausmodell (3xTg AD) verwendet.

Fragestellung: Es wurde die Wirkung des PPARα Agonisten Asx mit der Wirkung und den Risiken von Bex verglichen. Um die Effekte von Bex und Asx *in vitro* zu erforschen, wurden pBCEC in An- oder Abwesenheit der Substanzen kultiviert und die Auswirkungen auf die zelluläre Prozessierung des Amyloid-Precursor-Proteins (APP), die Aufnahme und den Transport von Aβ, den zellulären Cholesterinstoffwechsel und die Bildung von Sauerstoffradikalen analysiert. Für die *in vivo* Versuche wurde zwei unterschiedlich (nämlich <1 Jahr und >1 Jahr) alten Versuchstiergruppen Asx oder Bex für 6 Tage verabreicht. Anschließend wurden neben Gesamthirnlysaten und Cryoproben, die Hirnkapillarendothelzellen isoliert und einerseits die Gene die am Cholesterolstoffwechsel beteiligt sind untersucht, andererseits der Aβ-Gehalt beurteilt.

Ergebnisse: Die Aktivität des amyloidogenen Enzyms BACE1 wurde sowohl von Asx als auch Bex reduziert, gleichzeitig wurde der nicht-amyloidogene Stoffwechselweg, gekennzeichnet durch das Enzym ADAM10, verstärkt. Auch der Transport von Aβ in das Plasmakompartiment der BBB konnte durch die Behandlung mit jeder der beiden Substanzen erhöht werden. Die Gene ABCA1, LRP-1 und/oder APOA-I wurden bei behandelten Zellen vermehrt exprimiert. In pBCEC konnten sowohl Bex als auch Asx

das Transportprotein APOA-I und den High-density Lipoprotein (HDL)- induzierten Efflux von Cholesterin erhöhen, wohingegen die endogene Biosynthese und Veresterung von Cholesterin verhindert wurde. Bex und Asx reduzieten Aβ-Oligomere und eine ~80 kDa intrazelluläre 6E10-reaktive APP/Aβ Spezies in pBCEC. Dieser Effekt konnte durch LRP-1-Silencing oder die Inhibierung von ABCA1 mittels Probucol umgekehrt werden. Murine (m)BCEC, die aus mit Bex behandelten 3xTg AD Mäusen isoliert wurden, zeigten für APOE und ABCA1 erhöhte Level Sowohl Asx als auch Bex erhöhten den LRP-1 Level und senkten den von BACE1, verglichen mit transgenen Kontrolltieren und nicht transgenen, behandelten Tieren. Sowohl in Gesamthirnproteinlysaten als auch Proteinlysaten aus mBCEC von mit Bex oder Asx behandelten 3xTg AD Tieren, war der Gehalte an löslichen Aβ-Oligomeren fast zur Gänze gesenkt.

Schlussfolgerung: Unsere Ergebnisse lassen den Schluss zu, dass durch beide Kernrezeptoragonisten ein ähnlicher protektiver Effekt in Hinblick auf die Cholesterinhomöostase und auf den Abtransport von Aβ durch zerebromikrovaskuläre Endothelzellen ausgeübt wird.

ABSTRACT

Background: Alzheimer's disease (AD) is the most common neurodegenerative disease which is induced by the accumulation, oligomerization, and aggregation of amyloid-β peptides (Aβ) due to overproduction and impaired clearance. Cholesterol has reached interest as important risk factor for AD as cholesterol may trigger amyloidogenesis. Since the blood-brain barrier (BBB) is involved in these processes, we investigated the impact of the pharmacologic retinoid-X receptor (RXR) agonist, bexarotene (Bex), and the peroxisome proliferator-activated receptor-α (PPARα) agonist, carotenoid, and strong antioxidant, astaxanthin (Asx), on regulation of cellular cholesterol metabolism, amyloid precursor protein (APP) processing, Aβ generation and transport at the BBB *in vitro* using primary porcine brain capillary endothelial cells (pBCEC) and in 3xTg AD model mice.

Questions addressed: we here applied the PPARα agonist Asx in order to compare risks and the potential of such treatment to those of Bex. To investigate effects of Bex and Asx *in vitro,* pBCEC were incubated in the presence or absence of either of both compounds. We investigated amyloidogenic and non-amyloidogenic APP processing pathways, cellular cholesterol metabolism, Aβ clearance and trafficking across the *in vitro* BBB, and formation of reactive oxygen species. Furthermore, we conducted two mouse studies: in study I, female 3xTg AD and non-Tg mice (C57BL/6; 32-49 weeks) and in study II, aged (68-92 weeks) female 3xTg AD mice were gavaged for 6 days with Bex (100 mg/kg) or Asx (80 mg/kg). Brains and murine (m)BCEC were isolated and transcription and/or protein levels of APP/Aβ species as well as *BACE1* and genes involved in cholesterol transport and metabolism were determined.

Results: Activity of amyloidogenic BACE1 in response to Bex or Asx was reduced while non-amyloidogenic ADAM10 transcription was up-regulated in pBCEC. Aβ clearance to the apical/plasma compartment of the *in vitro* BBB model was enhanced after administration of either compound. Applying Bex or Asx increased expression levels of ABCA1, LRP-1, and/or apoA-I. ApoA-I- and HDL_3-mediated cholesterol efflux from pBCEC was induced by Bex or Asx in part through RXR/ PPARα activation, while cholesterol biosynthesis and esterification were diminished. Bex or Asx decreased Aβ oligomers and an ~80 kDa intracellular 6E10-reactive APP/Aβ species. Silencing of LRP-1/inhibition of ABCA1 by probucol showed opposite effects of Asx/Bex on levels

of ~80 kDa intracellular APP/Aβ in pBCEC. Murine (m)BCEC isolated from 3xTg AD mice treated with Bex showed elevated expression of apoE and ABCA1, while Bex and Asx increased LRP-1 expression and diminished BACE1 expression in mBCEC when compared to vehicle-treated or non-Tg, treated animals. Reduced levels of soluble Aβ oligomers in mBCEC and in brains of 3xTg AD mice were observed upon Bex or Asx administration. In parallel, Asx/Bex diminished Aβ species in brain soluble and insoluble fractions of 3xTg AD mice.

Conclusion: Our results strongly suggest that these two different nuclear receptor agonists establish similar protective effects on cholesterol homeostasis and Aβ clearance at the BBB thereby significantly reducing cerebral Aβ burden.

1. Introduction

1.1 Alzheimer's disease (AD)

Alzheimer's disease (AD) is a polygenetic and progressive neurodegenerative brain disorder which implies short-term and languid long-term memory loss (2). At an advanced stage, symptoms include language problems, disorientation, loss of motivation, cognitive decline, and loss of body functions which eventually lead to death. Reports from the National Institute on Aging show that the AD prevalence for individuals above the age of 65 doubles every five years (3).

In contrast to this prevalent late-onset sporadic form of AD, the early-onset form of AD is caused by a genetic predisposition and happens to people who are younger than 65 years (4).

Notably, it has been reported that higher blood pressure (5), cardiovascular disease (6), depression (7), physical activity, diabetes (8) and apoE genotype (ε4 allele carriers) are risk factors for AD (9).

By now, two acknowledged cerebral hallmarks in the pathology of the AD are reported. Amyloid-β peptides (Aβ), and neurofibrillary tangles generated by abnormally hyperphosphorylated tau (p-tau) (10) both are clearly visible by post mortem microscopy in brains of AD patients.

Increasing evidence supports the involvement of major mechanisms such as chronic oxidative stress as well as mitochondrial dysfunction in parallel with Aβ production and accumulation of neurofibrillary tangles, hormone instability, inflammation, calcium dysregulation, and genetic factors underlying AD pathogenesis (11).

Aβ can be intracellularly formed by proteolytic cleavage of amyloid precursor protein (APP) localized in the plasma membrane, in endoplasmic reticulum (ER), trans-golgi network, endosomal, lysosomal and mitochondrial membranes, or extracellular Aβ is internalized through receptors such as scavenger receptor for advanced glycation end-products (RAGE), or deposits as a major component in senile plaques (12).

Among different Aβ isoforms (in length 39-43 amino acids), $A\beta_{1-40}$ is the predominant Aβ species under normal physiological conditions; but it is known that $A\beta_{1-42}$ is the more toxic species as it aggregates way faster than $A\beta_{1-40}$. On the other side, oligomer size distribution is different between $A\beta_{1-40}$ and $A\beta_{1-42}$ (13).

Aβ forms various oligomeric states from <10 kDa to >100 kDa. For example, it has been shown that Aβ 56 kDa (dodecamers) caused memory deficits in Tg2576 model mice (14).

It has been reported that soluble Aβ is more cytotoxic compared to Aβ aggregates as the soluble form blocks activities of the neurons and causes memory loss *in vivo* (15). It is worthy to note that toxicity and cell death caused by Aβ happens through various pathways, for example, extracellular Aβ monomers. interact on the cell membrane with GM1 ganglioside (16) and form Aβ oligomers which induce neuronal death via nerve growth factor (NGF) receptors (17). Aβ oligomers also bind to NMDA-type receptor glutamate receptor (NMDAR) causing calcium dysregulation, more oxidative stress, and synaptic loss (18).

The concentration of Aβ in the brain depends on many factors such as APP regulation or in other words Aβ production and oligomerization, Aβ clearance and transport across BBB, and Aβ degradation. These factors cause 90% of sporadic AD cases and just 10-15% of AD reports are caused by mutations either in APP or the presenilin (PSEN) genes (19).

1.2 Amyloid precursor protein (APP) processing in the brain

The APP is a transmembrane protein (~110 kDa), the mammalian gene consists of 18 exons that go through several alternative splicing actions. The glycosylated form of APP695 is expressed predominantly in the CNS. 751 and 770 amino acid (aa) forms of APP (~120 kDa) (20) are more ubiquitously expressed.

APP is metabolized by a series of proteolytic enzyme-catalyzed cleavages. APP can be cleaved at the cell surface by metalloproteinase domain-containing protein 10 (ADAM 10), also called α-secretase cleavage (α-cleavage takes place in the Aβ domain), thereby generating the soluble fragment sAPPα in the extracellular environment and the membrane-bound C-terminal fragment CTFα/C83 **(Figure 1)**. Neurotrophic and proliferative properties of sAPPα in fibroblasts were shown (21). Previous studies have reported that sAPPα regulates calcium homeostasis in neurons (22) and increases potassium-channel conductance in hippocampal neurons (23).

Beta-site APP-cleaving enzyme 1 (BACE-1) is the main β-secretase that cleaves APP in early endosomes (24) **(Figure 1)**. BACE1 cleaves APP in the acidic environment (pH optimum is 4.5–5.5) (25), resulting in membrane-associated CTFβ/C99 and sAPPβ. In the brains of AD patients, BACE1 is elevated (26). In animal models and in humans, inhibition of BACE1 can prevent Aβ production (27,28). BACE1 deletion in mice reversed Aβ deposition and cognitive decline (29), for these reasons BACE1 inhibitors are promising targets for AD treatment (30,31).

Intraneuronal accumulation of CTFβ/C99 as a consequence of impaired lysosomal-autophagic function was reported in the 3xTg AD mouse model (32). Also In human AD post-mortem brains, elevated C99 was detected (33). It has been reported through NMR analysis that a C99-cholesterol complex formed in the presence of cholesterol in membrane mimetic environments and the production of Aβ was enhanced at high cholesterol concentration (34).

Soluble APPβ has some neurotrophic properties similar to sAPPα, such as cell adhesion, and it increases axonal outgrowth (35). On the opposite side, sAPPβ binds to the death receptor 6 (DR6) causing cell death (36). It has been reported that sAPPα and sAPPβ may be able to differentially regulate cholesterol synthesis (37).

Sequential cleavage of APP through BACE1 and γ secretase (amyloidogenic pathway) generates Aβ peptide and an APP intracellular domain (AICD) **(Figure 1)**. About 90% of all generated Aβ fragments are $A\beta_{1\text{-}40}$, but a minor fraction (as mentioned above

more fibrillogenic or oligomerization-prone) $A\beta_{1-42}$ (and $A\beta_{1-43}$) peptides are found in amyloid plaques (38). Insoluble fibrillar aggregated Aβ in extracellular amyloid plaques and soluble oligomers induce the neurodegenerative cascade of AD-related synaptic dysfunction (39). Decreased production of Aβ was shown also by lowering of γ-secretase activity (40).

APP regulates lipoprotein metabolism through interactions with lipoprotein receptor-related proteins (LRPs) such as LDL receptor-related protein 1 (LRP-1) (Trommsdorff et al., 1998). LRPs themselves control APP endocytic trafficking and processing, APP trafficking and processing are also altered by cellular cholesterol content (Marzolo and Bu, 2009).

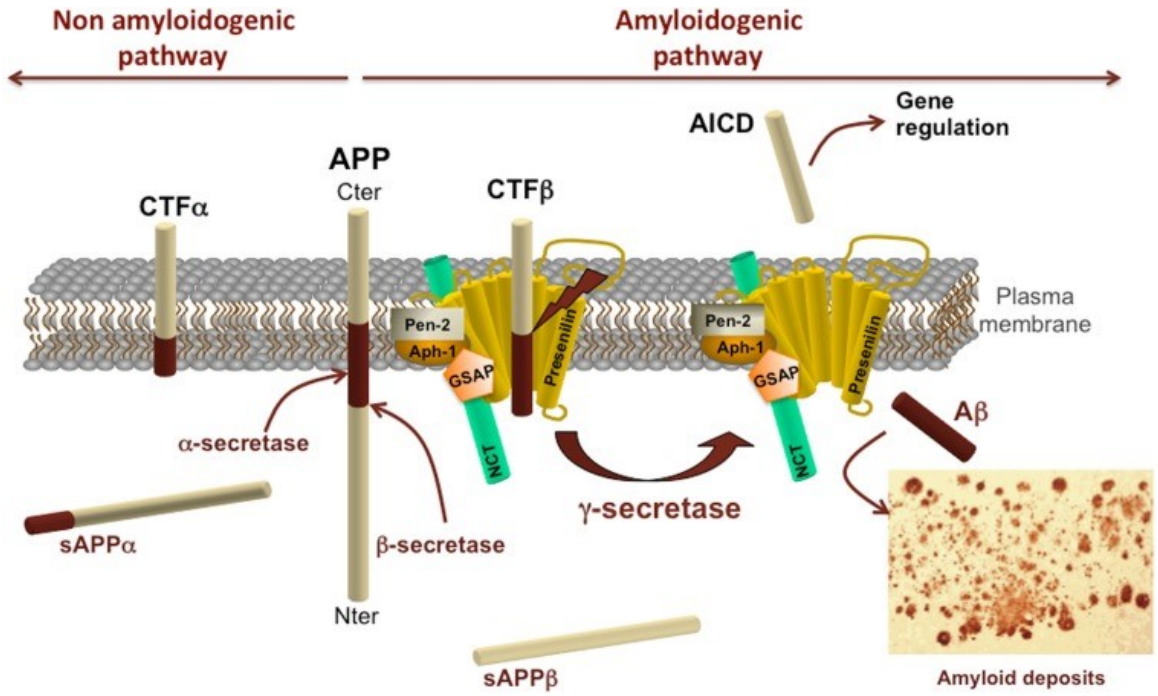

Figure 1: Amyloid precursor protein structure and metabolism

Schematic representation of APP processing by α-, β-, and γ-secretases. APP processing by secretase activities is divided into the non-amyloidogenic pathway on the left and the amyloidogenic pathway on the right. α- and β-secretase activities cleave APP in its extracellular domain to release, respectively, a soluble fragment sAPPα or sAPPβ in the extracellular space and generate carboxy-terminal fragments CTFα or CTFβ. These CTFs can subsequently be processed by γ-secretase complex to generate AICD and Aβ. The γ-secretase complex is composed of presenilin, nicastrin (NCT), γ-secretase activating protein (GSAP), pen-2, and aph-1 [Reproduced from Vingtdeux V et al. with permission of Front Physiology (41)].

1.3 Cerebral amyloid angiopathy (CAA)

The term cerebral amyloid angiopathy (CAA) describes various disorders, biochemically and genetically, in the CNS. All kind of disorders share morphological or pathological examination, i.e. amyloid fibrils accumulate in the walls of mostly arteries, arterioles, and, less often, capillaries and veins of the CNS, although amyloid deposits have been also detected in the capillaries of CNS parenchyma and of the leptomeninges. CAA appears mostly in the sporadic form in the elderly (42), familial forms occur rarely in younger patients (43). All sporadic and some hereditary forms of CAA in the human brain are Aβ type (Aβ-CAA). In Aβ-CAA, the sequential cleavage of APP by β- and γ-secretases leads to production and deposition of Aβ (as described above and presented in Fig. 1) in cerebral vessels, reflecting AD pathophysiology (44). CAA happens with a frequency of 80-90% of all AD cases when Aβ generation and clearance in the cerebrovasculature is imbalanced (45). Blood-brain barrier (BBB) dysfunction, changes in vascular density or diameter of capillaries, and impaired clearance of cerebral Aβ across the BBB may consequently contribute to AD pathogenesis (46). Therefore, the preservation of BBB integrity is critical to prevent AD and other neurological disorders.

Risk of developing sporadic Aβ-CAA is associated with ApoE4 (47) but almost no vascular and parenchymal amyloidosis was resulted by E3 allele (48).

CAA is graded according to the severity of pathological changes in blood vessels: mild, when amyloid is controlled in the tunica media and smooth muscle cells are not destructed; moderate, when the tunica media is replaced by amyloid and this layer is thicker than normal; severe, when extensive amyloid deposition with vessel wall fragmentation, necrosis, and leakage of blood in the vessel wall occurs (49).

Immunosuppressant treatments in order to reduce the course of inflammatory CAA (50), blood pressure control, or antiplatelet treatment (51) are suggested to reduce the risk of CAA. However, further research is essential in order to find therapeutic and preventive medications, aimed for restricting mortality and disability associated with CAA.

1.4 The blood-brain barrier (BBB)

The semipermeable cerebrovascular barrier forms the interior surface of blood vessels and is formed primarily by brain capillary endothelial cells (BCEC) which are tightly linked with tight junction proteins (claudin, occludins, VE-cadherin, ZO-1) (52) **(Figure 2)**. Pericytes wrap around the endothelial cells to stabilize them and display the maturation of endothelial cells by means of direct communication between the cell membranes by paracrine signaling (53). This barrier is a tightly regulated interface between the CNS and the blood circulation. Other cell types such as microglia and neurons are found in the perivascular space around the BBB.

These BBB-associated brain cells, in particular astrocytic glia with its perivascular endfeet modulate barrier permeability over a time-scale of seconds to minutes by releasing chemical factors. Endothelial cells, pericytes, smooth muscle and neural cells, astrocytes, neurons, interneurons, and extracellular matrix are named as the neurovascular unit (NVU).

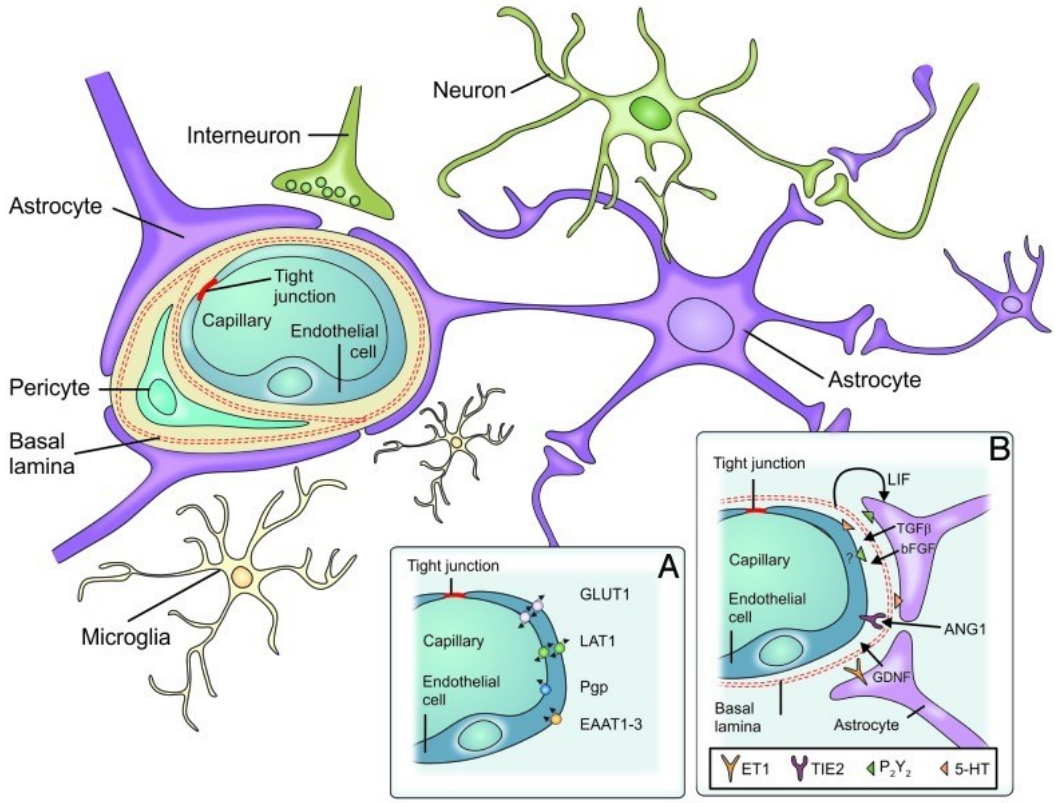

Figure 2: Components of the blood-brain barrier

The blood-brain barrier consists of specialized capillary endothelial cells that are lined by the basal lamina, astrocytic endfeet, pericytes and microglial cells. (A) Among several other transporters and receptors brain endothelial cells express excitatory amino acid transporters (EAAT1–3), glucose

transporter 1 (GLUT1), L-system for large neutral amino acids (LAT1) and P-glycoprotein (Pgp). (B) Surrounding cells intensely interact with endothelial cells and release soluble agents in order to support the maintenance of BBB functions [5-HT (5-hydroxytryptamine [serotonin]), angiopoetin 1 (ANG1), basic fibroblast growth factor (bFGF), endothelin 1 (ET1), glial cell line-derived neurotrophic factor (GDNF), leukemia inhibitory factor (LIF), purinergic receptor (P2Y2), transforming growth factor-β, endothelium-specific receptor tyrosine kinase 2 (TIE2)]. [Reproduced from Feustel SM et al. with permission of Virulence (54)].

The BBB is selective at preventing the entry of macromolecular substances from accessing the brain. The majority of potential drug treatments do not cross the barrier, posing disability to treat neurological disorders. Lipophilic and non-polar molecules can cross the BBB by passive diffusion while polar molecules require transport proteins to pass the BBB (55). BBB dysfunction develops early in AD which is caused by 1) BBB disruption leading to leakage of neurotoxic circulating substances into CNS, 2) transporter dysfunction which consequences insufficient nutrient supply and/or impaired Aβ efflux from the brain (56), 3) alteration of protein expression or secretion of any cell type in the NVU which affect the inflammatory response, oxidative stress and cell damage (57) .

1.5 Transporters and receptors at the blood-brain barrier

There are several transporters and receptors located either to the basolateral side (brain parenchymal side) or apical side (blood side) of the barrier. Receptors at the BBB have some regulatory function for example transcytosis of ligand from blood to brain and reverse transcytosis from brain to blood or only endocytosis into BBB cells. Thus, transporters in cerebrovascular endothelial cells control the transport of specific classes of substrate and their metabolites, Aβ levels and drug penetration into the brain (58). Numerous transporters are expressed at the BBB/in BCEC including LRP-1, receptor for advanced glycation end products (RAGE), insulin receptor (INSR), transferrin receptor 1 (TfR1), and several members of the large ATP binding cassette (ABC) transporter family, namely ABCA1, ABCA2, ABCA8, ABCC4, ABCB1 (also P-glycoprotein, Pgp; gene name multidrug-resistance-protein 1, MDR1), ABCC8, ABCG1, ABCG2 (breast cancer resistance protein, BCRP). Also members of the solute carrier (SLC) transporter family are present, like glucose transporter type 1 (GLUT1) (59) and amino-acid transporter type1 (LAT1, CAT1), nucleoside transporter type 2 (CNT2) have been so far identified at BBB (60).

1.6 ATP-binding cassette (ABC) transporters

Active transporters require energy in the form of adenosine triphosphate (ATP) to translocate substrates such as fatty acids, cholesterol, cholesterol derivatives (bile acids) and phospholipids across the BBB, and their functionality as ion channels for chloride or controlling the regulation of ATP-sensitive potassium channels have been reported (61). ABC transporters are integral membrane proteins, vary greatly in size (human ABCA13 is the largest ABC transporter protein described to date with >450 kDa (62)) and are ubiquitously expressed (63), with highest expression levels reported at the BBB, blood-testis barrier, in liver, intestine, placenta, and kidney (64).

The human ABC transporters which have 49 genes are classified into 7 subfamilies, A-G, due to their structure (65). ABC transporters containing two transmembrane domains (TMD) and two ATP or nucleotide-binding domains (NBD) are called full-size ABC transporters. On the other hand, ABC transporters which have only one TMD and one NBD are called half-size. ABC transporters with two TMDs and two NBDs are quarter-size (66).

The ABCA1 transporter protein contains 2201 amino acids, two transmembrane domains, six transmembrane helices and two nucleotide-binding domains (NBD-1 and NBD-2) containing two conserved peptide motifs known as Walker-A and Walker-B. ABCG1 protein has one transmembrane domain comprising six transmembrane helices and one NBD that contains two conserved peptide motifs, Walker-A and Walker-B (67).

These transport proteins have various substrates such as drugs, vitamins, lipid metabolites, heme, hormones, iron, peptides, and nucleosides (68). Most eukaryotic ABC transporters are effluxers such as ABCA1 (~ 254 kDa) and ABCG1 (~ 110 kDa) which are involved in cholesterol transport/efflux. ABCA1 not only mediates the first step in reverse cholesterol transport (69) **(Figure 3)** but was also identified as an anti-inflammatory receptor that suppresses the expression of inflammatory cytokines, proteins, and lipids, and the inflammatory process mediated by endotoxin. This suggests that ABCA1 plays a crucial role for the interaction between inflammation and reverse cholesterol transport (70). Overexpression of ABCA1 leads to the reduction of Aβ in the PDGF-driven human APP minigene with the V717F (Indiana) mutation

(PDAPP) mouse model of AD (71), implying that ABCA1 is also linked to Aβ homeostasis. ABCA2 is overexpressed in the adult brain, ABCA3 is primarily expressed in the lung but expressed at low levels in the brain. ABCA (1-4), ABCA7, ABCA8 as well as ABCB1, ABCB4, ABCD1 and ABCD2; ABCG1, ABCG2, and ABCG4 are involved in brain lipid transport or homeostasis (72).

Among the ABC transporter G subfamily, ABCG1 (highly expressed in endothelial cells and CNS (73)), ABCG4 (the expression is highly limited to the brain and eye (74)), ABCG5 and ABCG8 (restrict sterol absorption in the intestine and facilitate sterol efflux from hepatocytes into the bile (75)) contribute to sterol transport. ABCG1 specifically has complementary activity with ABCA1 (both are LXR target genes). ABCG1 induces cholesterol efflux to HDL particles **(Figure 3)** while ABCA1 promotes cholesterol efflux to lipid-poor apoA-I thereby initializing the biogenesis of HDL particles (76) **(Figure 3)**. It has been reported in contradictory findings that in humans, cholesterol efflux to HDL by LXR agonists in foam cells is mediated by ABCA1 and independent of ABCG1 expression (77). The roles and mechanisms of regulation of ABCA1 and ABCG1 expression and function in cholesterol efflux in pBCEC have been characterized in previous studies in our laboratory (73,78–80).

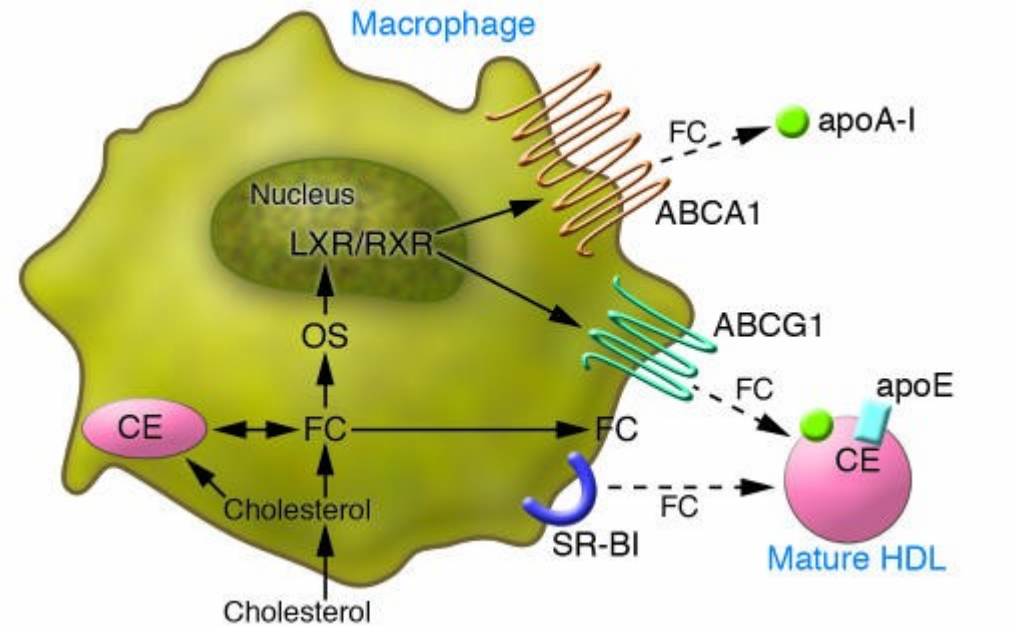

Figure 3: Role of ABCA1 and ABCG1 in cellular cholesterol efflux

Macrophages have several pathways for efflux of cholesterol. Free cholesterol can be effluxed to lipid-poor apoA-I via the ABCA1 pathway and to mature HDL via the ABCG1 pathway. Nuclear receptor liver-

X receptor (LXR) activation by oxysterols regulates both ABCA1 and ABCG1. Free cholesterol can be effluxed to mature HDL via SR-BI. [Reproduced from Daniel J. Rader with permission of the Journal of Clinical Investigation (81)].

1.7 Role of LRP-1 in the brain and at the blood-brain barrier

Low-density lipoprotein receptor-related protein 1 (LRP-1) is a promising receptor for employing the receptor-mediated transcytosis (RMT) pathway for substance/drug delivery to the brain and some macromolecules (peptides, proteins, and nucleic acids) can enter the CNS through this pathway. The 600 kDa LRP-1 precursor protein can be proteolytically processed and generates 515 kDa and 85 kDa subunits. The mature receptor has 85 kDa. LRP-1 contains cysteine-rich complement-type and epidermal growth factor (EGF) repeats, as well as three domains like β-propeller, transmembrane, and a cytoplasmic domain (82). LRP-1 ligand peptide (angiopep-2) or artificial LRP-1-binding peptide (L57:(TWPKHFDKHTFYSILKLGKH-OH)) with BBB permeability were reported to cross the BBB and pass drugs into the CNS (83). LRP-1 uptakes cholesterol into the brain via cholesterol-containing apoE (84). LRP-1 found in the membrane of endothelial cells plays an important role in the integrity of vasculature (85). Importantly, LRP-1 represents the probably major receptor responsible for Aβ clearance. Not only does LRP-1 facilitate cellular uptake of Aβ in endothelial cells (86,87), but is also required in the effective clearance of Aβ from the brain to the blood across the BBB **(Figure 4)** (88,89). LRP-1 is thought to either bind to Aβ directly (90) (although this finding was not confirmed by other groups (91)) or mediates Aβ uptake into the cells via heparan sulfate proteoglycans (Aβ-binding proteins) (92).

LRP-1 has the potential to couple with several other receptors on human primary fibroblasts (WI-38) cell surface such as platelet-derived growth factor (93) and N-methyl-D-aspartate (NMDA) receptor (94) thereby regulating signaling pathways. LRP-1 can be cleaved by different secretase (α/β secretase) (95,96) that either leads to the formation of the intracellular domain of LRP-1, a domain that may regulate transcription of genes similar to APP (97), or secreted/soluble form of LRP-1 (sLRP-1) affecting Aβ metabolism (98).
Overexpressing LRP-1 can lower Aβ generation in neuronal cell lines (95).

Receptor-associated protein (RAP), a 39 kDa molecular chaperone and potent LRP antagonist which causes the folding of LRP, apart from its ability to prevent ligand binding (99). In contrast to previous findings, one study reported that inhibiting LRP-1 function by RAP reduced Aβ production in H4 cells (human neuroglioma cells) transfected with human APP751 (100).

These and several other findings suggest that LRP-1 may modulate APP processing and Aβ generation in addition to its crucial function in clearing Aβ from brain to blood via transcytosis across the BBB.

Aβ transport mediated through LRP-1 at the BBB was shown in AD mouse models (89). Most study outcomes support that LRP-1 aids to maintain Aβ homeostasis in the brain via the above mentioned Aβ dependent pathways; in addition, indirect pathways with the involvement of apoE have also been proposed **(Figure 4)** (86).

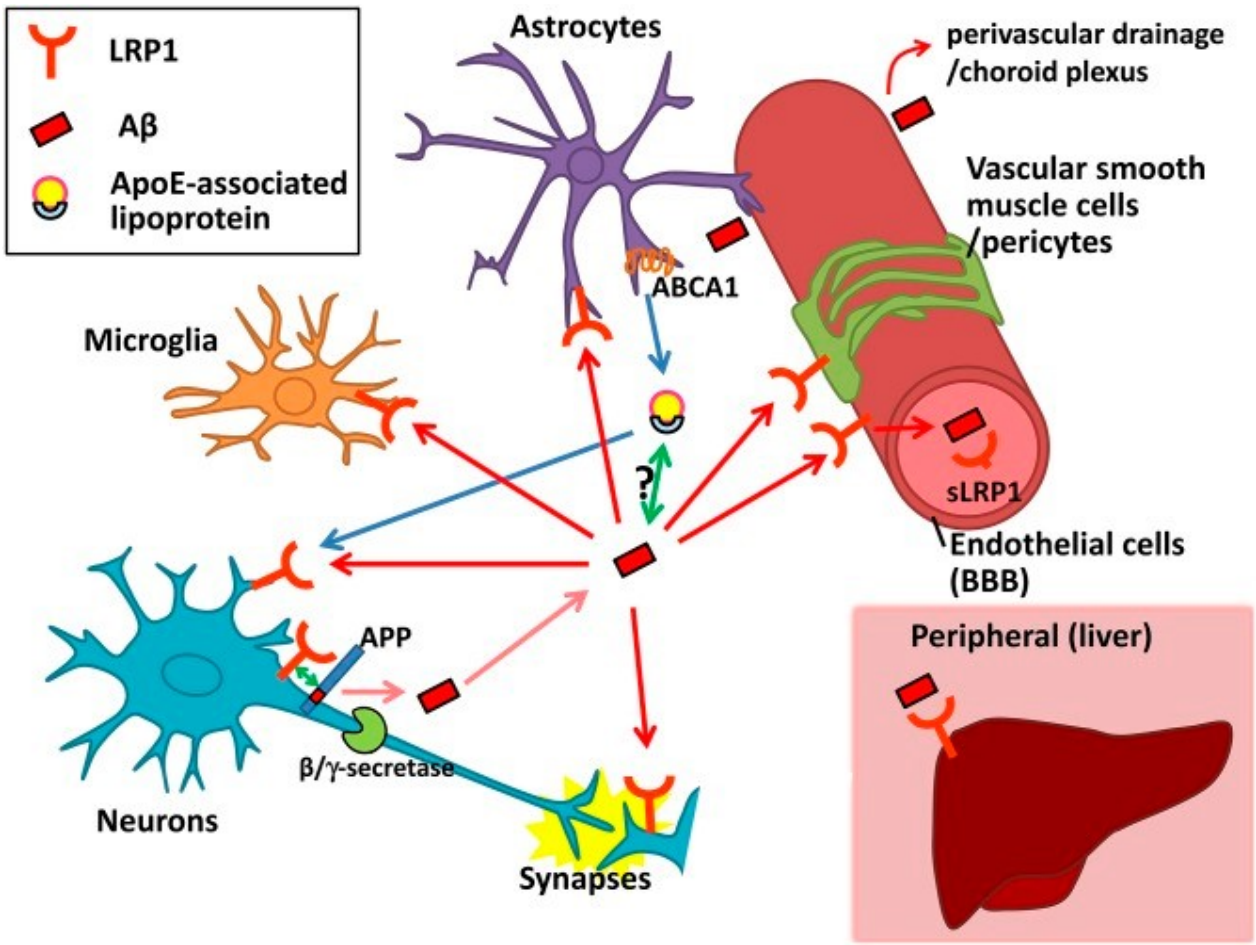

Figure 4: Proposed LRP-1-related pathways for Aβ production, clearance, and accumulation and their relationship with apoE

Aβ production from APP in neurons might be influenced by LRP-1 through its interaction with APP or competition with the β/γ-secretase cleavage of APP. Once Aβ is produced and secreted into the extracellular space in the brain, LRP-1 is involved in cellular uptake of Aβ in neurons, microglia, astrocytes, vascular smooth muscle cells, pericytes, endothelial cells, and the choroid plexus. It might be context-de-pendent whether internalized Aβ is degraded in lysosomes or accumulated in the cells provoking cellular toxicity. A portion of Aβ may be transported through LRP-1 at the BBB or pulled out by sink activity of soluble LRP-1 into the blood. LRP-1 in the liver might also help clear Aβ from the blood, possibly leading to the elimination of Aβ from the brain. ApoE, which is mainly produced and secreted from astrocytes in the brain, is lipidated by ABCA1 to supply cholesterol/lipids to neurons and other cells through LRP-1. ApoE isoforms likely affect LRP-1-mediated Aβ metabolism by directly interacting with Aβ or competing with Aβ for receptor binding. [Reproduced from Shinohara et al. with permission of Journal of Lipid Research (86)].

1.8 The role of cholesterol and lipoproteins in the brain and at the blood-brain barrier

Neurodegenerative diseases, such as AD have been linked to brain cholesterol metabolism deficiency and increased serum/plasma cholesterol levels were observed when the disease progresses (101,102). Around 20% of the whole body's cholesterol content is found in the brain (103). The majority of cholesterol in the adult brain resides in myelin sheaths and plasma membranes of neurons and glia cells. Brain cholesterol is primarily supplied by *de novo* synthesis and entry with lipoproteins from plasma is restricted due to the presence of the BBB.

The cholesterol concentration in the brain stays constant under normal physiological conditions. Excess of free cellular cholesterol in neurons or astrocytes can be esterified and stored in lipid droplets and/or secreted with HDL or associated apolipoproteins via ABCA1, ABCG1 or converted to the brain-specific cholesterol metabolite and oxysterol 24S-hydroxycholesterol, then crossing through the BBB (84). In the CNS, lipid-free/poor and HDL-associated apoA-I and apoE play a major role in lipid transport and cholesterol homeostasis (104). Lipidation of both apoA-I and apoE happens via ABCA1 (105), thereby ABCA1 mediates cholesterol efflux to acceptors like apoA-I (106) and may influence whole-brain cholesterol homeostasis.

On the other side, binding of Aβ to apoE plays a major role in the final excretion of Aβ from the brain (107).

It has been shown that APP processing machinery products such as sAPPα and C-terminal fragments (CTFs, cleavage products from α-secretase- and β-secretase (described above) are expressed in brain capillary endothelial cells (Schweinzer et al., 2011; Zandl-Lang et al., 2018) (described under section 1.2), BCEC express (i) receptors or transporters associated in HDL metabolism such as scavenger receptor, class B, type 1 (SR-BI), ABCA1, ABCG1 **(Figure 5)** (described under section 1.6) (ii) phospholipid transfer protein (PLTP, engaged in HDL remodelling (78) **(Figure 5)** and (iii) synthesize HDL-associated apolipoproteins like apoA-I (in porcine BCEC, pBCEC) (80) (described under section 1.8), apoE (in murine BCEC, mBCEC) (described under section 1.8), apoM (73), and apoJ (109). Nuclear receptor agonists for liver X receptors (LXRs) and peroxisome-proliferator activated receptors (PPARs) boost cholesterol efflux, HDL formation and restoration at the BBB (80,110). LXR agonists restrain APP processing and Aβ production (108,109).

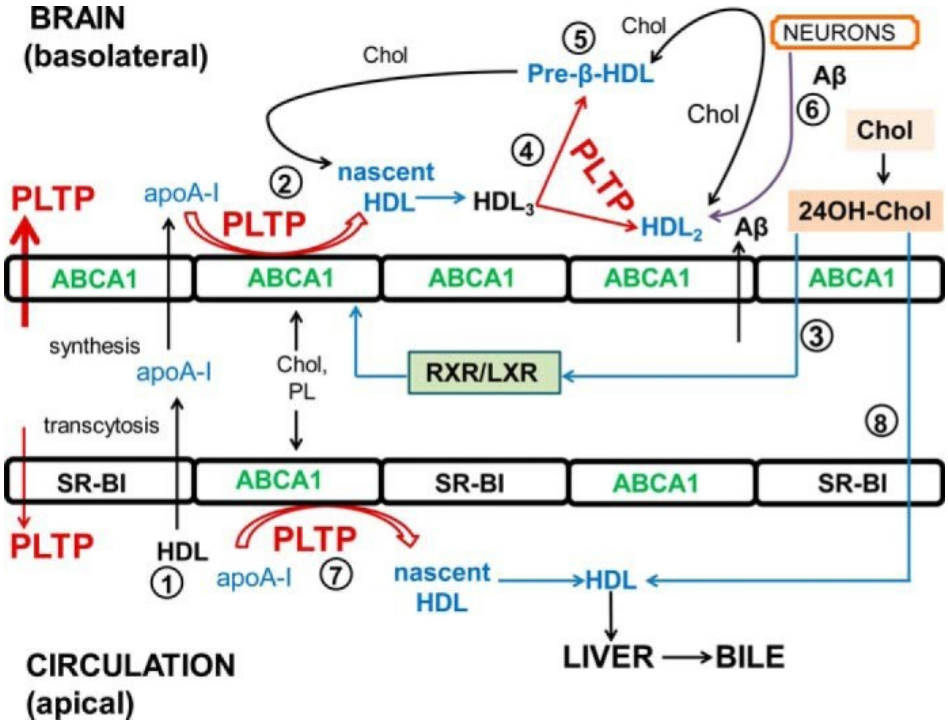

Figure 5: Model of proposed PLTP functions in HDL metabolism and HDL functions at the BBB

A small fraction of apoA-I from circulating HDL can transcytose across cerebrovascular endothelial cells. In addition, apoA-I is expressed by BCEC and released bidirectionally but mainly to the basolateral compartment. 2, active PLTP is also secreted bidirectionally but mainly to the basolateral compartment.

Nascent HDL particles are formed at the brain side with the aid of ABCA1 and PLTP. 3, LXR activation by 24OH-cholesterol (or synthetic agonists) promotes the formation of nascent apoA-I containing particles. 4, nascent HDL particles mature to form spherical HDL_3, and PLTP further remodels HDL_3 into HDL_2 and pre-β-HDL particles. 5, pre-β-HDL (and also HDL_2) accepts excess cellular cholesterol. 6, HDL may directly bind excess Aβ (from neurons and from BCEC); both PLTP and HDL may reduce intracellular Aβ oligomers, and HDL may facilitate the elimination of excess Aβ into the circulation. 7, HDL particles are also formed and remodeled at the apical side, through endogenous and exogenous (plasma) PLTP. 8, HDL in the circulation with the help of SR-BI accepts 24(S)-hydroxycholesterol, which will be finally removed through bile. (HDL, high density lipoproteins; ABCA1, ATP-binding cassette transporter A1; RXR, retinoid X receptor; PL, phospholipid; 24OH-Chol, 24(S)-hydroxycholesterol; Chol, cholesterol; SR-BI, scavenger receptor, class B, type I).[Reproduced from Chirackal Manavalan et al. with permission of Journal of Biological Chemistry (78)].

ApoA-I (a 28-kDa protein) is the major apolipoproteins in the CSF (0.37 ± 0.08 mg/dl) in parallel with apoE (0.3 ± 0.2 mg/dl) (111). ApoA-I is implicated in cerebrovascular and CNS functions (112).

Neither human primary nor murine brain microvascular endothelial cells express apoA-I mRNA (113). ApoA-I protein (not mRNA) has been found in brain tissue which is derived from plasma and crosses the BBB (114).

ApoA-I is a multifunctional apolipoprotein, and as part of HDL, plays a major role in cholesterol transport and in inflammation. It serves for cholesterol or phosphatidylcholine efflux from the lipid bilayer (115). ApoA-I is lecithin-cholesterol acyltransferase (LCAT) activator (LCAT is expressed in the brain) which contributes a mechanism for CNS cholesterol transport (116). Free cholesterol can be exported from cells for subsequent transport to the liver through initial interaction of lipid-free (or lipid-poor) apoA-I with ABCA1 on peripheral cells (117), on the other side this interaction cause Janus kinase 2 (JAK2) activation and lipid transport are impaired when JAK2-specific inhibitor is applied (118). Two different mechanisms have been shown in macrophages for ABCA1-mediated cholesterol efflux to apoA-I. One is that apoA-I at the cell surface makes complexes with phospholipid and cholesterol which is induced by ABCA1 activity (119). The other is that apoA-I interacts with ABCA1 at the cell surface and gets internalized into late endosomes, where apoA-I binds to lipids and the apolipoprotein-lipid complexes are then resecreted from the cell by exocytosis (120).

ApoA-I has antioxidant and anti-inflammatory effects and after brain injury increased apoA-I is reported in CSF (121). ApoA-I/ABCA1 interaction activates signal transducer and activator of transcription 3 (STAT3) linked to anti-inflammation (112).

ApoA-I was detected in senile plaques (122) and its expression in the hippocampus was found to be altered in neurodegenerative diseases such as AD. The risk of dementia was decreased with increased serum apoA-I levels (123) since apoA-I binds to Aβ (124) and to prevent β-sheet or toxicity of Aβ *in vitro* (125) or *in vivo* (126).

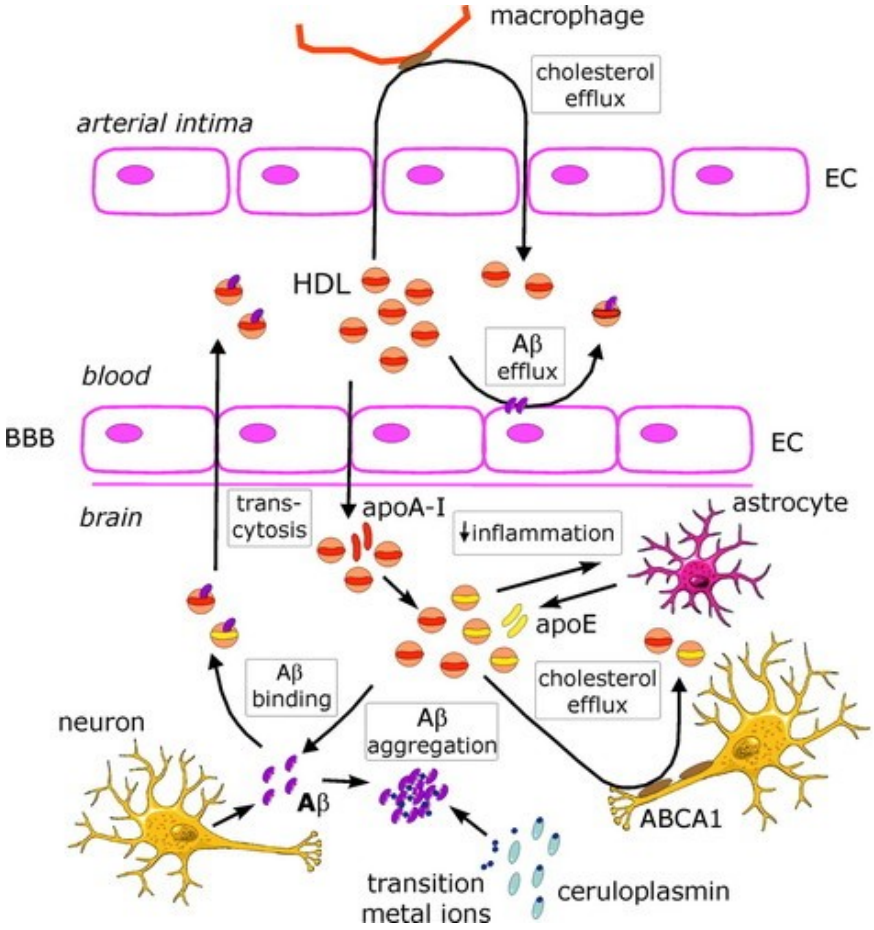

Figure 6: Neuroprotective actions of HDL and apoA-I

Underlying mechanism of the neuroprotective action of HDL. Aβ production can be suppressed by decreasing cellular cholesterol mediated by ABC transporters. ApoA-I can directly bind excess Aβ and thereby inhibit its oligomerisation. [Reproduced from Kontush et al. with permission of Arterioscler Thromb Vasc Biol (127)].

Apolipoprotein E (a 36 kDa protein) represents the major cholesterol carrier in the brain and has been identified as an essential factor for synaptic plasticity, neuronal activity,

and neuronal injury repair (128–130). ApoE has three different isoforms namely apoE2, apoE3, and apoE4, and apoE4 carriers are significantly worse in terms of brain aging and dementia risk. ApoE4 causes neurovascular dysfunction and increases BBB susceptibility to injury (131). ApoE4 is also associated with hyperlipidemia, hypercholesterolemia, and cardiovascular disease (132). In a mouse model of AD, apoE4 enhanced Aβ levels and reduced its clearance leading to plaque formation (133) and elevated Aβ-induced lysosomal leakage (134). As mentioned above, apoE (like apoA-I) contributes to cellular cholesterol efflux mechanism with ABCA1 (105) and silencing of the ABCA1 gene lowers levels of apoE (135) and increases Aβ load. Different isoforms of apoE also differ in their efficiency to promote cholesterol efflux from cells, with apo E2 having the most and apoE4 the least (136,137). In comparison to apoE3 and apoE4, apoE2 tends to bind weaker to LDL receptors and stronger to small, phospholipid-enriched HDL, whereas apoE4 tends to bind to larger, triglyceride-enriched lipoproteins (138) which, however are absent from the brain.

In addition, in AD patients apoE4 is associated with a higher density of amyloid plaques (139). ApoE4 may cause mitochondrial damage (140). On the other hand, apoE2 and apoE3 are more functional in AD, they cleared more Aβ than apoE4 in transgenic mice (133,141). Interestingly, a beneficial role of apoE2 was detected in male but not female subjects (142) and the link between apoE4 and AD is stronger in women than men which could explain the higher incidence of AD cases in women.

Cerebral amyloid deposition in living human beings is related to elevated levels of LDL cholesterol and reduced levels of HDL cholesterol in serum (143). Elevated cholesterol contents have been detected in human AD-brains and are enriched in amyloid plaques (144,145). Aβ-overproduction is also caused by increased cellular cholesterol which leads to higher membrane lipid raft content (146). Aβ-aggregation and -toxicity can be promoted in the presence of cholesterol (147). In animal models a reduction of accumulated Aβ and improved behavioral memory was shown with cholesterol-lowering drugs, including the hydroxyl-methyl-glutaryl coenzyme A (HMGCoA)-reductase inhibitors statins (148,149), although opposite effects of statins regarding cerebral Aβ content have been also reported *in vivo* (150). A regulatory feedback cycle, in which Aβ production is promoted by cholesterol while high cellular $A\beta_{1\text{-}40}$ concentrations inhibit cholesterol *de novo* synthesis has been proposed (151).

Another link between cholesterol and Aβ homeostasis appears to be ABCA1, although the underlying mechanisms have not been clearly established. Thus, Aβ oligomers

deposited in the hippocampus as a cause of memory deficits in aged APP23 mice were reported to be ABCA1-dependent (152). Furthermore, Aβ aggregation capacity could be neutralized by ABCA1 in an apoE-dependent manner via Aβ elimination from the brain (153).

1.9 Bexarotene and astaxanthin in AD

Bexarotene (Bex [Targretin, 4-[1-(5,6,7,8-tetrahydro-3,5,5,8,8-pentamethyl-2-naphthalene) ethenyl] benzoic acid) (154) is a retinoid X receptor (RXR) agonist, and FDA approved antineoplastic drug, applied in current clinical trials to treat advanced cutaneous T cell lymphomas (155), lung cancer (156) and breast cancer (157). Bex has recently been reported to have beneficial effects in many animal models of CNS disorders such as AD, amyotrophic lateral sclerosis (158), Parkinson's disease (159), multiple sclerosis (160), epilepsy (161), hypertension (162), and stroke (163).

Regarding AD mouse studies, Cramer and coworkers first reported that in the mutant, APP-overexpressing APPswe/PS1ΔE9 (APP/PS1) mice, more than 50% of cerebral Aβ plaques were cleared after Bex administration within just 72 h and behavioral and cognitive deficits were reversed (164). Subsequent studies in part, however, have shown opposite results on amyloid deposition. (165–167). Because Aβ clearance is facilitated by apoE and apoE transcription can be induced by RXR agonists, apoE was identified as a primary target of Bex which promotes microglial phagocytosis (164). Bex has some useful effects of endosomal vesicular trafficking through apoE (168). Lee et al have shown that apoE raised endosomal trafficking to lysosomes in microglia. When RXR forms heterodimers it regulates the expression of ABCA1 (169) which promote brain-to-blood transcytosis of Aβ or prevent Aβ entrance into the brain. ApoE, as a target of Bex may further improve synaptic health through increased signaling by LRP-1. Thus, postsynaptic proteins that regulate synaptic plasticity are decreased with aging Bex did not increase pre-synaptic marker synaptophysin or post-synaptic marker PSD95 expression in aged neuronal LRP-1$^{-/-}$ mice but they were regenerated by Bex treatment in the brains of control mice (170).

Bex treatment also stimulated ABCA1 expression in hippocampus and cortex of APP/PS1 mice (164,171). Bex was further reported to induce the expression of the phagocytic receptors Axl and family of receptor tyrosine kinases (MerTK). Consequently, Aβ phagocytosis by myeloid cells in the brain was promotedand

inhibiting the MerTK receptor abolished the induction of phagocytosis by Bex in brain slices of the AD mouse model, APP/PS1 (172).

Bex-dependent plaque reduction due to increased phagocytosis by microglia and macrophages in APP/PS1 mice may lead to reduced inflammatory gene expression, i.e. of TNFα, IL-1β, and IL-6 in the neuron environment. Bex reduced GFAP positive astrocytes and accompanying inflammatory cytokine production in subiculum of 4 months old, and in cortex of 8 months old 5XFAD mice which may have contributed to enhanced neuronal survival (168).

Interestingly, in an animal model of Parkinson's disease, Bex treatment induced the activity of the nuclear receptor related 1 protein (Nurr1) through formation of Nurr1-RXR heterodimers (159). In that study, increased retention of dopaminergic neurons and improved behavioral performance was observed in 6-hydroxydopamine (6-OHDA) lesioned rats with very low dose Bex (approximately 6 μg/kg/day).

Recently, small molecule OAB-14, a derivative of Bex, was reported to rapidly clear 71% of Aβ by promoting microglia phagocytosis and increasing insulin-degrading enzyme (IDE) and neprilysin expression in APP/PS1 transgenic mice after administration for 15 days or 3 months. This compound also ameliorated the downstream pathological events of Aβ accumulation, such as synaptic failure, neuronal loss, hyperphosphorylation of tau, and neuroinflammation in APP/PS1 mice (173).

Surprisingly, neuroprotective effects of Bex have also been reported in the SOD1(G93A) mouse model of amyotrophic lateral sclerosis (ALS) (158), a murine tauopathy model (174), as well as in murine and human Huntington’s disease neurons *in vitro* (175).

Table 1: Chemical names and structure of compounds

Compound	Chemical name	CAS	Chemical structure	Reference
Bexarotene (Targretin) C24H28O2	4-[1-(5,6,7,8-tetrahydro-3,5,5,8,8-pentamethyl-2-naphtalenyl) ethenyl] benzoic acid)	153559-49-0	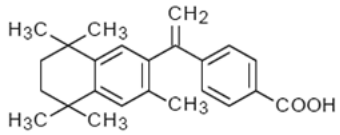	(176)
Astaxanthin C40H52O4	3,3′-Dihydroxy-β,β-carotin-4,4′-dione	472-61-7	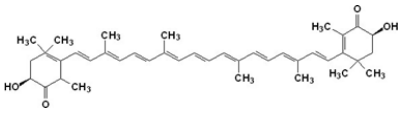	(177)

[Reproduced from Fanaee-Danesh E et al. with permission of Biochim Biophys Acta Mol Basis Dis (1)].

The role of PPARs as regulators of lipid metabolism (178) and energy homeostasis (179) is already known.Upon activation by their ligands, PPARs form obligatory heterodimers with RXR. It has been described that PPAR/RXR activation causes interactions with various cell signaling pathways (180). They have been proposed as targets for neurodegenerative diseases (181). All PPAR isoforms are more highly expressed in neurons than other cell types. It has been indicated that PPAR(α, β/δ, γ) activation induces some changes at the BBB. It has been shown that PPARδ reduces Aβ burden in AD murine models (182), PPAR α increased expression of ABCG2 (183) and protective effects against deprivation stimuli (184) in BBB models, but so far no studies have reported on changes in Aβ levels after PPARα activation at the BBB.

The order of quantities in the brain was found to be PPARβ/δ>PPARα≥PPARγ, among them PPARα was the only isotype to colocalize with all cell types in both adult mouse and adult human brain tissue (185). PPARα has been related to the regulation of energy homeostasis (186), synaptic function (187), neuroprotection, and anti-inflammatory response (188). Recently, PPARα activation by WY14643 or Gemfibrozil augmented α-secretase ADAM10 expression, thereby pushing APP processing toward the non-amyloidogenic pathway, decreasing Aβ levels and increasing sAPPα in mouse hippocampal neurons (189). Knocking out PPARα from 5XFAD mice aggravated Aβ

deposition and, interestingly, the same effect was observed in PPARα$^{-/-}$ mice, which exhibited increased levels of endogenous Aβ.

Asx ([3,3′-Dihydroxy-β,β-carotin-4,4′-dione]), a PPARα agonist (190) and carotenoid is used as a dietary supplement, and its widely beneficial effects are largely ascribed to its unique antioxidant capacity. This is caused by Asx's many double bonds at the center of the molecule which donate electrons to reduce a reactive oxidizing molecule (191) and due to the two hydroxylated ionone rings at both ends of the lipophilic domain (Table 1). This structure of Asx allows the molecule in a cell to get integrated vertically through the phospholipids bilayers and the precise position of Asx can interfere with lipid peroxidation in the membrane. Asx has the capacity to protect the cell membrane against oxidative parameters (192) Production of superoxide dismutase (SOD) and heme oxygenase-1 (HO-1), potent endogenous antioxidant defense mechanisms, are also augmented by Asx (193). Microglial activation is alleviated by Asx whereby the amount of produced cytotoxic substances are decreased (194).

Hippocampal neurogenesis, plasticity, and spatial memory in mice are improved by Asx (195). Proliferation of neural precursor cells *in vitro* is increased by Asx, and when these cells were exposed to an oxidative insult they were directly protected by Asx treatment (196).

Algae is the richest source of Asx, commonly found in *Chlorella zofingiensis*, *Chlorococcum*, and *Phaffia rhodozyma* (197). While, *Haematococcus pluvialis* is the primary natural source for Asx. Due to dietary ingestion (natural or supplemented), salmon, trout, krill, shrimp, crayfish, and crustaceans contain Asx which can be seen by the typical reddish/pink colour. The molecule has a high BBB permeability and has been reported to significantly ameliorate BBB disruption (198). Neuroprotective effects of Asx (199) against oxidative stress (197), anti-inflammatory (198) effects like lowered C-reactive protein (CRP), and anti-apoptotic properties (200) have been reported. Furthermore, Asx improved spatial memory in Swiss albino male mice (201) and improved memory performance of BALB/c mice in the Morris water maze has been achieved (202). Asx also improved cognitive function in a group of 10 healthy men (age 50-69), who were complaining of forgetfulness, and received Asx (12 mg/day) for 3 months. By a computerized test sensitive to detect early cognitive deterioration, an improvement in measuring reaction time and of working memory was observed (203) Short-term effects have been reported for Asx, albeit in rats: Asx treatment (30 mg/kg) improved CA1 hippocampal neuronal density after a 7 day treatment in a rat global

cerebral ischemia model (204). Asx (10-40 mg/kg) effectively improved cognitive function and reduced cerebral inflammation in diabetes mellitus in a rat model (Male Wistar rats) after 5 days of treatment (205).

2. Rationale and aims

Alzheimer's disease (AD) is the most common cause of dementia. Despite decades of research no significant therapeutic benefits have been achieved. Both, AD and atherosclerosis share several risk factors as well as protective factors, indicating that vascular mechanisms critically contribute to the development of AD. A hallmark in AD is the formation and accumulation of neurotoxic Aβ peptides in the brain and in the cerebrovasculature. Although several risk factors for AD have been identified, the molecular pathways of how they affect Aβ metabolism are widely unknown.

Using an *in vitro* model of the BBB we have shown that primary pBCEC express and release apoA-I that may assemble with cellular cholesterol to form HDL, a pathway that is enhanced by treatment with nuclear receptor (i.e., LXR and PPAR) agonists (80,110). These apo/lipoproteins may also interact with Aβ or its APP. We confirmed APP expression and processing by pBCEC indicating that the BBB may actively contribute to Aβ synthesis. Moreover, modulation of cellular cholesterol metabolism (with LXR agonists or simvastatin) regulated APP processing in pBCEC. Our findings strongly implied that pharmacological modulation of cellular cholesterol metabolism could contribute to redirect APP synthesis and processing by cerebromicrovascular endothelial cells towards the beneficial, non-amyloidogenic pathway (108).

In a striking recent paper, another synthetic agonist that potently activates RXR and RAR, Bex, treatment has been reported to reverse the effects of neurodegeneration (and improve cognitive skills) in a mouse model of AD via increasing the clearance of Aβ (164). However, no significant clearance of Aβ was so far reported in response to Asx treatment.

The AIM of the present thesis was to investigate the effects of the pharmacologic retinoid-X receptor agonist, bexarotene (Bex), and the peroxisome proliferator-activated receptor-α agonist and strong antioxidant, astaxanthin (Asx) in Aβ and cholesterol metabolism at the blood-brain barrier.

We addressed the following specific questions:

- To examine the effects of Bex and Asx on APP processing and Aβ levels using pBCEC and murine (m)BCEC. Therefore, pBCEC were incubated with [10, 100]

nM of Bex and [1,10] nM of Asx for 24 h in SF conditions or 3xTg AD mice were gavaged with Bex (100 mg/kg) or Asx (80 mg/kg) for 6 days and isolating mBCEC.

- To investigate the effect of Bex or Asx on cellular cholesterol metabolism at the BBB *in vitro* using pBCEC.
- To study Aβ trafficking and clearance at the BBB after Bex or Asx administration *in vitro* using pBCEC or *in vivo* using murine (m)BCEC isolated from 3xTg AD mice.

3. Materials and methods

Parts of this chapter are literally published in:

Fanaee-Danesh E, Gali CC, Tadic J, Zandl-Lang M, Carmen Kober A, Agujetas VR, et al. Astaxanthin exerts protective effects similar to bexarotene in Alzheimer's disease by modulating amyloid-beta and cholesterol homeostasis in blood-brain barrier endothelial cells. Biochim Biophys Acta Mol Basis Dis. 2019 Sep 1;1865(9):2224–45. (1).

Martina Zandl-Lang. Interactions of simvastatin and apoJ with APP processing and amyloid-β clearance in blood-brain barrier endothelial cells [Internet]. Medizinische Universität Graz; 2017 (206).

Yidan Sun. The Impact of Gestational Diabetes Mellitus on Regulating Cholesterol Homeostasis in Human Fetoplacental Endothelium [Internet]. Medizinische Universität Graz; 2018 (207).

3.1 Materials

3.1.1 Chemicals and solutions for isolation and culture of primary pBCEC

Purchased chemicals are listed in (Table 2) . 75 cm² cell culture flasks, 6- and 12- well plates were obtained from Greiner Bio-One. Transwell 12-well plates (0.4 µm polyester membrane) were obtained from Corning Life Sciences. Evohm ohmmeter was from World Precision Instruments (206).

Table 2: Chemicals/solutions used for cell isolation, culture, and cell culture experiments

Product	Company
TO 901317	Cayman Chemicals
Bexarotene	Calbiochem (Merk Millipore)

Astaxanthin	AdipoGen
PA 452	Tocris
GW 6471	Sigma- Aldrich
Probucol	Sigma- Aldrich
MCDB 131 Medium(1x)	Life Technologies
Minimum Essential Medium (MEM, 10x)	Life Technologies
Medium 199 (1x)	Life Technologies
DMEM/ F-12 (Ham)	Life Technologies
Dispase	Life Technologies
Collagen G from bovine calf skin	M&B Stricker
Penicillin/streptomycin/ Gentamycin	PAA Laboratories
Trypsin- EDTA	PAA Laboratories
Horse Serum	PAA Laboratories
L-Glutamine	PAA Laboratories
Collagenase/dispase	Roche
Amyloid β protein fragment (1-40)	Sigma- Aldrich
Hydrocortisone	Sigma- Aldrich
Percoll® pH 8.5- 9.5	Sigma- Aldrich

Dextran	VWR

Contents of this table are literally published in (206).

1x PBS, pH 7.38-7.42, 5 liters

40 g NaCl
1.5 g KCl
0.1 g KH_2PO4
0.457 g $Na_2HPO_4 + H_2O$
10 g glucose or dextrose
Fill up to 5 liters with d_2H_2O, filter the solution and autoclave it (206).

Collagenase/dispase solution

Sterile-filter (0.2 µm pore size) 100 mg collagenase/dispase and 10 mg plating medium A and store 350 µl aliquots at -20 °C (206).

Dextran solution

200 g Dextran
2.4 g $NaHCO_3$
109.1 ml MEM (10x)
Fill up to 1.2 liters with d_2H_2O, stir overnight at 4°C, determine and adjust density to 1.0612 and final solution was autoclaved.and stored at 4°C (206).

Percoll® biphase

1.03 g/ml density

40 ml PBS, 1x
9 ml Percoll® pH 8.5- 9.5
1 ml MEM (10x)

1.07 g/ml density

20 ml PBS, 1x
27 ml Percoll® pH 8.5-9.5
3 ml MEM (10x)

Collagen G solution (60 µg/ml and 120 µg/ml)

Mix 450 µl (for 60 µg/ml) or 900 µl (for 120 µg/ml) of collagen G stock solution (4 mg/ml) with 30 ml PBS (206).

Preparation medium

500 ml medium M199 (1x)
1% penicillin/streptomycin
1% gentamycin
1 mM L-glutamine.

Plating medium A

500 ml medium M199 (1x)
10% horse serum
1% penicillin/streptomycin
1% gentamycin
1 mM L-glutamine

Plating medium B

Same components as the medium A but without gentamycin

Medium serum-free (SF)

500 ml medium M199 (1x)
1% penicillin/streptomycin
1 mM L-glutamine

DMEM/Ham's F12 medium

1% penicillin/streptomycin
0.7 mM L-glutamine
0.4% hydrocortisone stock solution [50 µg/ml]

Hydrocortisone stock solution [50 µg/ml]

Dissolve 1 mg hydrocortisone in 1 ml ethanol and 19 ml DMEM/Ham's F12 medium. Store aliquots at -20°C (206).

Carbonate-bicarbonate (CBC) buffer pH 9.0

0.5 M Na_2CO_3
0.5 M $NaHCO_3$

Fluorescent labeling of $A\beta_{1-40}$

100 µl of $A\beta_{1-40}$ [1mg/ml] was labeled fluorescently while incubating with 3 µl Alexa Fluor 488 5-TFP for 1 h at 37°C in 18 µl CBC buffer. Unbound fluorescent dye was removed via size-exclusion on a PD-10 column. Elution was performed with 1 ml of PBS (206).

Bexarotene stock solution

3.5 mg of bexarotene was dissolved in 1 ml ethanol (10 mM) as a stock solution and then was further diluted to (1:50) to the 200 µM concentration, stored in aliquots at -20 ºC. For 100 nM bexarotene, cells were incubated with 0.5 µl/1 ml of the 200 µM stock solution.

Astaxanthin stock solution

5,96 mg of astaxanthin was dissolved in 1 ml DMSO [10 mM] as a stock solution and stored in aliquots at -20 ºC. Further dilutions (1:50) were prepared freshly in SF medium at the day of treatment.

PA 452 stock solution

44,4 mg of PA452 was dissolved in 1 ml DMSO [0.1 M] as a stock solution and stored in aliquots at -20 ºC. Further dilutions (1:100) were prepared freshly in SF medium at the day of treatment, [10 µM] of PA 452 used for experiment.

GW 6471 stock solution

5 mg of GW 6471 in 800 µl DMSO [0.01 M] as a stock solution and stored in aliquots at -20 ºC. Further dilutions (1:10) were prepared freshly in SF medium at the day of treatment, [10 µM] of GW 6471 used for experiment.

Probucol (P9672) stock solution

51,7 mg of probucol was dissolved in 1 ml DMSO [0.1 M] as a stock solution and stored in aliquots at -20 ºC. Further dilutions (1:100) were prepared freshly in SF medium at the day of treatment, [10 µM] of probucol used for experiment.

3.1.2 Chemicals and solutions used for RNAi, RNA isolation, cDNA synthesis, and RT-qPCR

All products and reagents used for isolation and RT-qPCR are listed in (Table 3) (206).

Primers used for RT-qPCR (Table 4) for RNA silencing are listed in (Table 5, Table 6) (1).

Table 3: Materials used for RNA isolation, cDNA synthesis, and RT-qPCR

Product	Company
iQ SYBR® green supermix	Biorad
Hard-Shell® Low-profile thin-wall 96-well skirted PCR plates	Biorad
Microseal ‘B’ Adhesive seals for PCR plates	Biorad
0.2 ml PCR tubes	Biorad
C-1000™ thermal cycler	Biorad
Icycler iQ™, Real-time PCR detection system	Biorad
Molecular imager ChemiDoc XRS System	Biorad
Power Pac HC, power supply	Biorad
Biozym LE agarose	Biozym

OneTouch filter-tips, 10 µl	Biozym
Nuclease-free water	Carl Roth
HE 33 Mini submarine electrophoresis unit	Hoefer® Inc.
High capacity reverse transcriptase kit	Life Technologies
Ethidiumbromide (10 mg/ml)	Life technologies
Taqman gene expression master mix	Life technologies
TriReagent RT	Molecular Research Center, Inc
2-Log DNA ladder	New England laboratories
Gel loading dye, blue (6x)	New England laboratories
NanoDrop® ND-1000 UV-Vis spectrophotometer	Peqlab

Contents of this table are literally published in (206).

Table 4: Primers used for RT-qPCR

Gene	Sequence (5'-3')	Amplicon size (bp)
ssADAM10	F,AGCAACATCTGGGGACAAAC	219
	R,CTTCCCTCTGGTTGATTTGC	
ssBACE1	F,TGGACTGCCTCATGGTGTG	155
	R,GTGACCAAAGTGAACCACCG	
ssHPRT1	F,AGGACCTCTCGAAGTGTTGG	247
	R,CAGATGGCCACAGGACTAGA	
ssLRP-1	F,GCAGATGTATCAACATCAACTGG	98
	R,GGGTGCTAGAGCAAGAGTGG	
ssABCA1	F,GCCATTCTCCGGGCCAAC	252
	R,GGCTTCACGCCGCTGAT	
ssAPOA-I	F,GATGCGATCAAAGACAGTGG	98
	R, CTGTCCCAGTTGTCCAGGAG	
mmLRP-1	F,CCGCATCTTCTTCAGTGACA	96
	R, ACAGAGCCCACATTTTCCAC	
mm ABCA1	F,ATTGCCAGACGGAGCCG	103
	R,TGCCAAAGGGTGGCACA	
mm APOE	F,CTGACAGGATGCCTAGCCG	107
	R,CGCAGGTAATCCCAGAAGC	
mm CD31	F,AGGCTTGCATAGAGCTCCAG	278
	R,TTCTTGGTTTCCAGCTATGG	
mm CD13	F,CCCCGGGGCTGCTGTTCTTT	1208
	R,ACCACCCGCTCCTTGTTGCTAATG	

mm GFAP	F,TCCTGGAACAGCAAAACAAG	224
	R,CAGCCTCAGGTTGGTTTCAT	
mm SYP	F,CATTCAGGCTGCACCAAGTG	60
	R,TGGTAGTGCCCCCTTTAACG	
mm IBA1	F,GGATTTGCAGGGAGGAAAAG	92
	R,TGGGATCATCGAGGAATTG	
mm SMA	F,CTGACAGAGGCACCACTGAA	285
	R,GAAATAGCCAAGCTCAG	
mm PDGFRβ	F,AGCTACATGGCCCCTTATGA	367
	R,GGATCCCAAAAGACCAGACA	
mm HPRT1	F,GCCTAAGATGAGCGCAAGTTG	101
	R,TACTAGGCAGATGGCCACAGG	
mmHPRT1 mmBACE1	QUANTITECT PRIMER ASSAY (QIAGEN)	

Primer sequences, forward (F) and reverse (R) for porcine (ss) and murine (mm) genes used for qPCR analysis. [Reproduced from Fanaee-Danesh E et al. with permission of Biochim Biophys Acta Mol Basis Dis (1)].

Table 5: Chemicals and solutions used for silencing

Product	Company
ON target plus siRNA	Dharmacon
DharmaFECT 1 Transfection Reagent	Dharmacon

Table 6: siRNA used for LRP-1 silencing

siRNA	Sequence	Company
LRP1-1	5’-GGAGGAUGACUGUGAACAU-3’	Microsynth
LRP1-2	5’-ACAACGCUGUCGCCUUGGA-3’	Microsynth
LRP1-3	5’-CCUGUACUGGUGUGACAAA-3’	Microsynth

3.1.3 Chemicals and solutions used for protein isolation, SDS-PAGE, and immunoblotting

All purchased products and solutions used for protein precipitation, isolation and immunoblotting are listed in (Table 7) (206).

Table 7: Materials used for protein isolation and immunoblotting

Product	Company
XT sample buffer (4x)	Biorad
XT sample reducing agent (20x)	Biorad
Blotting-Grade blocker, nonfat dry milk	Biorad
Clarity western ECL substrate	Biorad
IKA® model MS1 mini shaker	Carl Roth
Combi- shaker KL 2	Carl Roth
Microcentrifuge, Qualitron DW- 41	Carl Roth
Chemicals	Carl Roth or Sigma Aldrich
Concentrator plus	Eppendorf
IKA® Model MS1 mini shaker	Carl Roth
Combi- shaker KL 2	Carl Roth
Microcentrifuge, Qualitron DW- 41	Carl Roth
ELMA Transsonic 460, ultrasonic unit	Carl Roth
PVDF membrane, Hybond-P	GE Healthcare
NuPage® Novex 4-12% Bis- Tris midi gel	Life technologies
NuPage® MES SDS running buffer (20x)	Life Technologies
NuPage® MOPS SDS running buffer (20x)	Life Technologies
Pierce® BCA protein assay kit	Thermo Scientific
Bovine serum albumin, 2 mg/ml	Thermo Scientific
CL- Xposure film (12.5 x 17.5 cm)	Thermo Scientific
Cell proliferation reagent WST-1	Roche

Sunrise photometer with Magellan software	Tecan
Centrifuge Sigma 3K15 with angle rotor 12154-H	Sigma
Protease Inhibitor cocktail tablets	Sigma Aldrich
Magnetic stirrer with heating, MR 3001, Heidolph	VWR
Ratek RSM7, Rotary suspension mixer	VWR

Contents of this table are literally published in (206).

Protein lysis buffer

- 50 mM Tris, pH 7.5
- 10 mM EDTA
- 1% Triton-X-100
- 1 tablet of protease inhibitor cocktail

Fill up to 10 ml with d_2H_2O and store in aliquots at -20°C (206).

Running buffer (10x, pH 8.3)

- 30.3 g Tris
- 144.0 g glycin
- 10.0 g SDS

Transfer buffer (1x, 2.4 l)

- 240 ml running buffer, 10x
- 480 ml methanol

Fill up to 2.4 ml with d_2H_2O and store at 4°C (206).

TBS-TT (1x, 5 liters)

- 100 ml Tris, 1 M, pH 7.5
- 250 ml NaCl, 5 M
- 10 ml Triton-X-100

- 2.5 ml Tween 20

Fill up to 5 l with d_2H_2O and store at 4°C (206)

Blocking solution

Dissolve 5% blotting-grade blocker in 1x TBS-TT

3.1.4 Antibodies

Primary and secondary antibodies used for immunoblotting were dissolved in 5 % skim milk powder in TBST-T and are listed in (Table 8) (1,206).

Table 8: Antibodies used for immunoblotting

Antibody	Working dilution	Company	Protein detected
Primary antibody			
Rabbit-anti- β -actin	1:5000	Sigma Aldrich	β-actin
Rabbit-anti-β-amyloid precursor protein	1:1500	Invitrogen	full- length APP
anti-amyloid precursor protein, C-terminal A8717	1:1000	Sigma Aldrich	APP/ CTF
A11 rabbit-anti-amyloid oligomer	1:10 000	Millipore	Aβ oligomers
Mouse-anti-beta-amyloid 1-16 (6E10)	1:1000	Biolegend	sAPPα
Polyclonal rabbit-anti-human apoA-I antiserum	1:2500	Behring	secreted apoA-I
mouse anti-ABCA1	1:8000	Abcam	ABCA1
anti-LRP-1 antibody ab192308	1:10000	Abcam	LRP-1
Secondary antibody			
Goat anti-rabbit IgG-HRP	1:10 000	Santa Cruz Biotechnology	

Goat-anti-mouse-HRP	1:5000	Sigma Aldrich	

Contents of this table are literally published in (207).

3.1.5 Materials used for Aβ transport and uptake studies

Table 9: Materials and reagents used for Aβ transport studies

Gamma 5500B	Beckman
Ultima gold scintillation cocktail	New England Nuclear
Tri-carb 2100 TR liquid scintillation Analyzer	Packard
^{14}C-sucrose	Perkin Elmer
^{125}I-Aβ_{1-40}	Phoenix Peptides

Contents of this table are literally published in (206).

3.1.6 Material used for radiometric assay

Table 10: Reagents and materials used for cholesterol efflux, cholesterol biosynthesis and esterification

Product	**Company**
[1,2-^{3}H(N)]-Cholesterol	PerkinElmer
Ultima gold scintillation cocktail	New England Nuclear
[1-^{14}C]-Acetic acid	Perkin Elmer
TLC Silica gel 60	Merck
Cholesterol standard	Sigma-Aldrich
Cholesteryl oleate standard	Sigma-Aldrich

Iodine	Roth
Acetic acid	Roth
Diethylether	Roth
Methanol	Roth
Chloroform	Roth
Isopropanol	Roth
n-hexane	Roth
β-counter	Packard

Contents of this table are literally published in (207).

3.1.7 Reagents used for measuring total cholesterol

Table 11: Chemicals and materials for total cholesterol measurement

Product	**Company**
Cholesterol detection kit	DiaSys Diagnostic Systems
Sodium3,5-dichloro-2-hydroxybenzenesulfonate (DHBS)	Sigma-Aldrich
Absorbance detection	Sunrise

Contents of this table are literally published in (207).

3.1.8 Material used for measuring reactive oxygen species

Table 12: Reagents used for ROS detection

Product	Company
H_2DCFDA fluorescent dye	Biotium
Tiron	Sigma-Aldrich
Triton- X100	Sigma-Aldrich

Contents of this table are literally published in (207).

3.1.9 Equipment used for ultracentrifuged HDL_3 and apoA-I isolation

Table 13: Materials used for HDL_3 and apoA-I isolation

Product	Company
PD10 size-exclusion columns	GE healthcare
Qubit Quant-iT Protein Assay Kit	Invitrogen
Optima L-90K ultracentrifuge	Beckman coulter
Sephacryl S-200 column	GE healthcare

Contents of this table are literally published in (207).

3.1.10 Materials for *in vivo* studies

Table 14: Materials used for mouse studies

Material	Company
Corn oil	Sigma-Aldrich
Bexarotene	LC Laboratories
Astaxanthin	Sigma-Aldrich
Diethylamine (DEA)	Sigma-Aldrich
Formic acid (FA)	Sigma-Aldrich

3.1.11 Reagents used for Aβ extraction from murine brain homogenates

Table 15: Materials and equipment required for Aβ extraction from mouse brain

Materials	Company
1.5 ml open-top Eppendorf tubes	Thermo Scientific
DEA (≥99.5%)	Sigma-Aldrich
95% formic acid (FA)	Carl Roth
100 mM NaCl	Sigma-Aldrich
Tris base	Thermo Scientific
0.5 M sodium phosphate dibasic (Na_2HPO_4)	Carl Roth
0.05% sodium azide (NaN3)	Thermo Scientific
250 mM sucrose	Thermo Scientific
0.5 mM Ethylenediaminetetraacetic Acid, Disodium Salt Dihydrate (EDTA)	Thermo Scientific
0.5 mM Ethylene glycol-bis (2-aminoethylether)-N, N, N′, N ′-tetraacetic acid (EGTA)	Thermo Scientific
Protease Inhibitor Cocktail	Sigma-Aldrich
Beckman Coulter optima L-90K ultracentrifuge with a SW50.1 rotor	Beckman

3.1.12 Reagents and products required for immunocytochemistry

Table 16: Reagents used for immunohistochemistry

Reagent	**Concentration/ dilution**	**Company**
1st antibody	polyclonal rabbit anti-human Aß (Ab9234) 8µg/ml	Millipore
2nd antibody	Goat anti-rabbit Cy-3 (red) 1.88µg/ml	Jackson ImmunoResearch Lab, Inc. PA, USA)
Negative control	Normal rabbit immunoglobulin fraction	Millipore Corp., Temecular, Ca, USA
Dako Cytomation antibody diluent		(Dako, Inc., Carpinteria, Ca, USA).

3.2 Methods

3.2.1 Isolation and culture of primary porcine brain capillary endothelial cells (pBCEC)

Porcine BCEC were isolated according to the protocol previously described by Franke et al. (208) with minor modifications (78) from 3 pooled hemispheres of freshly slaughtered pigs (~6 months old, male and female) from the local slaughterhouse. Forceps were used to remove meninges and capillaries and a scalpel and a cutter with rolling plates were used to mince the gray and white matter of the brain cortex. To isolate the capillaries, dispase (70 mg/brain) was mixed with 40 ml of Preparation Medium described under (3.1.1) and incubated at 37°C in the water bath for 1 h with gentle stirring. After the incubation time, 150 ml dextran solution was added and the suspension was centrifuged (8000x*g*, 10 min, 4°C). The pellet was resuspended in Medium A described under (3.1.1) and the capillaries were disrupted mechanically by filtering the suspension through a nylon mesh and enzymatically by adding 350 µl collagenase/dispase. The suspension was carefully pipetted onto a percoll bi-phase gradient (15 ml of 1.07 g/ml percoll solution on the bottom, 20 ml of 1.03 g/ml percoll solution on top) and centrifuged (1300x*g*, 10 min, RT) in a swinging bucket rotor. Endothelial cells were aspirated from the interphase and washed once with Medium A. Cells were plated onto collagen-coated 75 cm² cell culture flasks in Medium A and incubated at 37°C in humified air containing 5% CO_2. After 24 h of incubation, BCEC were washed twice with 1x PBS and cultured in Medium B until confluency (206).

After 3 days, confluent pBCEC were trypsinized (using trypsin, 0.5%) and split onto collagen-coated 6-well or 12-well plates (60 µg/ml collagen) or Transwells (120 µg/ml collagen) for further experiments (206).

3.2.2 Isolation of intracellular and secreted proteins

Porcine BCEC were plated on 6-well plates and incubated with SF medium containing vehicle (0.05% ethanol), Bex [10 nM], or [100 nM], Asx [1 nM] and [10 nM]. To isolate secreted proteins, the medium was collected and centrifuged at 10000 rpm for 10 min

at 4°C. Proteins were precipitated by adding 3% (v/v) trichloroacetic acid. After 1 h incubation on ice, the suspension was centrifuged at (10000x*g*, 10 min, 4°C), the pellet was washed twice with ice-cold acetone and dissolved in 1x sample buffer (Biorad) and 1x reducing agent (73).

After removing the medium from the 6-well plates, cells were washed twice with cold 1x PBS and lysed in protein lysis buffer [40 µl/well] (206). Cell lysates were transferred to a fresh 1.5 ml tube, vortexed, and sonicated in a water bath sonicator for 2x3 min (206). To remove residual DNA, the suspension was centrifuged (12000 rpm, 10 min, 4°C) and the supernatants were transferred to fresh tubes. After measuring the protein concentration by BCA assay (Thermo Scientific) Concentrated loading buffer and reducing agent were added to 10 µg of the proteins and filled up with double-distilled water (ddH_2O) to 20 µl and loaded onto the gel.

3.2.3 SDS-PAGE and immunoblotting

Porcine BCEC were cultured in 6-well plates and incubated with SF medium (Earle´s medium M199 1X, 1% P/S, 1 mM L-glutamine) containing 0.5% ethanol (control), Bex [10,100 nM] or Asx [1,10 nM] for 24 h at 37°C (1). After 24 h, immunoblot analysis of mBCEC cell protein lysates and secreted proteins precipitated by trichloroacetic acid (TCA) (described under 3.2.2) were performed (73). Lysates mixed with sample buffer, and proteins denatured at 95°C for 5 min in a thermocycler. Equal amounts of protein (20 µg) were loaded onto gradient NuPage® Novex 4-12% Bis-Tris Midi Gels (Thermo Scientific) and subjected to SDS-PAGE under reducing conditions as described (1,206). Proteins were electrophoretically transferred (210) to 0.45 µm PVDF membranes (GE healthcare) (1). 10% non-fat dry milk (Bio-Rad) in Tris-buffered saline containing Tween 20 (TBST) for 1 h was used for blocking (1), then the membranes were probed with the primary antibodies (listed in Table 8) diluted in TBST containing 5% milk powder (1). ECL was used for detecting chemiluminescent signals and blots were imaged by using a ChemiDoc system (Bio-Rad). ImageLab software (version 5.2.1, Bio-Rad) was applied for quantification of Immunoreactive bands.

3.2.4 BACE activity assay

The fluorometric Beta-Secretase Activity Assay Kit (Abcam) was used to measure the activity of BACE1. The two reporter molecules EDANS and DABCYL are attached to a secretase-specific peptide. Upon cleavage of this peptide by BACE1, the reporter molecules are released and the fluorescent signal can be detected. In brief, pBCEC were incubated with either vehicle control (0.5% ethanol), Bex [100 nM] or Asx [10 nM] in SF medium for 24 h at 37°C (1). Cells were harvested by scraping and centrifuged for 5 min at 700x*g* (1). Supernatants were removed, 0.1 ml of ice-cold extraction buffer was added to the pellets and incubated on ice for 10 min, centrifuged 10000x*g*, 5 min. The supernatant was transferred to new tube and was kept on ice. A fluorimeter (Flexstation 2 Molecular Devices) (Ex=345 nm/Em=500 nm) was used for determination of the activity (1,109).

3.2.5 Isolation of RNA and quantitative real-time PCR

Porcine BCEC were grown in collagen-coated 6-well plates and incubated with SF medium containing vehicle control (0.5% ethanol), Bex [10,100 nM], or Asx [1,10 nM] for 24 h at 37°C. Cells from 3 wells were pooled and resuspended in 1 ml TriReagent RT (MRC, USA). To reach a phase separation, 50 µl of 4-bromoanisole (BAN) was added, incubated for 5 min at RT and centrifuged (12000x*g*, 15 min, 4°C). The aqueous phase of the suspension was isolated and mixed with isopropanol 1:1 (v/v) (206). After 10 min incubation time at RT and one centrifugation step (12000x*g*, 8 min, 4°C), the pellet was washed once with 75% ethanol (206). The RNA pellet was air-dried and resuspended in 40 µl RNase free water. To dissolve the RNA, the samples were incubated for 10 min in the thermocycler (55°C, 300 rpm) before checking the concentration and the purity in the Nanodrop (206). For cDNA synthesis, the High Capacity Reverse Transcriptase Kit by Life Technologies was used (206). On average 250 ng RNA was reversed to receive a final concentration of 2.5 ng/µl of cDNA. Relative gene expression was analyzed by using Sybr Green Master Mix (Biorad) on a CFX96 PCR detection system (Bio-Rad) (206). Gene expression levels were normalized to HPRT1 using the $^{\Delta\Delta}$CT method (211). The relative gene expression was quantified by using the $^{\Delta\Delta}$Ct method described by Livak and Schmittgen (212). Primers used throughout the study are listed in (Table 4).

3.2.6 Transwell studies

For transcytosis experiments, cells were cultured on 12-well transwells filters at a density of 40,000 or 80,000 cells/cm^2, upon confluence, pBCEC were washed with 1x PBS and incubated in DMEM/ Ham's F12 medium containing 1% P/S, 0.25% glutamine and 500 nM hydrocortisone (Sigma Aldrich) added for inducing tight junctions (206). Increasing transendothelial electrical resistance (TEERs) of pBCEC was monitored using Endohm tissue resistance chamber and the Evohm ohmmeter (World Precision Instruments) (206) to record tight junctions formation (intact BBB), and wells with 150–300 ohms/cm^2 were used for experiments.

3.2.7 Purification of human plasma HDL and apoA-I

EDTA plasma from healthy, female volunteers were used to isolate HDL_3 (1.125–1.21 g/ml) by KBr-density gradient ultracentrifugation (213). HDL_3 was stored at 4 °C, PD10 size-exclusion column chromatography and PBS (pH 7.4) were used for HDL_3 desalting. Protein content was determined by Qubit Quant-iT Protein Assay Kit (1). ApoA-I isolation from delipidated HDL by size-exclusion chromatography was performed on a Sephacryl S-200 column 3 x 150 cm (GE healthcare) as described (Bergt et al. Biochem J 2000) (1,214).

3.2.8 Radiometric assay for cholesterol efflux

Porcine BCEC were cultured in collagen-coated (60 µg/ml) 12-well plates (207). The cells (70-80 % confluent) were labeled with 0.5 µCi/ml [^{3}H]-cholesterol in M199 medium during incubation at 37°C for 24 h (1,78). After incubation, cells were pre-incubated with PA 452 or GW 6471 for 15 min and then incubated in the presence of ethanol (vehicle control % 0,05), bexarotene [100 nM], bexarotene in addition to PA 452 or astaxanthin [10 nM], astaxanthin in addition to GW 6471 in SF medium for 16 h at 37°C (PA 452, GW 6471 were applied to verify whether RXR/PPARα activation was involved in cholesterol efflux). Then cells were rinsed and cholesterol acceptors HDL_3 (200 µg/ml) or apoA-I (10 µg/ml) was added in the fresh SF medium (1). From cell supernatants, 200 µl were taken at 90 and 240 min and analyzed on a β-counter. Cells were rinsed with ice-cold PBS and in order to lyse the cells, 0.3 M NaOH over night at

4°C was used. After 24 h, the [^{3}H]-cholesterol radioactivity in the cell lysates was counted, and total cellular protein concentration was quantified using the Qubit fluorometer (Quanti-IT protein assay kit, Invitrogen). Cholesterol efflux was indicated as cpm/mg cell protein in the supernatants relative to the total counts in the supernatants plus cell lysates (1).

3.2.9 Quantification of cellular cholesterol levels

Cells cultured in 6-well plates were incubated in SF medium containing vehicle (ethanol), Bex [100 nM], or Asx [10 nM] for 24 h (1). Cells were rinsed twice with PBS and incubated for 30 min under mild agitation with cholesterol reagent (Greiner Bio-one) in the presence of 5 mg/ml enhancer sodium 3,5-dichloro-2-hydroxybenzenesulfonate (DHB; Sigma Aldrich) (1). A spectrophotometer with Magellan software (Tecan) was used to measure the absorbance at 562 nm and the obtained values were normalized to intracellular protein content (1).

3.2.10 Radiometric assay for cellular cholesterol synthesis and esterification

Porcine BCEC were incubated with [^{14}C]-acetate (2 µCi/mL) in the presence of vehicle control (0.5% ethanol), Bex [100 nM] or Asx [10 nM] in SF medium for 24 h (1). [^{14}C]-acetate incorporated into cellular cholesterol and cholesterol esters was evaluated as previously described (1,108). Cells were rinsed twice in PBS, and in order to extract cellular lipids cell were incubated with n-hexane/isopropanol (3:2, v/v) (2 x 1 ml for 30 min) under gentle agitating at 25°C (1). A stream of nitrogen was used to dry the lipid extracts and further resuspended in 50 µl of chloroform/methanol (2:1, v/v). Aliquots of the samples were counted on a β-counter to obtain total counts/well. Lipid extracts were loaded onto silica thin layer chromatography (TLC) plastic plates (Merck). As a mobile phase, n-hexane/diethylether/acetic acid (70:29:1, v/v/v) was used to separate lipid classes. Standards (Sigma Aldrich) for free and esterified cholesterol (1 mg/ml) were subjected in parallel to TLC plates. Respective lipid spots were stained with iodine vapour, cut out, and radioactivity in free cholesterol and cholesteryl esters was determined by β-counting (Liquid Scintillation Analyzer, Packard). Intracellular protein

content was estimated by the Qubit fluorimeter and the Quant-iT Protein Assay kit, Invitrogen. Total counts per sample were normalized to intracellular protein content (1).

3.2.11 Cellular Aβ uptake assay

Porcine BCEC were seeded in collagen-coated 24-well plates and incubated in the presence of vehicle control (0.5% ethanol), Bex [100 nM] or Asx [10 nM] for 24 h (1). Measurement of Aβ uptake by pBCEC was followed as recently described (1,109). Concisely, 3 µl Alexa Fluor 488 5-TFP were used to label 100 µl of $A\beta_{1-40}$ [1mg/ml] fluorescently in 18 µl carbonate-bicarbonate buffer (incubating 1 h, 37°C) (1). Size-exclusion chromatography on a PD-10 column was used to remove unbound fluorescent dye (108). Characterization by immunoblotting confirmed that Alexa-Aβ secondary structure to be identical to unlabelled $A\beta_{1-40}$ (data not shown). After 24 h, Alexa Fluor 488 labelled $A\beta_{1-40}$ [0.5 µg/ml] was added to cells for 2 h at 37°C, and fluorescence was measured in the cellular supernatants at 490-525 nm using the Promega Glomax detection system (1). In order to lyse the cells, 0.3 M NaOH was added to the wells and cellular protein content was measured using the Qubit fluorometer (Quant-IT protein assay kit) (1,109). Alternatively, in parallel with Aβ transport studies [^{125}I]-$A\beta_{1-40}$ uptake was also determined (see below).

3.2.12 Aβ transcytosis across the *in vitro* BBB model

Porcine BCEC were cultured on collagen-coated [120 µg/ml] 12-well transwell filters, incubated in the presence of vehicle control (0.5% ethanol), Bex [100 nM], or Asx [10 nM] for 24 h in DMEM/Ham's F12 medium containing 1% P/S, 0.25% glutamine and 500 nM hydrocortisone (Sigma Aldrich). In parallel, the increased changes in TEER was measured (1). Aβ transport across the *in vitro* BBB model was determined by adding 0.3 nM of [^{125}I]-$A\beta_{1-40}$ and 100 nM [^{14}C]-sucrose (as paracellular transport control which is not taken up by cells or transcytosed) to the basolateral compartment. Transport of [^{125}I]-$A\beta_{1-40}$ from the basolateral, abluminal ('brain parenchymal') to the apical, luminal ('blood') compartment was assessed after 2 h (1). From each basolateral (input) compartment 100 µl and from each apical (acceptor) compartment 50 µl were taken to count the radioactivity of [^{125}I]-$A\beta_{1-40}$ or [^{14}C]-sucrose using a

gamma (Beckman)- and beta-counter (Packard), respectively. To measure transcytosis of intact [^{125}I]-Aβ_{1-40} to the apical side, 50 µl of apical media were precipitated with 15% TCA and incubated for 10 min at 4°C (to precipitate iodine bound Aβ) (1). Samples were then centrifuged at 10,000x*g* for 10 min at 4°C, and radioactivity associated to pellets was counted on a γ-counter, the supernatant was transferred to a new vial, the same steps were repeated with basolateral samples and uptake of [^{125}I]-Aβ_{1-40} was calculated as the percentage of cpm/mg cell protein in the pellet of cell lysates relative to the cpm/mg of supernatant. To examine the passive diffusion of [^{14}C]-sucrose across the BBB, 50 µl of apical media were counted on a β-counter in 5 ml Ultima Gold scintillation cocktail (1). The transcytosis quotient (TQ) was calculated as described in equation 1 (109):

Equation 1: Transcytosis quotient (TQ)

$$\text{A}\beta\ \text{TQ} = \frac{\frac{[125\text{I}] - \text{A}\beta\ acceptor}{[125\text{I}] - \text{A}\beta\ input}}{\frac{[14C] - \text{sucrose}\ acceptor}{[14C] - \text{sucrose}\ input}}$$

3.2.13 Cytotoxicity assay

The cell proliferation Reagent WST1 from Roche was used for the cytotoxicity assay . In brief, pBCEC were cultured onto collagen-coated [60 µg/ml] 96-well plates. Upon approaching 80-90% confluency, cells were treated for 24 h with vehicle control (0.5% ethanol), Bex [100 nM] or Asx [10 nM] (1). Magellan software (SUNRISE TECAN) was used to measure absorbance of the formazan product photometrically at 450 nm and 650 nm (1).

3.2.14 Reactive oxygen species (ROS) assay

The experiment was performed according to the protocol described by Kozina et al. (215). Porcine BCEC were plated in 12-well plates and treated with control (0.5% ethanol), Bex [100mM] or Asx [10 nM]. Cells were washed once with warm PBS and 600 µL of pre-warmed 10 µM H_2DCFDA/PBS solution for 20 min at 37°C. Cells were then washed once with ice-cold PBS and lysed in 300 µL 3% (v/v) Triton X-100 in PBS for 30 min with shaking on ice in the dark. To improve solubilization of the fluorescent

dye, 50 µl of absolute ethanol was added and the plates were shaken for an additional 15 min. Lysates were transferred to microfuge tubes and cellular debris was removed by centrifugation (13000 rpm, 10 min, 4°C). 100 µl of the supernatants were transferred in duplicates to a black 96-well microtiter plate. Fluorescence was measured at excitation and emission wavelengths of 485 and 530 nm respectively using a Promega glomax detection system (1). Protein contents of the cell lysates were determined using the BCA TM Protein Assay Kit and fluorescence was normalized to protein content (1).

3.2.15 RNA-mediated interference for silencingLRP-1 in pBCEC

Primary pBCEC were cultured in 6-well plates for 3 days to get ~70% confluency. DharmaFECT transfection reagent 1 was used for transfecting the cells according to manufacturer's instructions and as described with minor modifications (1,73). In brief, three targeting siRNAs for target gene LRP-1 (described in Table 6) were mixed in nuclease-free water to access 5 µM stock solutions (1). The stocks were then diluted in SF (SF) medium (1:10), Dharmafect was diluted (1:40) in SF medium, each was incubated for 5 min at RT, diluted stocks and diluted Dharmafect were pooled and incubated for 25 min at RT. Medium in the 6-well plate was replaced to 1.6 ml complete medium (M199, containing 10% horse serum, without antibiotics) (1). Transfection mix (400 µl) was added one drop at a time to each well and incubated for 24 h in 37°C (1). Cells were treated with Bex [100 nM] and Asx [10 nM] for another 24 h in 37°C (1).

3.2.16 Mouse studies

Animal experiments were implemented after ethical approval of the Austrian Department of Science, Research and Economy (approval number 66010/0052-WF/V/3b/2015). 3xTg AD mice, harboring the mutant genes APP_{Swe}/$MAPT_{P301L}$/$PSEN1_{M146V}$ were from the Jackson Laboratory. Progressively generated plaques and tangles are present in the brains of these mice (1,216). Female mice were used in the study since they were reported to form significantly larger Aβ burden and behavioral deficits compared to age-matched males (1,217,218). Female 3xTg AD and non-transgenic C57/BL6 (non-Tg) mice were kept at a 12 h light/12 h dark cycle in a humidity- and temperature-controlled environment and given ad libitum

access to food and water (Ssniff, Germany). Before treatment, blood was collected from the submandibular vein (1).

Two individual studies were performed:

In *study I*, younger than 1-year-old (32-49 weeks old) female 3xTg AD mice were gavaged for 6 days with vehicle (10% DMSO in corn oil, [v/v]; vehicle control group, n=10), Bex (100 mg/kg in DMSO/corn oil; n=9), or Asx (80 mg/kg in DMSO/corn oil; n=8) and compared to non-Tg mice (37-49 weeks; n=5 for vehicle control group; n=6 for Bex; n=7 for Asx) (1).

In *study II*, aged (68-92 weeks old) female 3xTg AD mice were gavaged for 6 days with vehicle (n=8), Bex (100 mg/kg; n=6), or Asx (80 mg/kg; n=8). Body weights were taken ahead of treatment, at day 4, and before scarification (1).

On day 7, mice were fasted for 6 h prior to sacrification using a gentle CO_2 stream (1). EDTA blood samples were taken via cardiac puncture and plasma lipids were measured enzymatically using colorimetric assay kits (DiaSys Diagnostic Systems) (1). Murine brains were removed from the skull and divided into two hemispheres. One hemisphere was sliced into 3 pieces, two were frozen for protein and RNA isolation at -20°C, the third one was snap frozen and stored at -70°C for immunostaining. The other hemisphere was pooled with up to three hemispheres from mice of the same group, and mBCEC were isolated (see below) on the day of scarification (1).

3.2.17 Isolation of murine brain capillary endothelial cells (mBCEC)

One hemisphere of each animal was used (109) and 3 hemispheres were pooled to isolate mBCEC. In brief, the hemispheres were washed in PBS (pH 7.4, containing 2% P/S) and the olfactory bulb was removed. Scalpel and douncer were used to mince the grey and white matter of the cortex. To isolate capillaries, the homogenate was mixed with dispase (10 mg/3 hemispheres) in 5 ml MCDB131 medium (containing 2% FBS, 1% L-glutamine and 1% P/S), and incubated at 37°C in the water bath for 1 h. After adding dextran (5 ml), the suspension was centrifuged (10,000x*g*, 10 min, 4°C) and the pellet was resuspended in 5 ml medium and filtered through a nylon mesh (180 µM). In order to disrupt capillaries and removing the basement membrane and adhering pericytes (219), 40 µl collagenase/dispase (1 min in a water bath) was supplemented, the suspension filled up to 5 ml medium and centrifuged (900 rpm, 5 min, 25°C). Endothelial cells were harvested using a Percoll bi-phase gradient as

referred above for pBCEC. Cells were rinsed with PBS and stored at -20°C for protein and RNA isolation. RT-qPCR for mRNA expression of cell-specific markers was performed to prove the purity of isolated mBCEC. These markers such as cluster of differentiation 31 (CD31) for endothelial cells, aminopeptidase N (CD13) and beta-type platelet-derived growth factor receptor (PDGFRβ) for pericytes, glial fibrillary acidic protein (GFAP) for astrocytes, synaptophysin (SYP) for neurons, ionized calcium-binding adaptor molecule 1 (IBA1) for microglia, and smooth muscle actin (SMA) for smooth muscle cells The lack of CD13 or PDGFRβ mRNA demonstrated the absence of pericytes in the isolated mBCEC fraction, which was highly enhanced in CD31 identifying endothelial cells (1).

3.2.18 Immunofluorescent staining on mouse brain cryosections

Mouse brain 18 µm cryosections were used for staining. Before immunofluorescent staining, sections were fixed in cold acetone (5 min) and air-dried (20 min). Sections were rinsed with TBST (pH7.4) and subsequently blocked with Ultra-V block (7 min) and following incubation with polyclonal rabbit anti-Aβ, A11 (Ab9234, 8 µg/ml) or mouse anti-β-Amyloid (6E10, 5 µg/ml, SIG-39320) as primary antibodies for 1 h at 25°C. In order to reduce background in staining, primary antibodies were diluted with Dako antibody diluent. Sections were washed for 5 min with TBST. As secondary antibody, goat anti-rabbit Cy-3 (red, 1.88 µg/ml, 30 min) was applied. All incubation procedures were performed in a dark moist chamber at 25°C. Slides were rinsed by TBST, for nuclear staining DAPI was added to the slides (20 min). Sections were rinsed again with TBST and mounted with Vectashield mounting medium. A Leica DM4000 B microscope (Leica Cambridge Ltd) supplied with Leica DFC 320 video camera was used to acquire and analyse computerized images of all sections and cells. As negative control Non-immune rabbit IgG was used (1).

3.2.19 BCEC double-staining of mouse brain cryosections

Double staining of vWF (a specific endothelial cell marker) and Aβ was performed on 18 µm cryosections of mouse brain samples (1). In advance of immunofluorescence staining, tissue sections were fixed with 4% paraformaldehyde (10 min), rinsed in distilled water. All incubations were carried out at 25°C. Sections were washed with

TBST (pH 7.4) then, blocked with donkey serum (1 h) and incubated with primary antibody (1 h at 25°C). Rabbit anti-vWF (0.16 µg/ml) and mouse anti-β-Amyloid (6E10, 5 µg/ml) antibodies were applied. All incubation steps were performed in a dark moist chamber at 25°C. Slides were rinsed by TBST and then, as secondary antibodies donkey anti-mouse Cy-3 (red, 1.88 µg/ml) and donkey anti-rabbit Dylight 488 (green, 1.66 µg/ml) were used (30 min). Slides were rinsed again with TBST and for nuclear staining, DAPI was added (20 min). Sections were rinsed again with TBST and mounted with vectashield mounting medium. As negative controls, non-immune mouse or rabbit IgG were used (1). A Leica DM4000 B microscope (Leica Cambridge Ltd) equipped with Leica DFC 320 video camera was used to take and analyse computerized images of sections and cells.

3.2.20 Immunohistochemistry on paraffin-embedded mouse brain sections

Studies were carried out on 4% paraformaldehyde fixed, paraffin-embedded mouse brain hippocampus tissue sections (5 µm) (1). Slides were deparaffinised in xylene, and rehydrated with decreasing concentrations of ethanol according to standard methods. Antigen retrieval was used for tissue sections submerged in 10 mM sodium citrate buffer (0.05% Tween 20, pH 6.0) and microwaved for 10 min in a domestic microwave oven. Slides were allowed to cool for 45 min at 25°C prior to immunohistochemistry.

Immunohistochemistry was performed using the ultravision LP detection system (Thermo Scientific) according to the manufacturer's suggestions. Sections were washed with 0.01 M PBS (pH 7.4) and then blocked with hydrogen peroxide for 12 min and UV treatment for 7 min. Sections were then incubated for 1 h at 25°C with mouse anti-β-Amyloid (6E10, 5.0 µg/ml) as the primary antibody. Primary antibody enhancer (30 min) and HRP-polymer (20 min) were added; then sections were incubated with 3-amino-9-ethylcarbazol (Thermo Fisher) for 10 min. As a negative control, non-immune mouse IgG was used. All sections were rinsed with PBS in between each incubation steps. Sections were counterstained with Mayer's Hematoxylin and mounted with Kaiser's glycerol gelatin (Merck Corp). To acquire and analyze computerized images of respective sections, an Aperio ImageScope (Leica Biosystems) was used to scan all images (1).

3.2.21 Aβ extraction from mouse brains

Frozen brain cortical hemispheres from female 3xTg AD mice and wild-type C57BL6 mice (non-Tg) were utilized (1). Extraction of both soluble proteins such as (DEA: Aβ isoforms, APP) and insoluble (FA: Aβ isoforms associated with plaques) were performed explicitly as defined (1,220). Shortly, brain (250 µl) were mechanically homogenized and blended with 0.4% DEA solvent (250 µl), (DEA: 1 ml of 5 M NaCl and 50 ml of ddH_2O) and centrifuged at (135,000 rpm,1 h at 4°C), the supernatant (425 µl) was neutralized with 0.5 M Tris-HCl (42.5 µl) and saved at -80°C. The pellet was sonicated on ice for 1 min in 95% FA for ~20 s with 15 mA amplitude until the pellet dissolved, centrifuged at 109,000 rpm for 1 h at 4°C. FA neutralization buffer (1 M Tris, 0.5 M Na_2HPO_4 and 0.05% NaN_3) was used to neutralize the supernatant (105 µl) and the samples were stored at -80°C. Immunoblotting was performed to classify Aβ species and to assess the amyloid burden in mice (1).

3.2.22 Immunoblotting for insoluble (FA) and soluble (DEA) Aβ fraction

Insoluble (FA) and soluble (DEA) Aβ fractions from murine whole brains were extracted as described under (3.2.21). For both fractions, 12% NuPage (Thermo Fisher) gels and MES buffer (ThermoFisher) for electrophoresis were used. Immunoblotting was performed using Tris-glycine buffer (25 mM Tris, 0.5 M glycine, 20% methanol) and nitrocellulose membrane (GE Healthcare Protran BA83) for 3 h, 50 mA at 4°C. Subsequently, membranes were stained with Ponceau S. In order to unfold respective epitopes, membranes were heated for 5 min in PBS in a microwave oven and blocked (5% milk powder, 1x TBS) for 1 h (1). Blots were incubated with primary antibody 6E10 (1:750) and secondary antibody goat-anti-mouse IgG-HRP was used. ECL was used for detecting chemiluminescent signals and blots were imaged by using a ChemiDoc system (Bio-Rad). ImageLab software (version 5.2.1, Bio-Rad) was applied for quantification of Immunoreactive bands (1).

3.2.23 Nissl staining on mouse brain cryosections

Staining was carried out on 18 µm cryosections from mouse brains (hippocampus). Initially, sections were fixed in 4% paraformaldehyde for 15 min and then stained with 0.1% thionine for 5 s. Sections were washed with ddH_2O. Slides were dehydrated and mounted with permount. To acquire and analyze computerized images of sections, a Motic microscope (MOTIC Deutschland GmbH) equipped with Moticam Pro 285B camera was used (1).

3.2.24 Statistical analysis

Experiments were performed at least three times in triplicates and data are indicated as means±SEM unless stated variously. Statistical significances (*p≤0.05; **p≤0.01; ***p≤0.001; ****p≤ 0.0001) were defined by one-way or two-way ANOVA performed by using Prism 6 software (Graphpad version 6) (1).

4. Results

Parts of this chapter have been literally published in:
Fanaee-Danesh E, Gali CC, Tadic J, Zandl-Lang M, Carmen Kober A, Agujetas VR, et al. Astaxanthin exerts protective effects similar to bexarotene in Alzheimer's disease by modulating amyloid-beta and cholesterol homeostasis in blood-brain barrier endothelial cells. Biochim Biophys Acta Mol Basis Dis. 2019 Sep 1;1865(9):2224–45 (1).

4.1 Asx and Bex shift APP processing towards the non-amyloidogenic pathway in pBCEC

Although pathological functions of APP are not well understood, several observations have shown that APP may contribute to cellular stress as well as inflammation at the vascular barrier (221,222). Endothelial cells express APP which regulates immune cell adhesion and stimulates a tyrosine kinase-dependent response in endothelial cells (223), Platelet APP can also inhibit a blood coagulation factor (224). Thus, APP-mediated events may contribute to the pathogenesis of cerebrovascular disease and AD.

To investigate effects of both compounds on mRNA expression levels of APP, pBCEC were treated for 24 h with vehicle (0.5% ethanol), Bex [10 and 100 nM] or Asx [1 and 10 nM]. APP mRNA levels with Bex [10 nM] by 1.2±0.04-fold, and with Bex [100 nM] by 2.2±0.10-fold was dose-dependently upregulated **(Figure 7A).** One-way ANOVA for treatment revealed a significant effect ($p<0.0001$). Significantly elevated APP mRNA levels with Asx [1 nM] by 1.2±0.04-fold and with Asx [10 nM] by 1.7±0.04-fold **(Figure 7B)** ($p=0.0008$) was observed (1).

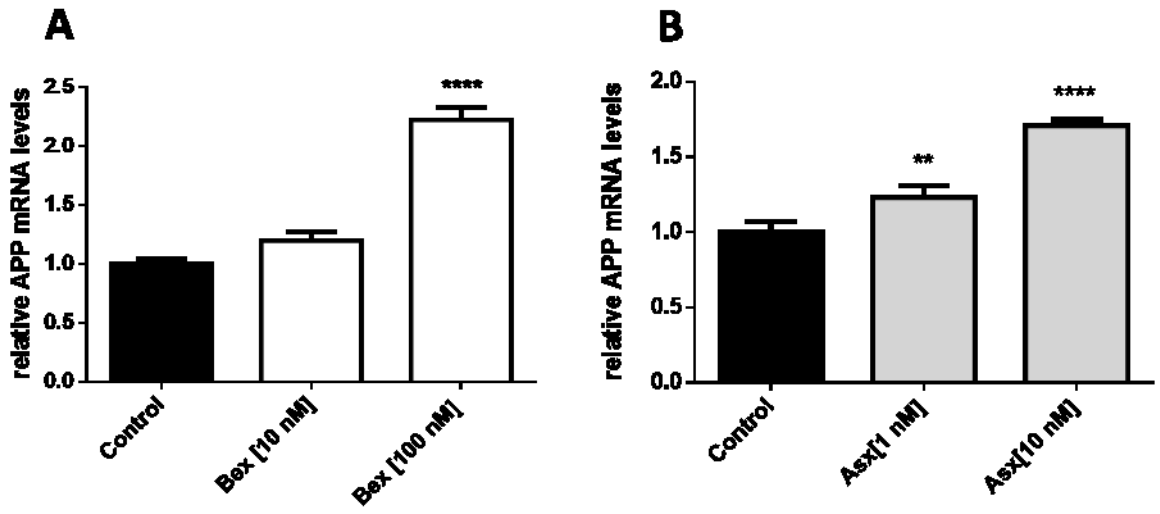

Figure 7: Bex and Asx increase APP mRNA expression in pBCEC

(A-B) Porcine BCEC cultured on 6-well plates were incubated with 0.5% ethanol (vehicle control), Bex [10 and 100 nM] or Asx [1 and 10 nM]. Total RNA was isolated, reverse-transcribed, and subjected to qPCR analysis using SYBR Green technology and HPRT1 as house-keeping gene. The $^{\Delta\Delta}$Ct method was applied to quantify relative mRNA expression levels of *APP*. Data shown are mean±SEM of 3 independent experiments performed in triplicates (***p≤0.001; ****p≤0.0001 vs controls). [Reproduced from Fanaee-Danesh E et al. with permission of Biochim Biophys Acta Mol Basis Dis. (1)].

Soluble amyloid precursor protein-α (sAPP-α) has a proposed significant therapeutic potential as AD prophylactics and therapeutics (225,226). The level of endogenous sAPP-α may be suppressed by various factors such as physical inactivity, abnormal glucose metabolism, abnormal lipid metabolism and oxidative stress (227).

sAPP-α may reduce Aβ generation by directly binding to BACE1 and thereby modulate APP processing, since in sAPP-α overexpressing AD transgenic mice, a reduction of Aβ plaques and soluble Aβ was reported (226). In addition, sAPP-α immunoneutralization imposed APP amyloidogenic processing in these mice. These findings together suggest that low levels of sAPP-α in brain of AD patients may cause a polarization of APP processing toward the amyloidogenic, Aβ-producing route. When analyzing amounts of sAPP-α secreted by pBCEC, TCA-precipitated protein levels of sAPPα were increased with Bex [100 nM] by 5.9±0.92 (p=0.0079) **(Figure 8A)**with Asx [10 nM] treatments by 7.7±1.65 (p=0.0004) **(Figure 8B)**. This suggests that both compounds could considerably promote the non-amyloidogenic pathway of APP processing (1).

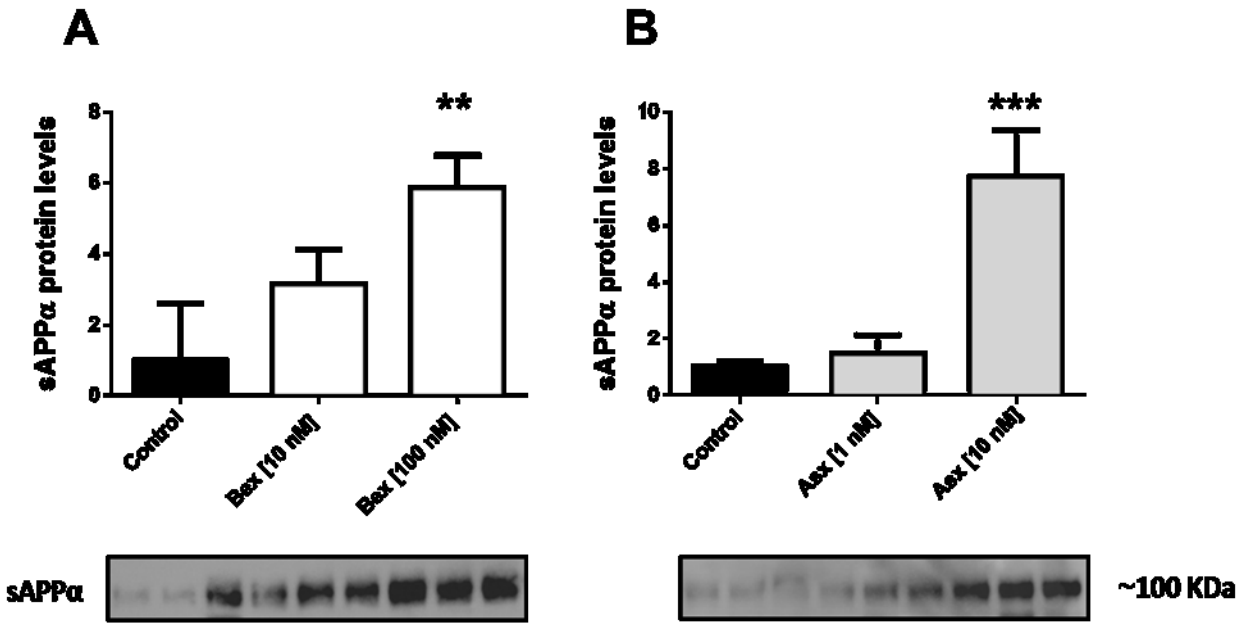

Figure 8: Bex and Asx enhance sAPPα protein levels in pBCEC

(A-B) Proteins were extracted from cells and TCA-precipitated from supernatants, separated by SDS-PAGE, and levels of secreted sAPPα (normalized to Ponceau stained bands) were detected by immunoblot experiments using 6E10 as primary antibody. One representative blot out of 3 is shown. The graphs represent densitometric analysis, data shown are mean±SEM of 3 experiments performed in triplicates (**p≤0.01; ***p≤0.001 vs controls). [Reproduced from Fanaee-Danesh E et al. with permission of Biochim Biophys Acta Mol Basis Dis (1)].

Several enzymes in the “a disintegrin and metalloprotease” (ADAM) family, including ADAM9, ADAM10, and ADAM17 have α-secretase activity, although recent studies have demonstrated that ADAM10 is the major α-secretase that cleaves APP in the brain (228). BACE1 competes with ADAM10 for cleavage of APP substrate, such that enhanced BACE1 activity causes decreased α-secretase processing of APP and higher Aβ generation and vice versa. This observation implys that increased ADAM10 activity should be expected to decrease Aβ production and AD pathogenesis.

When we next analysed effects on ADAM10 expression, a significant increase in relative ADAM10 mRNA levels in response to treatments with Bex 1.5±0.20-fold at [10 nM], 1.8±0.18-fold at [100 nM]) **(Figure 9A)** (p=0.0435), as well as Asx (1.6±0.11-fold

at [1 nM] and 2.2±0.03-fold at [10 nM]) **(Figure 9B)** (p=0.0001) was observed, supporting enhanced non-amyloidogenic APP processing on the enzyme level (1).

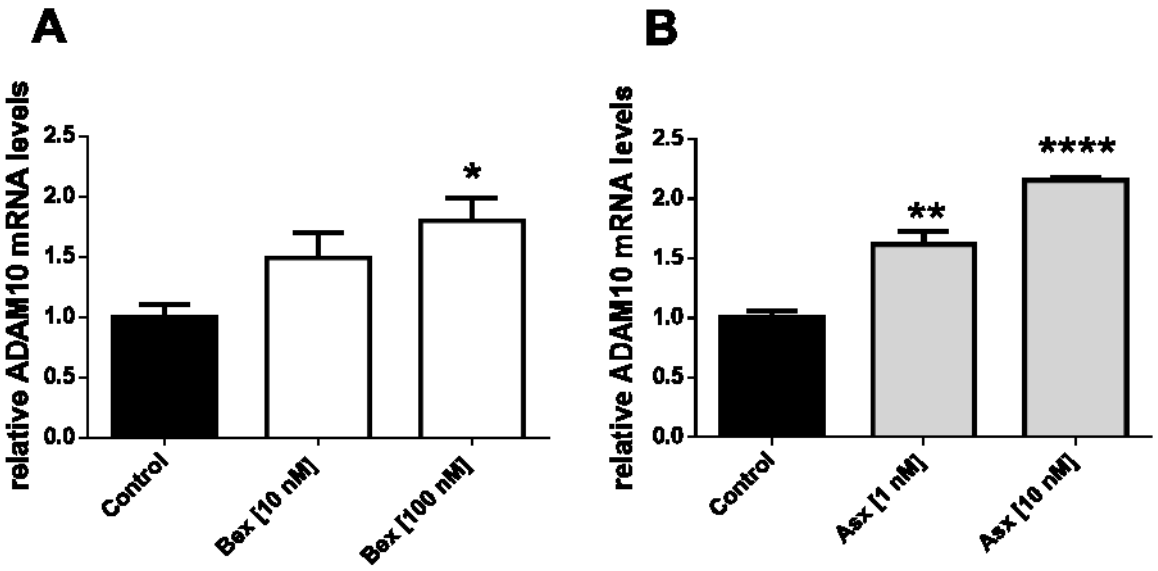

Figure 9: Bex and Asx elevate ADAM10 mRNA expression in pBCEC

(A-B) Primary pBCEC cultured on 6-well plates were incubated with 0.5% ethanol (vehicle control), Bex [10 and 100 nM] or Asx [1 and 10 nM]. Total RNA was isolated, reverse-transcribed, and subjected to qPCR analysis using SYBR Green technology and HPRT1 as house-keeping gene. The $^{\Delta\Delta}$Ct method was applied to quantify relative mRNA expression levels of *ADAM10*. Data shown are mean±SEM of 3 independent experiments performed in triplicates (*p≤0.05; **p≤0.01; ****p≤0.0001 vs controls). [Reproduced from Fanaee-Danesh E et al. with permission of Biochim Biophys Acta Mol Basis Dis (1)].

On the other side, APP proteolytic cleavage by β-site APP cleaving enzyme 1 (BACE1) leads to Aβ generation. Aβ reduction by chemical inhibition of BACE1 was reported in human trials and in animal studies (229). To date, inhibition of BACE1 activity appears to be one of the most promising targets for the treatment of AD patients.

Interestingly, BACE1 mRNA expression was down-regulated upon treatment with Bex [10 nM] 19±15.4% Bex [100 nM] **(Figure 10A)** (p=0.0007), with Asx [1 nM] by 17±0.6% and Asx [10 nM] by 22±1.5% **(Figure 10B)** (p=0.0092). Accordingly, total BACE1 activity was also significantly reduced upon treatment of pBCEC with Bex [100 nM] by 17±0.6% or Asx [10 nM] by 17±0.8% **(Figure 10C)** (p=0.0156) (1).

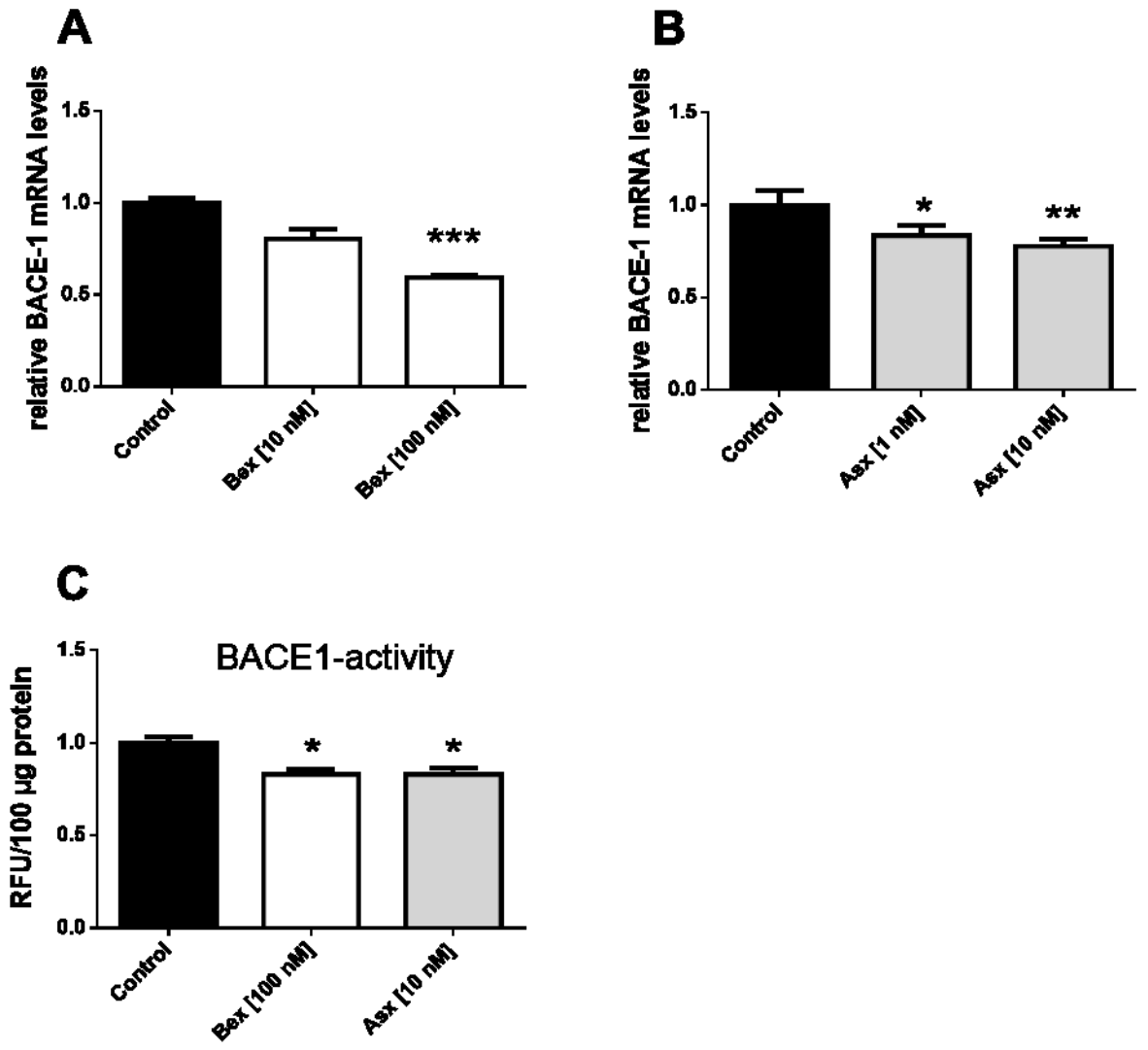

Figure 10: Bex and Asx down-regulate BACE-1 mRNA expression and reduce BACE1-activity in pBCEC

(A-B) Primary pBCEC cultured on 6-well plates were incubated with 0.5% ethanol (vehicle control), Bex [10 and 100 nM] or Asx [1 and 10 nM]. Total RNA was isolated, reverse-transcribed, and subjected to qPCR analysis using SYBR Green technology and HPRT1 as house-keeping gene. The $^{\Delta\Delta}$Ct method was applied to quantify relative mRNA expression levels of *BACE-1*. Data shown are mean±SEM of 3 independent experiments performed in triplicates (*p≤0.05; **p≤0.01; ***p≤0.001; vs controls). **(C)** Primary pBCEC cultured in 25 cm² flasks were incubated with 0.5% ethanol (control), Bex [100 nM] or Asx [10 nM] for 24 h. BACE-1 activity was measured by using the fluorometric BACE-1 activity assay kit (Abcam) using 100 µg of total protein Data represent mean±SEM from 3 experiments with different cell preparations performed in duplicates (*p≤0.05 vs controls). [Reproduced from Fanaee-Danesh E et al. with permission of Biochim Biophys Acta Mol Basis Dis (1)].

In addition to increased production, impaired clearance of Aβ contributes to the development of AD (230). In a mouse model of AD, it has been demonstrated that treatment with LXR agonists elevated levels of apoE and ABCA1, which correlated with cognitive improvements and lowered Aβ deposition (231).

Similarly, PPARγ activation can promote the degradation of Aβ and increase apoE and ABCA1 levels (232).

We treated pBCEC for 24 h with vehicle (0.5% ethanol), Bex [10,100 nM] or Asx [1,10 nM]. As expected in pBCEC, immunoblotting for Aβ oligomers revealed a prominent band at ~38 kDa (109), which was markedly reduced in response to Bex [100 nM] by 36±3.7% **(Figure 11A)** ($p=0.0343$) and Asx [10 nM] by 69±4.7% **(Figure 11B)** ($p=0.0166$) (1). These *in vitro* results demonstrate that both drugs prevent Aβ/oligomer production in pBCEC while stimulating non-amyloidogenic APP processing in parallel (1).

Strikingly, a prominent 6E10-reactive APP/Aβ species ~80 KDa band was detected in vehicle-treated pBCEC lysates (and APP/Aβ species not cross-reacting with C-terminal APP antibody, data not shown). This band was markedly reduced by Bex [100 nM] by 90±0.01% **(Figure 11C)** ($p<0.0001$) and almost completely dissipated upon treatment with Asx [10 nM] **(Figure 11D)**. These *in vitro* results demonstrate that both drugs significantly inhibit Aβ production in pBCEC while promoting non-amyloidogenic APP processing in parallel (1).

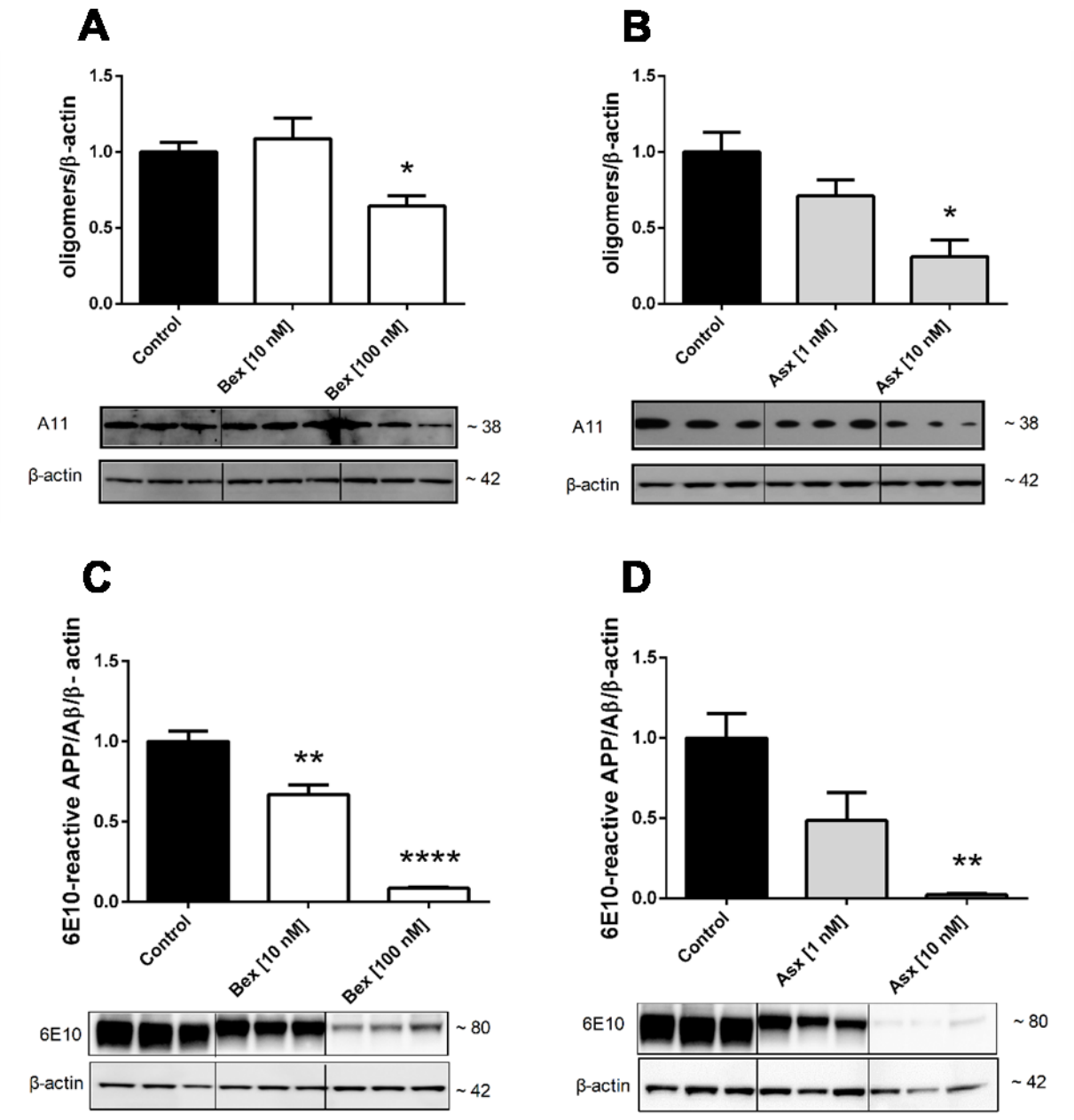

Figure 11: Bex and Asx reduce Aβ oligomers and an ~80 kDa 6E10-reactive APP/Aβ species in pBCEC

(A-B) Proteins were extracted from pBCEC, separated by SDS-PAGE, and levels of Aβ oligomers (normalized to β-actin levels) were detected by immunoblot experiments using A11 as primary antibody. β-actin was used as loading control. One representative blot out of 3 is shown. The graphs represent densitometric evaluation, data shown are mean±SEM of 3 experiments performed in triplicates (*p≤0.05 vs controls). **(C-D)** Proteins were extracted from pBCEC, separated by SDS-PAGE, and levels of Aβ species (normalized to β-actin levels) were detected by immunoblot experiments using 6E10 as primary antibody. β-actin was used as loading control. Data shown are mean±SD of one representative experiment out of two performed in triplicates (**p≤0.01 ; ****p≤0.0001 vs controls). [Reproduced from Fanaee-Danesh E et al. with permission of Biochim Biophys Acta Mol Basis Dis (1)].

4.2 Bex and Asx up-regulate genes/proteins responsible for cholesterol transport and metabolism in pBCEC

The role of apoA-I -containing HDL in cholesterol efflux from lipid-loaded cells *in vitro* has been shown long time ago (233,234). A deceleration in cholesterol removal has been reported in apoA-I-deficient mice (235). Oxidized apoA-I has a restricted capacity to mediate cholesterol efflux in plasma (236). Moreover, the lipidation state of lipoproteins can alter their affinity for lipid transporters. Lipid-poor apoA-I is a substantial determinant of ABCA1-mediated efflux to plasma.

We next investigated mRNA expression of apoA-I. Primary pBCEC were treated for 24 h with vehicle (0.5% ethanol), Bex [10 and100 nM]. Treatment with Bex [10 nM] and [100 nM] dose-dependently increased apoA-I mRNA levels by 1.3±0.09 and by 2.0±0.07-fold (p=0.0002) **(Figure 12A)**. Immunoblotting of TCA-precipitated proteins from the supernatants revealed that levels of secreted apoA-I were increased upon Bex treatment [100 nM] by 2.7±0.24 (p=0.0034) **(Figure 12C)** however, Asx had neither an effect on apoA-I mRNA expression nor on protein levels **(Figure 12B,D)** (1).

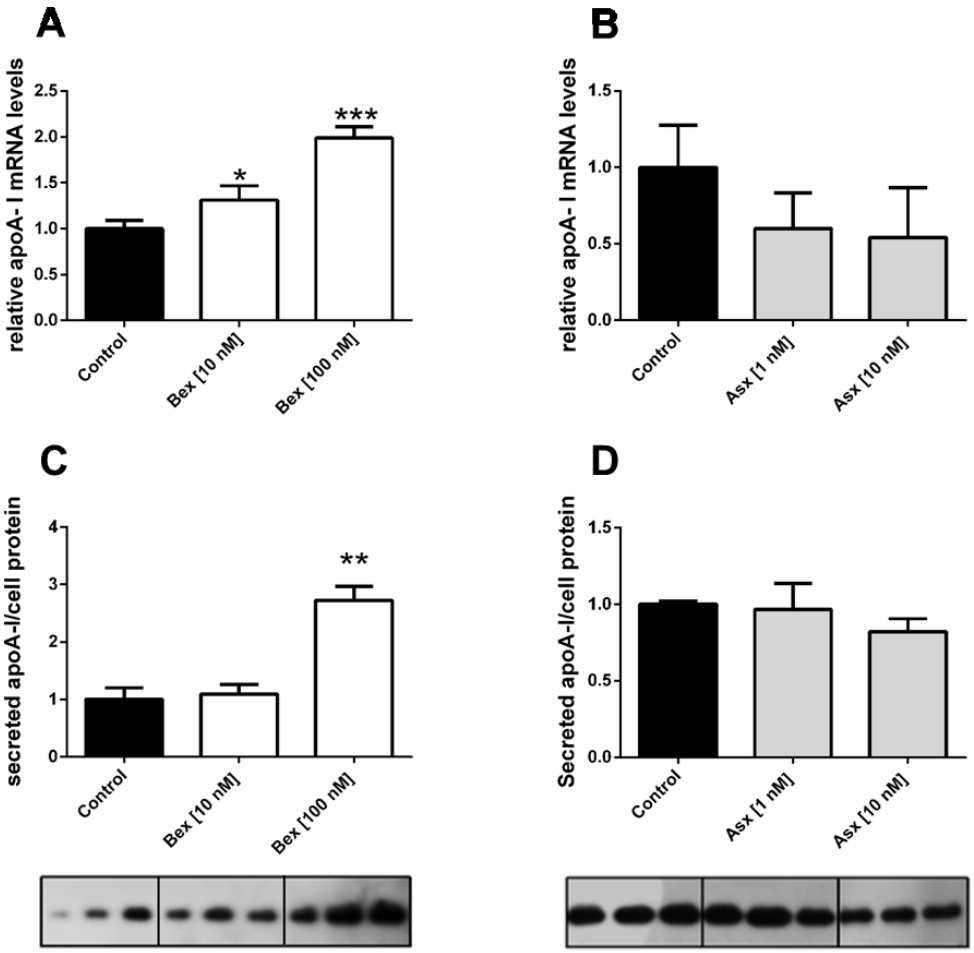

Figure 12: Bex but not Asx enhances apoA-I mRNA and protein levels

(A-B) Primary pBCEC cultured on 6-well plates were incubated with 0.5% ethanol (vehicle control), Bex [10 and 100 nM] or Asx [1 and 10 nM] for 24 h. Total RNA was isolated, reverse-transcribed, and subjected to qPCR analysis using SYBR Green technology and HPRT1 as house-keeping gene. The $^{\Delta\Delta}$Ct method was applied to quantify relative mRNA expression levels. Data shown are mean±SEM of 3 independent experiments performed in triplicates (*p≤0.05; ***p≤0.001 vs controls). **(C-D)** Proteins were extracted from cells and TCA-precipitated from supernatants, separated by SDS-PAGE, and levels of secreted apoA-I (normalized to total protein content) were detected by immunoblot experiments using anti-ABCA1 as primary antibodies. β-Actin was used as loading control. One representative blot out of 3 is shown. The graphs represent densitometric analysis, data shown are mean±SEM of 3 experiments performed in triplicates (**p≤0.01 vs controls). [Reproduced from Fanaee-Danesh E et al. with permission of Biochim Biophys Acta Mol Basis Dis (1)].

The outcomes of animal and human studies indicate that ABCA1-mediated cholesterol transport is exquisitely important in AD. Thus, mutation in ABCA1 were associated with a higher risk for AD (237). Elevated amyloid deposition was observed in APP23 mice with disrupted ABCA1 (238). In one study, the essential role of ABCA1 was shown to

clear hippocampal soluble Aβ and to ameliorate cognitive deficits in AD mice (239). Cellular cholesterol efflux supported by the apoA-I- or apoE/ABCA1-mediated pathway has also been reported to alter secreted Aβ levels (240). Thus, aggravated ABCA1 expression lowered Aβ levels in an AD mouse model (71) and ABCA1 deficit led to more Aβ deposition (241). Importantly, in an *in vitro* model of human BCEC, increased ABCA1 expression and stimulation of cholesterol efflux by Bex treatment has been also recorded (242) (1).

We next investigated mRNA expression of ABCA1. Primary pBCEC were treated for 24 h with vehicle (0.5% ethanol), Bex [10 and 100 nM], Asx [1 and 10 nM]. Bex also upregulated ABCA1 mRNA levels by 2.3±0.15-fold at [10 nM] and 3.8±0.36-fold at [100 nM] **(Figure 13A)** (p=0.0005). Similarly, Asx [10 nM] dose-dependently upregulated ABCA1 on mRNA levels by 2.7±0.20-fold **(Figure 13B)** (p=0.0010) (1).

A pronounced increase in ABCA1 protein expression levels in response to Bex [10 nM] by 4.8±0.60-fold and [100 nM] by 4.8±0.40-fold, respectively, was observed **(Figure 13C)** (p=0.002). Similarly, Asx increased ABCA1 protein expression levels: at low Asx concentrations [1 nM] by 2.5±0.78-fold while at higher Asx concentrations [10 nM] by 3.9±0.38-fold **(Figure 13D)** (p=0.0277) (1).

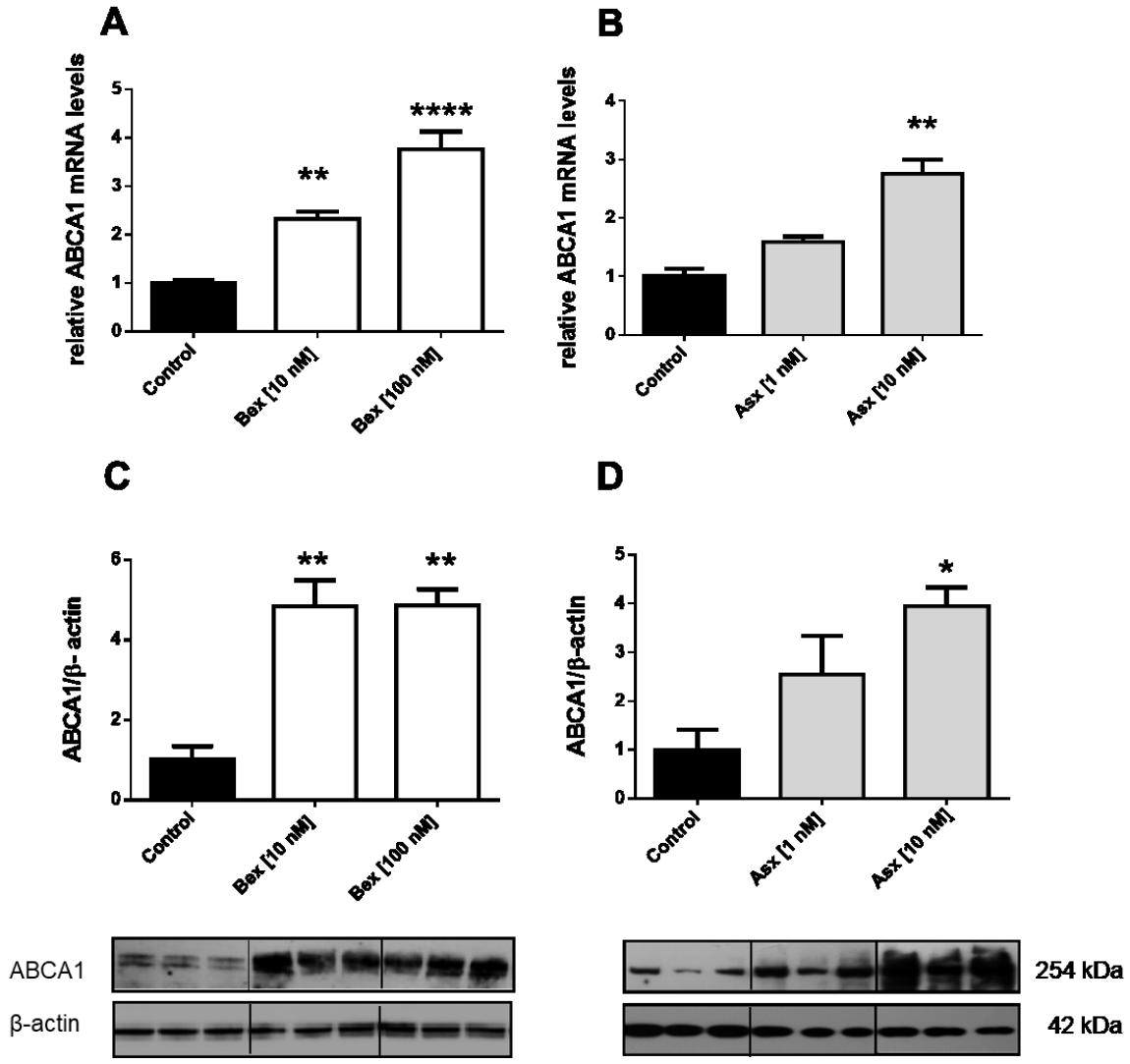

Figure 13: Bex and Asx enhance ABCA1 mRNA and protein levels in pBCEC

(A-B) Primary pBCEC cultured on 6-well plates were incubated with 0.5% ethanol (vehicle control), Bex [10 and 100 nM] or Asx [1 and 10 nM] for 24 h. Total RNA was isolated, reverse-transcribed, and subjected to qPCR analysis using SYBR Green technology and HPRT1 as house-keeping gene. The $^{\Delta\Delta}$Ct method was applied to quantify relative mRNA expression levels. Data shown are mean±SEM of 3 independent experiments performed in triplicates (**p≤0.01; ****p≤0.0001 vs controls). **(C-D)** Proteins were extracted from cells and TCA-precipitated from supernatants, separated by SDS-PAGE, and levels of ABCA1 (normalized to total protein content) were detected by immunoblot experiments using anti-ABCA1 as primary antibodies. β-Actin was used as loading control. One representative blot out of 3 is shown. The graphs represent densitometric analysis, data shown are mean±SEM of 3 experiments performed in triplicates (*p≤0.05; **p≤0.01 vs controls). [Reproduced from Fanaee-Danesh E et al. with permission of Biochim Biophys Acta Mol Basis Dis (1)].

ABCG1, the cholesterol transporter, facilitates cholesterol efflux to HDL and is expressed in the brain, consequently influencing the brain cholesterol biosynthetic pathway especially in the adjustment of neuronal cholesterol efflux to apoE and in the restriction of APP processing to generate Aβ peptides (240). The function of ABCG1 in pBCEC has been recently characterized in our laboratory (73).

We therefore investigated mRNA expression of ABCG1 upon Bex and Asx incubations. Primary pBCEC were treated for 24 h with vehicle (0.5% ethanol), Bex [10 and 100 nM], Asx [1 and 10 nM]. Treatment of pBCEC with Bex [100 nM] elevated ABCG1 mRNA expression by 2.9±0.99 fold **(Figure 14A)** (p=0.0219) and with Asx [10 nM] slightly upregulated ABCG1 mRNA expression by 1.2±0.03 fold **(Figure 14B)** (p=0.0034). Unexpectedly, treatment of cells with either Asx or Bex had no significant effect on ABCG1 protein expression **(Figure 14C, D)** (1).

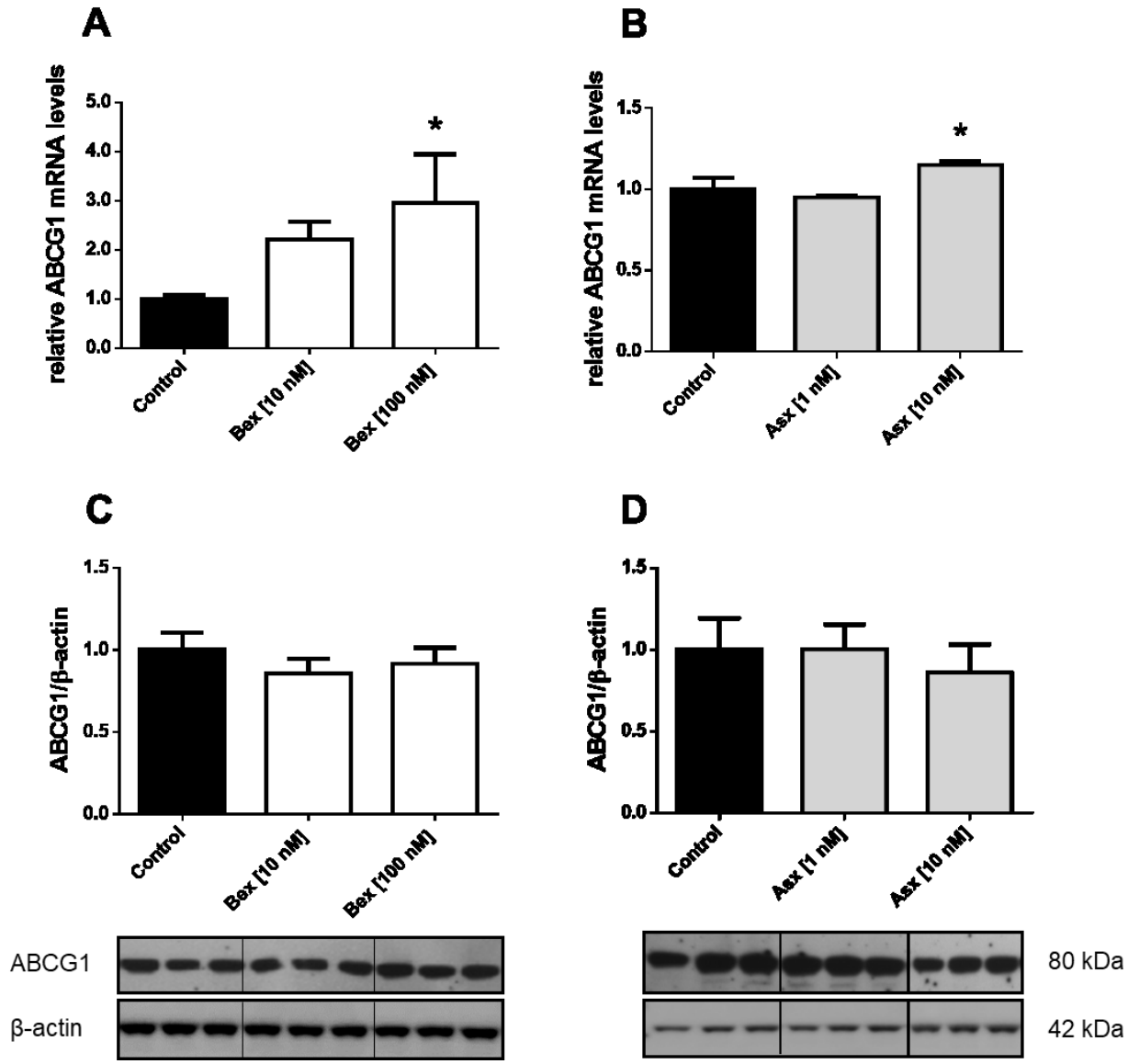

Figure 14: Bex and Asx enhance ABCG1 mRNA but not protein levels

(A-B) Primary pBCEC cultured on 6-well plates were incubated with 0.5% ethanol (vehicle control), Bex [10 and 100 nM] or Asx [1 and 10 nM] for 24 h. Total RNA was isolated, reverse-transcribed, and subjected to qPCR analysis using SYBR Green technology and HPRT1 as house-keeping gene. The $^{\Delta\Delta}$Ct method was applied to quantify relative mRNA expression levels. Data shown are mean±SEM of 3 independent experiments performed in triplicates (*p≤0.05 vs controls). **(C-D)** Proteins were extracted from cells and separated by SDS-PAGE, ABCG1 (normalized to β-actin levels) were detected by immunoblot experiments using anti-ABCG1 as primary antibody. β-actin was used as loading control. One representative blot out of 3 is shown. The graphs represent densitometric evaluation of immunoreactive bands. Data shown are mean±SEM (n=3, performed in triplicates). [Reproduced from Fanaee-Danesh E et al. with permission of Biochim Biophys Acta Mol Basis Dis (1)].

4.3 Bex and Asx enhance cholesterol release implicating PPARα- and RXR-mediated activation and suppress cholesterol synthesis in pBCEC

The human brain is the largest source of cholesterol in the body, and cholesterol dyshomeostasis was shown in the pathology of AD (243). In particular, the cholesterol content in neurons is dysregulated in AD, as constant neuronal damage may increase cholesterol biosynthesis (244).

We next studied effects of Bex and Asx on cellular cholesterol release to two cholesterol acceptors, namely apoA-I and HDL_3 and explored a potential contribution of nuclear receptor-dependent mechanisms by applying PPARα- and RXR-antagonists. We verified cholesterol efflux ability of pBCEC which were prelabelled with [^{3}H]-cholesterol for 24 h and pre-incubated with either antagonist (15 min) ahead of treatment with vehicle (0.5% ethanol), Bex [100 nM], Bex [100 nM] and RXR antagonist PA 542 [10 µM], Asx [10 nM], Asx [10 nM] and PPARα antagonist GW 6471[10 µM]. ApoA-I [10 µg/ml] or apoE-free HDL_3 [200 µg/ml] were added as cholesterol acceptors to the SF culture media. Hereupon, results acquired were consistent with the elevated ABCA1 (and ABCG1 mRNA) expression: Bex [100 nM] stimulated cholesterol efflux to apoA-I by 3.5-fold and 7.1-fold at 90 and 240 min, respectively. Two-way ANOVA revealed a significant effect of treatment ($p \leq 0{,}0001$) when compared to control cells (1). Treatment with Bex and PA 542 partially reversed this effect. Cholesterol efflux in the presence of the RXR antagonist versus untreated controls was still augmented, albeit to lower extent by (2.5-fold and 3.45-fold at 90 and 240 min; p=0.0009) **(Figure 15A)** (1).

Asx [10 nM] rised cholesterol efflux to apoA-I by 1.3-fold and 1.6-fold at 90 and 240 min when compared to untreated control cells (p=0.0004). Treatment with Asx and GW 6471 was not significantly different from untreated control cells (p=0.4888) **(Figure 15B)**, indicating that Asx induced cholesterol efflux via PPARα activation in pBCEC (1).

Bex [100 nM] also enhanced cholesterol efflux to HDL_3 particles by 2-fold and 1.7-fold at 90 and 240 min when compared to untreated control cells (p=0.007), whereas cholesterol release after treatment with Bex and PA 542 was not significantly elevated when compared to untreated control cells (p=0.2789) **(Figure 15C)**, indicating that Bex

enhanced HDL_3-mediated cholesterol efflux via RXR activation in pBCEC. In similar fashion, Asx [10 nM] enhanced cholesterol efflux to HDL_3 significantly by 1.9-fold and 1.5-fold at 90 and 240 min, respectively, when compared to untreated control cells, and treatment with Asx and GW 6471 was not significantly deviating from untreated control cells (p=0.2866) **(Figure 15D)** (1).

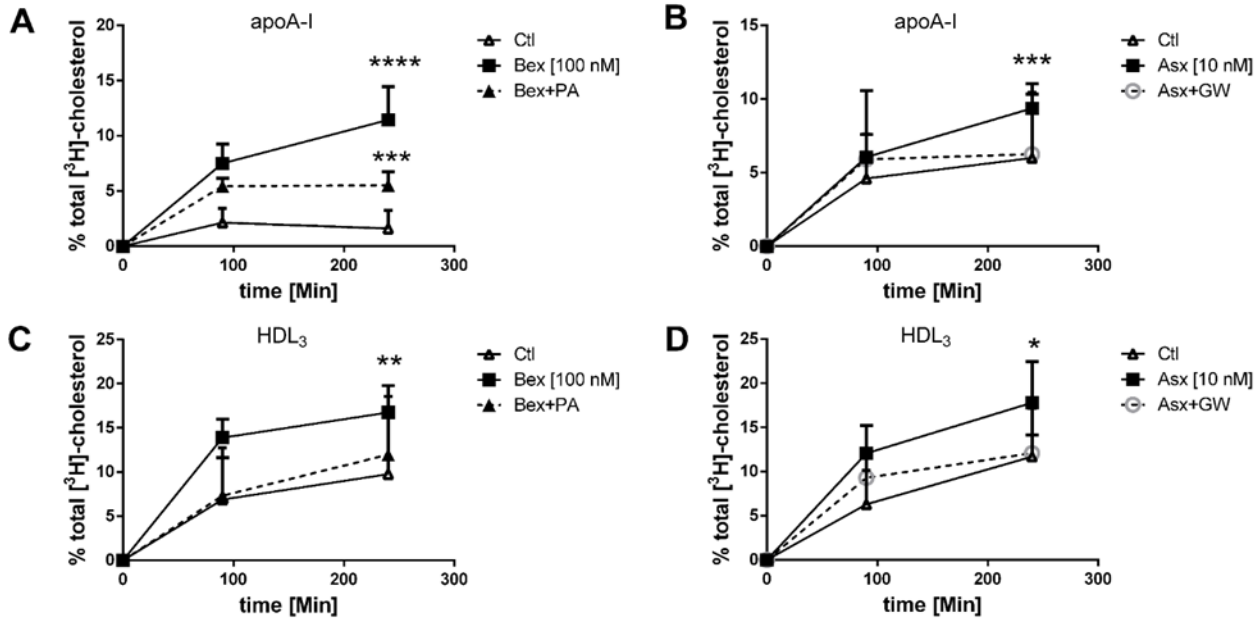

Figure 15: Bex and Asx enhance cholesterol efflux from pBCEC via PPARα- and RXR- activation

(A-B) Primary pBCEC cultured in 12-well plates were labeled with [³H]-cholesterol for 24 h. Then cells were equilibrated for 16 h in SF medium, preincubated with RXR antagonist PA 452 [10 µM] or PPARα antagonist GW 6471 [10 µM] for 15 min, during incubation with 0.5% ethanol (vehicle control), Bex [100 nM], Asx [10 nM], Bex and PA 452, or Asx and GW 6471. Medium was changed and (A-B) apoA-I [10 µg/ml] or (C-D) HDL_3 [200 µg/ml] were added, and time-dependent cholesterol release to the culture medium was measured by β-counting. Data shown are mean±SD of one representative experiment out of two (in presence of antagonists) or three (in absence of antagonists) performed in triplicates (*p≤0.05; **p≤0.01; ***p≤0.001; ****p≤0.0001 vs controls). [Reproduced from Fanaee-Danesh E et al. with permission of Biochim Biophys Acta Mol Basis Dis (1)].

4.4 Bex and Asx reduce cellular cholesterol mass, *de novo* cholesterol biosynthesis, and esterification in pBCEC

To further investigate the effects of both drugs on cellular cholesterol biosynthesis and esterification, pBCEC were metabolically labelled with [^{14}C]-acetate, the cholesterol precursor molecule. Extracted cellular lipids were separated by TLC and the radioactivity incorporated into the cholesterol and cholesterol ester fractions was measured. Treatment with Bex [100 nM] significantly diminished endogenous cholesterol biosynthesis by 15±1.1%; Asx [10 nM] lowered levels of free (unesterified) endogenous cholesterol by 41±1.8% **(Figure 16A)** ($p=0.0037$). Bex [100 nM] and Asx [10 nM] in parallel, reduced cholesterol ester synthesis by 51±1.1% and by 36±2.1%, respectively, when compared to controls **(Figure 16B)** ($p\leq0.0001$). The mean ratio of cholesterol ester to total cholesterol was 1.8±0.21%. In parallel, the cellular cholesterol content (photometric CHOD-PAP test was used for enzymatic measurements) was also suppressed in pBCEC. After a 24 h incubation time, Bex [100 nM] and Asx [10 nM] decreased intracellular cholesterol levels by 13±2.5% and 28±1.2% **(Figure 16C)** ($p\leq0.0001$). These results simultaneously, suggest that both Asx and Bex stimulate release of cellular cholesterol and lower endogenous cholesterol synthesis in pBCEC (1).

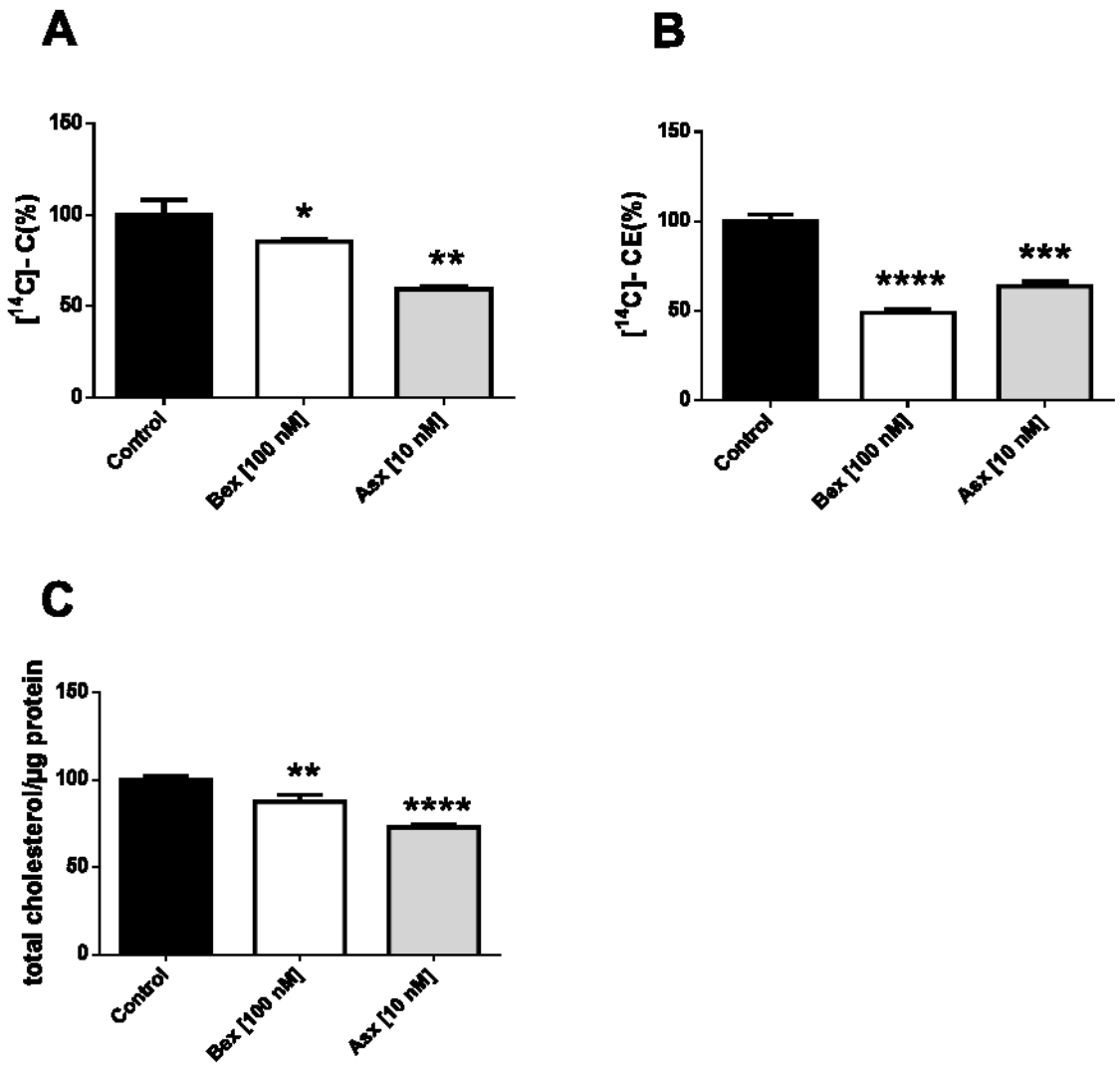

Figure 16: Bex and Asx reduce cellular cholesterol mass, *de novo* cholesterol biosynthesis, and cholesterol esterification in pBCEC

(A-B) Primary pBCEC were metabolically labelled for 24 h using cholesterol precursor [^{14}C]-acetate [2 µCi/ml] in the presence of 0.5% ethanol (vehicle control), Bex [100 nM] or Asx [10 nM]; Unesterified [^{14}C]-cholesterol **(A)** and esterified [^{14}C]-cholesterol **(B)** was determined after TLC separation of Folch extracts and subsequent β-counting of individual bands cut out from TLC plates. Activity in cpm/well was normalized to mg cell protein and percentage of total activity was calculated (*p≤0.05; **p≤0.01; ***p≤0.01; ****p≤0.0001 vs controls). **(C)** Cells were treated for 24 h in the presence of 0.5% ethanol (control), Bex [100 nM] or Asx [10 nM] and cellular cholesterol content was measured enzymatically. Data represent mean±SEM of 3 independent experiments performed in triplicates. *p≤0.05; **p≤0.01; ***p≤0.001 vs controls (**p≤0.01; ****p≤0.0001 vs controls). [Reproduced from Fanaee-Danesh E et al. with permission of Biochim Biophys Acta Mol Basis Dis (1)].

4.5 Bex and Asx upregulate LRP-1 in pBCEC

Aβ can be eliminated from the basolateral compartment by transcytosis across the BBB to the apical side via LRP-1 a multifunctional receptor accepted to be responsible for the majority of Aβ transport at the BBB (88–90). LRP-1 expression at the BBB is reduced in AD mouse models and in AD patients (90,245,246). Therefore, we were particularly interested in examining potential effects of both drugs on LRP-1. LRP-1 binds several ligands such as apoE-enriched lipoproteins (247,248). The major impact of apoE is, however, likely to be through interaction with Aβ and delivering Aβ to the lysosome for degradation. Quantitative PCR experiments revealed that Bex dose-dependently up-regulated mRNA expression of LRP-1 by 1.4±0.31-fold (10 nM Bex) and 2.4±0.29-fold (100 nM Bex), respectively **(Figure 17A)** (p=0.0291). Similarly, Asx enhanced *LRP-1* mRNA expression levels in pBCEC by 1.8±0.10-fold (1 nM Asx) and 2±0.18-fold (10 nM Asx) **(Figure 17B)** (p=0.0098) (1).

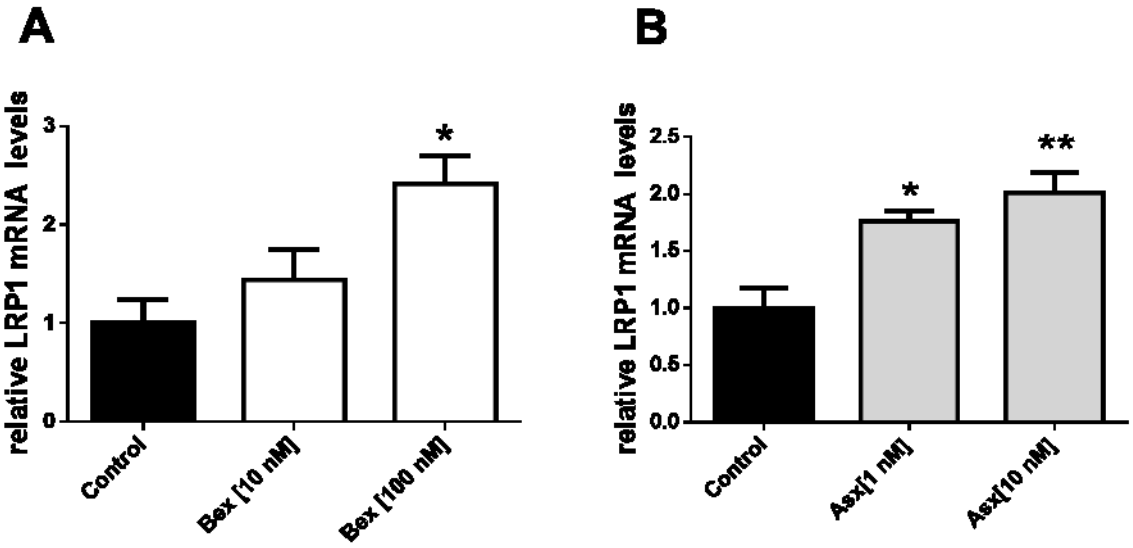

Figure 17: Bex and Asx increase LRP-1 mRNA expression level in pBCEC

(A-B) Primary pBCEC cultured on 6-well plates were incubated with 0.5% ethanol (vehicle control), Bex [10 and 100 nM], or Asx [1 and 10 nM] for 24 h. Total RNA was isolated, reverse-transcribed, and subjected to qPCR using SYBR Green technology and HPRT1 as a house-keeping gene. The $^{\Delta\Delta}$Ct method was applied to quantify relative mRNA expression levels. Data represent mean±SEM from 3 experiments with different cell preparations each performed in triplicates (*p≤0.05, **p≤0.01 vs controls). [Reproduced from Fanaee-Danesh E et al. with permission of Biochim Biophys Acta Mol Basis Dis (1)].

4.6 Bex and Asx induce Aβ uptake and transport by pBCEC

Since LRP-1 expression was increased by drug treatment and LRP-1 is known to facilitate Aβ transport at the BBB, we investigated effects of Bex and Asx on Aβ uptake and transcytosis in pBCEC. For uptake studies, cells pre-treated with vehicle control (0.5% ethanol), Bex [100 nM] or Asx [10 nM] for 24 h, were then incubated for 2 h with Alexa Fluor 488 labeled $A\beta_{1-40}$ [0.5 µg/ml]. Fluorimetric measurements revealed a decreased fluorescence intensity in the culture media of treated cells when compared to control cells. This suggested that cellular uptake of Aβ was enhanced by Bex (20±5.9%) and Asx (22±3.3%) **(Figure 18A)** (p=0.0325). In similar experiments, the relative uptake of [^{125}I]-$A\beta_{1-40}$ was also increased by Bex (35±11.7%) and Asx (55±6.6%) **(Figure 18B)** (p=0.005), confirming the outcome of experiments performed using the fluorescently labelled Aβ. To further examine the effects of Bex and Asx on Aβ transcytosis, [^{125}I]-$A\beta_{1-40}$ was added to the basolateral compartment (representing brain parenchyma) of pBCEC (seeded in transwell filter chambers), and Aβ transport to the apical compartment (mimicking the plasma environment) was measured after 2 h. Indeed, Bex [100 nM] and Asx [10 nM] moderately but significantly stimulated transcytosis of Aβ across the *in vitro* BBB model by 1.2±0.12-fold and by 1.5±0.08-fold, respectively **(Figure 18C)** (p=0.0022) (1).

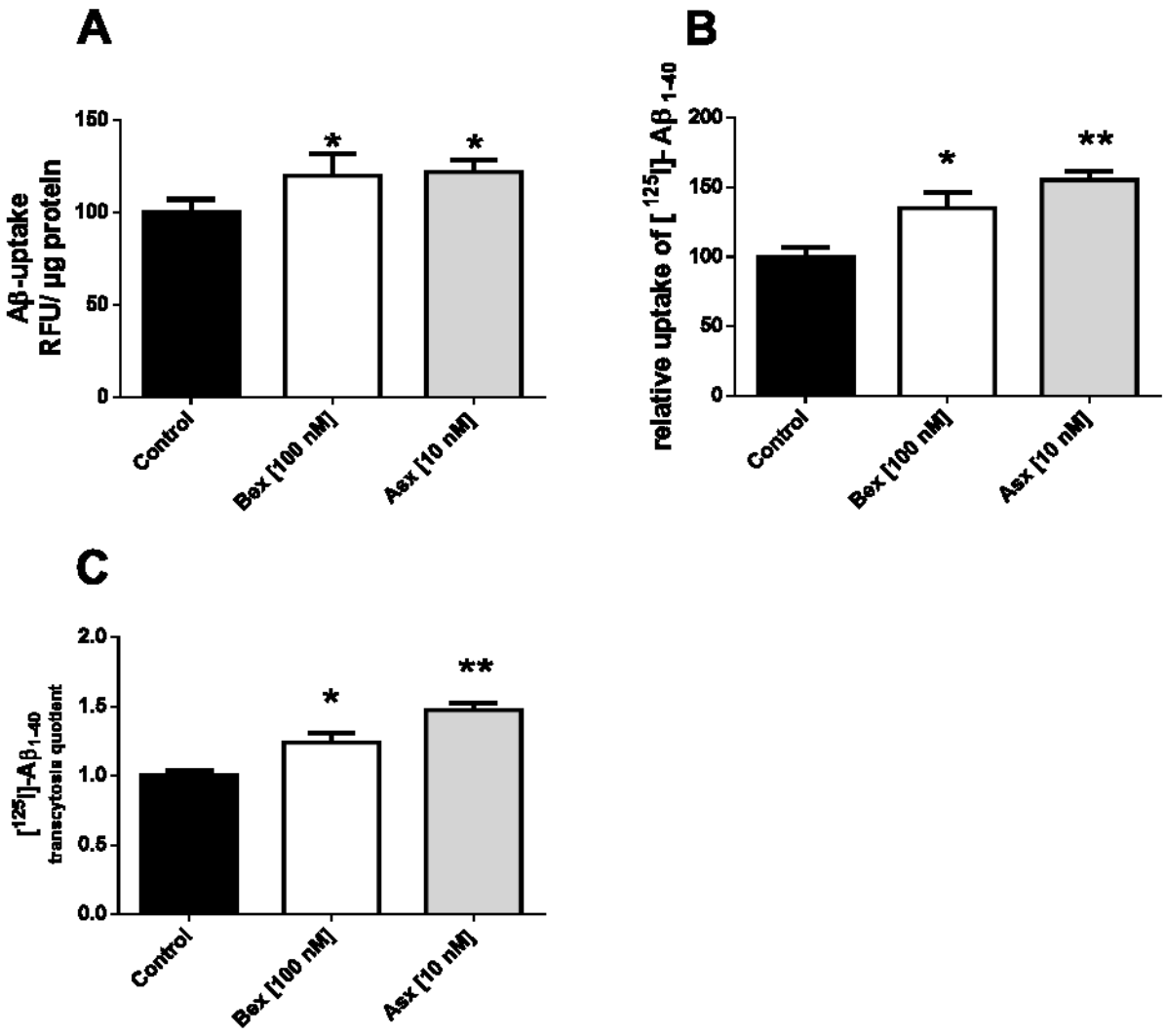

Figure 18: Bex and Asx promote Aβ uptake and transcytosis by pBCEC

Primary pBCEC were treated with 0.5% ethanol (control), Bex [100 nM] or Asx [10 nM] for 24 h. Cells were then washed and incubated with Alexa Fluor 488 labeled $A\beta_{1-40}$ [0.5 µg/ml] for 2 h, and fluorescence was measured at 490-525 nm using a Promega Glomax detection system (*p≤0.05 vs controls. RFU: relative fluorescent units). **(B)** pBCEC were plated on transwells and treated with 0.5% ethanol (control), Bex [100 nM] or Asx [10 nM] for 24 h and tight junction formation was induced (overnight) by adding 550 nM hydrocortisone. TEER was measured using an Endohm ohmmeter. Aβ uptake assay was performed by adding 0.3 nM [^{125}I]-$A\beta_{1-40}$, and 100 nM [^{14}C]-sucrose as non diffusion control, to the basolateral compartment. Uptake of [^{125}I]-$A\beta_{1-40}$ was counted at 2 h from the apical compartment. TCA-precipitated proteins isolated from apical and basolateral media, were incubated on ice for 10 min and centrifuged at 10,000 x *g* (10 min, 4°C) and radioactivity associated to pellets was counted on a γ-counter. The supernatant was transferred to a new vial and the uptake of [^{125}I]-$A\beta_{1-40}$ was calculated as the percentage of cpm/mg cell protein in the pellet relative to the cpm/mg of supernatant. Data represent mean±SEM from 3 experiments with different cell preparations each performed in triplicates (*p≤0.05, **p≤0.01 vs controls). **(C)** pBCEC were plated on transwells and treated with control (0.5% ethanol), Bex [100 nM] or Asx [10 nM] for 24 h, tight junction formation was induced (overnight) by adding 550

nM hydrocortisone. TEER was measured using an Endohm ohmmeter. Aβ transport assay was performed by adding 0.3 nM [^{125}I]-Aβ_{1-40}, and 100 nM [^{14}C]-sucrose as non diffusion control, to the basolateral compartment. Transport of [^{125}I]-Aβ_{1-40} was counted at 2 h from the apical compartment and normalized to [^{14}C]-sucrose activity. Data represent mean±SEM from 3 experiments performed in triplicates (*p≤0.05, **p≤0.01 vs controls). [Reproduced from Fanaee-Danesh E et al. with permission of Biochim Biophys Acta Mol Basis Dis (1)].

4.7 Time-dependent and PPARα-/RXR-dependent effects of Bex and Asx on ABCA1, LRP-1, and APP/Aβ species in pBCEC

Time-dependent experiments were performed to explore the potential of Bex and Asx in the absence or presence of RXR- and PPARα antagonists PA 542 and GW 6471, respectively, to influence the expression of ABCA1, LRP-1, CTFs, and APP/Aβ species at different incubation times (1).

Bex enhanced ABCA1 protein expression time-dependently up to 520% after 24 h (when compared to control cells). In the presence of the antagonist, protein expression of ABCA1 was completely reduced, indicating that RXR activation is required for Bex-mediated effect on ABCA1 through RXR pathway. Even after 8 h, treatment with RXR antagonist PA 542 in addition to Bex treatment reduced expression of ABCA1 close to completely when compared to Bex treatment at 8 h alone **(Figure 19C)** (1).

Asx also increased ABCA1 protein levels in a time-dependent manner up to 277% after 24 h (when compared to control cells), whereas treatment of pBCEC with PPARα antagonist GW 6471 together with Asx decreased expression of ABCA1 by 83% when compared to Asx treatment after 8 h alone **(Figure 19D).** Thus PPARα activation is required for Asx-mediated effect on ABCA1 protein expression in pBCEC (1).

Interestingly, induction of expression of LRP-1 in pBCEC by Bex and Asx, respectively, became apparent also to be mediated through RXR and PPARα activation. Thus, treatment of pBCEC with Bex enhanced LRP-1 protein level time-dependently by 46% after 24 h (versus controls). However, treatment with PA 542 in addition to Bex lowered LRP-1 expression level by 58% (after 24 h) when compared to Bex treatment alone **(Figure 19E)**. Furthermore, treatment of pBCEC with Asx enhanced LRP-1 levels by 63% after 24 h (when compared to controls), and treatment with GW 6471 along with

Asx diminished LRP-1 levels by 59% (after 16 h) when related to individual Asx treatment **(Figure 19F)** (1).

Regarding immunoblotting analyses of APP/Aβ species, Bex also time-dependently enhanced levels of CTFs of APP by 89% after 24 h (when compared to control cells). Interestingly, observed effects of Bex treatment on CTFs were as well mediated by RXR activation, considering a 91% reduction in CTFs upon treatment with the antagonist PA 542 in addition to Bex when compared to Bex treatment of pBCEC alone after 8 h **(Figure 19G)**. Similarly, treatment of pBCEC with Asx increased CTF protein levels by 305% (when compared to control cells after 16 h). Treatment with GW 6471 in addition to Asx, suppressed protein levels of CTF by 74% (when compared to Asx treatment after 16 h) **(Figure 19H)**. Interestingly, Bex significantly reduced the prominent ~80 kDa 6E10-reactive APP/Aβ species even after 8 h by 82% (when compared to control cells) **(Figure 19K)**. Asx also decreased the 6E10-reactive APP/Aβ species after 24 h by 82% (when compared to control cells) **(Figure 19L)** whereas no significant effect of antagonists was observed after treatment with antagonist PA 542 in addition to Bex or GW 6471 in addition to Asx (1).

In line with results shown above in **(Figure 19A)**, Bex increased sAPPα levels in a time-dependent manner by 110% after 24 h when compared to control cells **(Figure 19I)**. Asx enhanced sAPPα levels even more pronounced than Bex, by 150% after 24 h (when compared to control cells) **(Figure 19J)** whereas no significant effect of antagonists was observed after treatment with antagonist PA 542 in addition to Bex or GW 6471 in addition to Asx (1).

Thus, unlike formation of CTFs from APP, the almost complete reduction of the 6E10-reactive ~80 KDa APP/Aβ species in pBCEC along with augmented sAPPα release by pBCEC by Bex and Asx was not dependend on RXR or PPARα activation (1).

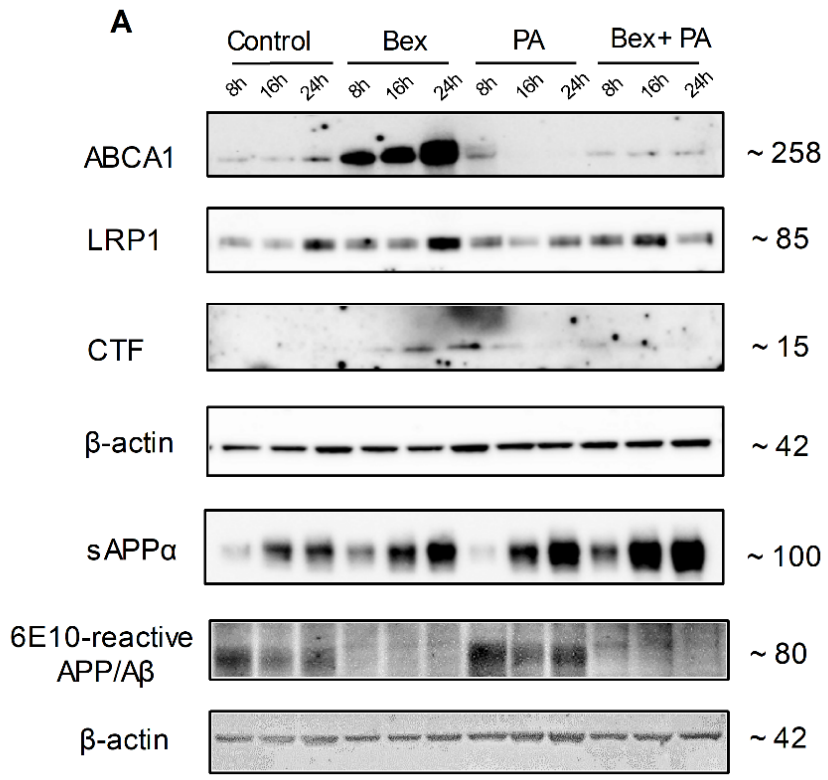
A
Control
Bex
PA
Bex+ PA
8h
16h
24h
ABCA1
~ 258
LRP1
~ 85
CTF
~ 15
β-actin
~ 42
sAPPα
~ 100
6E10-reactive APP/Aβ
~ 80
β-actin
~ 42

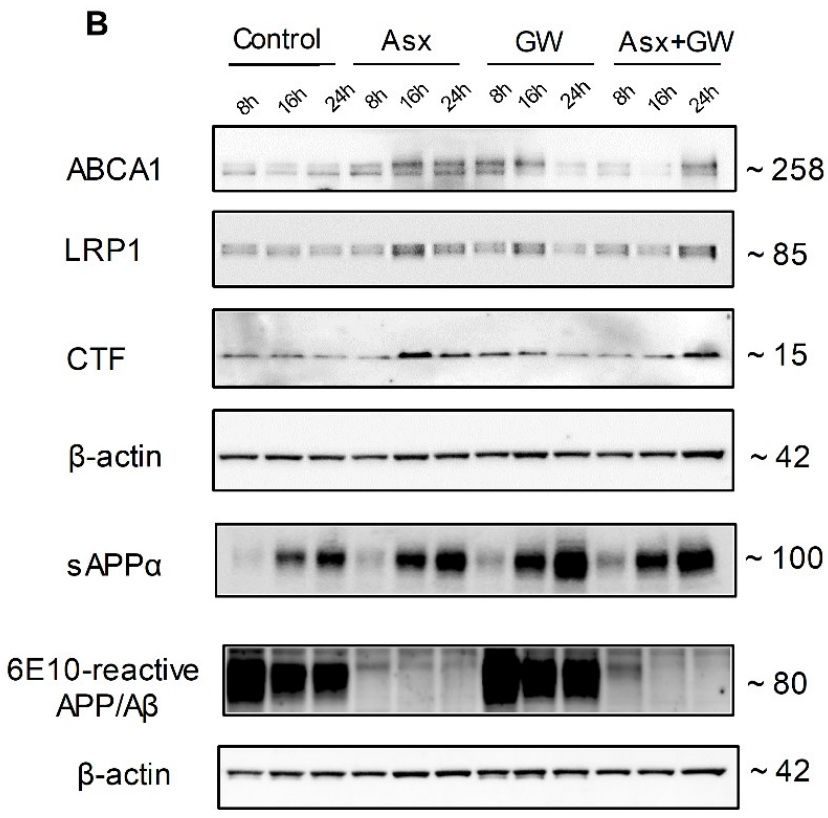
B
Control
Asx
GW
Asx+GW
8h
16h
24h
ABCA1
~ 258
LRP1
~ 85
CTF
~ 15
β-actin
~ 42
sAPPα
~ 100
6E10-reactive APP/Aβ
~ 80
β-actin
~ 42

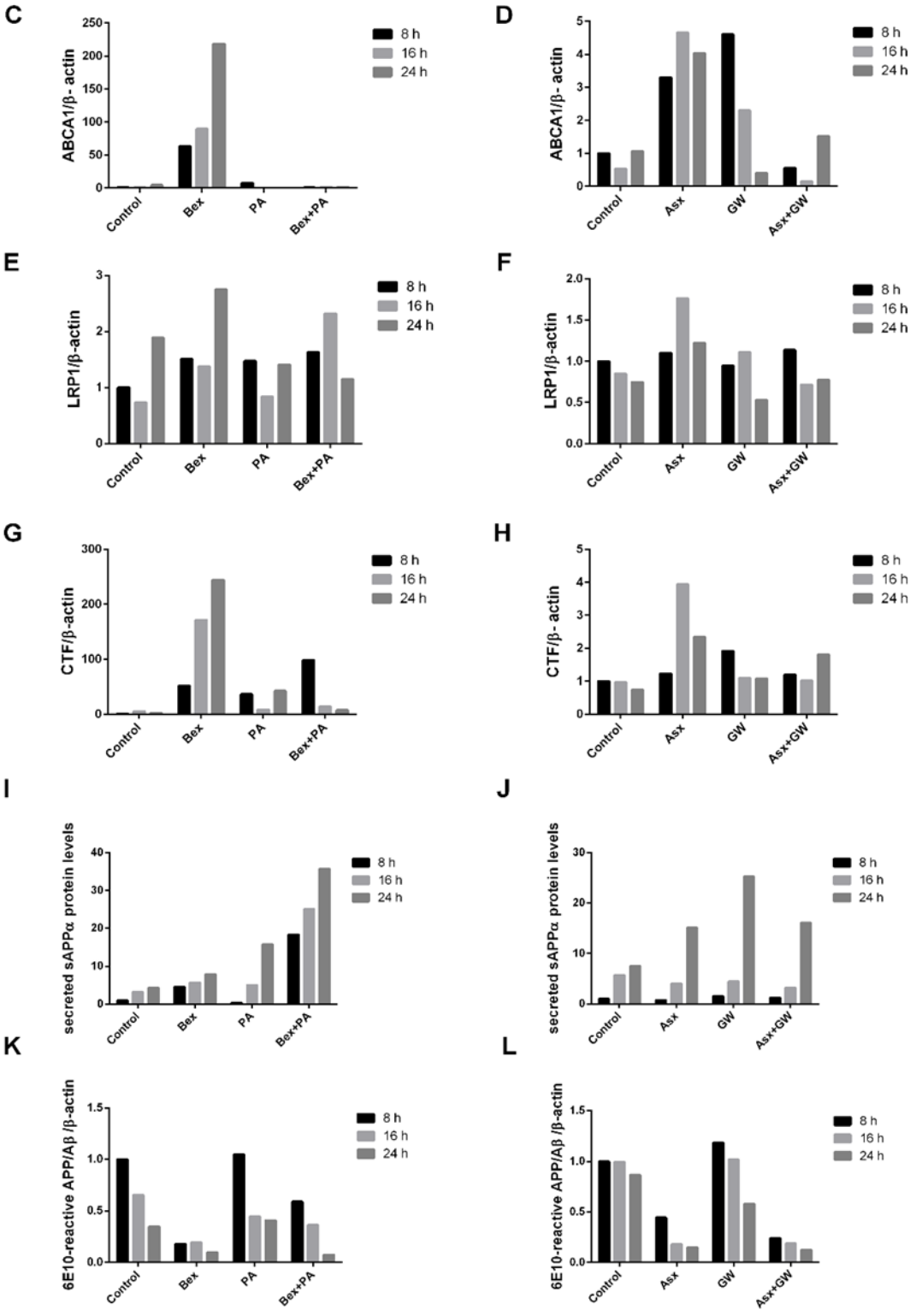
C
ABCA1/β- actin
250
200
150
100
50
0
8 h
16 h
24 h
Control
Bex
PA
Bex+PA
D
ABCA1/β- actin
5
4
3
2
1
0
8 h
16 h
24 h
Control
Asx
GW
Asx+GW
E
LRP1/β-actin
3
2
1
0
8 h
16 h
24 h
Control
Bex
PA
Bex+PA
F
LRP1/β-actin
2.0
1.5
1.0
0.5
0.0
8 h
16 h
24 h
Control
Asx
GW
Asx+GW
G
CTF/β-actin
300
200
100
0
8 h
16 h
24 h
Control
Bex
PA
Bex+PA
H
CTF/β- actin
5
4
3
2
1
0
8 h
16 h
24 h
Control
Asx
GW
Asx+GW
I
secreted sAPPα protein levels
40
30
20
10
0
8 h
16 h
24 h
Control
Bex
PA
Bex+PA
J
secreted sAPPα protein levels
30
20
10
0
8 h
16 h
24 h
Control
Asx
GW
Asx+GW
K
6E10-reactive APP/Aβ /β-actin
1.5
1.0
0.5
0.0
8 h
16 h
24 h
Control
Bex
PA
Bex+PA
L
6E10-reactive APP/Aβ /β-actin
1.5
1.0
0.5
0.0
8 h
16 h
24 h
Control
Asx
GW
Asx+GW

Figure 19: Bex and Asx increase protein levels of ABCA1/LRP-1/CTFs/sAPPα and decrease ~80 kDa 6E10-reactive APP/Aβ species in pBCEC in a time-dependent manner, via nuclear receptor-dependent and independent mechanisms

(A-H, K-L) Primary pBCEC cultured on 6-well plates were pre-incubated in absence or presence of RXR antagonist PA 542 [10 µM] or PPARα antagonist GW 6471 [10 µM] for 15 min and treated with 0.5% ethanol (control), Bex [100 nM] or Asx [10 nM], Bex and PA 542, or Asx and GW 6471 for 8 h, 16 h, and 24 h. Proteins were extracted from cells, separated by SDS-PAGE, and levels of ABCA1, LRP-1, CTFs and 6E10-reactive APP/Aβ species (normalized to β-actin levels) were detected by immunoblot experiments. β-Actin was used as loading control. One representative blot out of 2 experiments is shown. The graphs represent densitometric evaluation of immunoreactive bands.

(I-J) pBCEC cultured on 6-well plates were pre-incubated with PA 542 [10 µM] or GW 6471 [10 µM] for 15 min and treated with control (0.5% ethanol), Bex [100 nM] or Asx [10 nM], Bex and PA 542, or Asx and GW 6471 for 8 h, 16 h, and 24 h. Proteins (precipitated with TCA from supernatants) were separated by SDS-PAGE, and levels of secreted sAPPα (normalized to Ponceau stained bands) were detected by immunoblot experiments using 6E10 as primary antibody. One representative blot out of 2 experiments is shown. The graphs represent densitometric evaluation of immunoreactive bands. [Reproduced from Fanaee-Danesh E et al. with permission of Biochim Biophys Acta Mol Basis Dis (1)].

4.8 LRP-1 silencing and ABCA1 inhibition reverses impacts on APP processing/Aβ load in Bex- and Asx-treated pBCEC

In order to establish a potential link between LRP-1 and/or ABCA1 and Bex-/Asx-mediated influences on APP processing in pBCEC, we repeated cellular experiments under conditions of LRP-1 silencing and ABCA1 inhibition (1). In agreement with results shown in **Figure 19**, Bex [100 nM] and Asx [10 nM] treatment augmented LRP-1 protein levels in pBCEC by 327% and 358%, respectively, when compared to control cells **(Figure 20A)**. A mixture of previously validated short interfering RNA sequences was used in order to silence LRP-1. Primary pBCEC under normal conditions express constitutively low LRP-1 levels hence silencing showed minimal effects in reducing LRP-1 levels, moreover, Bex and Asx significantly elevated LRP-1 levels in pBCECs. An 48 h incubation with LRP-1 targeting siRNAs (50 nM). resulted in a marked downregulation of endogenous LRP-1 protein under Bex- and Asx treated conditions by 70% **(Figure 20A)**. Remarkably, the down-regulation of LRP-1 was accompanied by an increase in levels of the prominent ~80kDa 6E10-reactive APP/Aβ species by 230% in LRP-1-silenced Bex-treated [100 nM] pBCEC when compared to non-

silenced, Bex-treated cells **(Figure 20B)**, and by 420% in LRP-1-silenced Asx-treated [10 nM] cells (when compared to non-silenced Asx-treated cells) **(Figure 20B)**. Thus, LRP-1 appears to be required for increased 'clearance' or diminished generation and/or accumulation of the 80 kDa APP/Aβ species which is brought about by Bex and Asx treatment in pBCEC (1).

We ultimately analysed the consequence of blocking ABCA1 activity with probucol (which inactivates ABCA1 in the plasma membrane (1,249) on cellular APP processing cleavage products sAPPα, 6E10-reactive ~80 kDa band and ABCA1 protein levels in pBCEC. Bex [100 nM] and Asx [10 nM] increased ABCA1 protein level by 236%, and 180%, respectively (1). Pretreatment with probucol [10 µM] for 2 h and subsequent incubation with Bex [100 nM] or Asx [10 nM] for 24 h decreased ABCA1 protein levels by 68% and 75% when compared to Bex- and Asx-treated cells in the absence of probucol **(Figure 20C)**. As expected, treatment with Bex [100 nM] or Asx [10 nM] reduced intracellular ~80 kDa APP/Aβ species by 87% and 80%, respectively **(Figure 20D)**. In parallel, secreted sAPPα protein levels were enhanced by 150% (Bex) and 280% (Asx) when compared to control cells **(Figure 20E)**. Furthermore, cellular treatment with probucol [10 µM] together with Bex [100 nM] or Asx [10 nM] for 24 h also decreased ABCA1 protein levels by 68% and 75% when compared to Bex- and Asx-treated cells in the absence of probucol **(Figure 20C)**. In parallel, 6E10-reactive ~80 kDa APP/Aβ species was considerably increased by 490% (Bex) and 480% (Asx)**(Figure 20D)** while sAPPα protein levels were decreased by 75% (Bex) and 99% (Asx), accordingly **(Figure 20E)**. Taken together, these results strongly support a direct and beneficial link between ABCA1 activity and APP processing in Bex- and Asx-mediated effects in pBCEC (1).

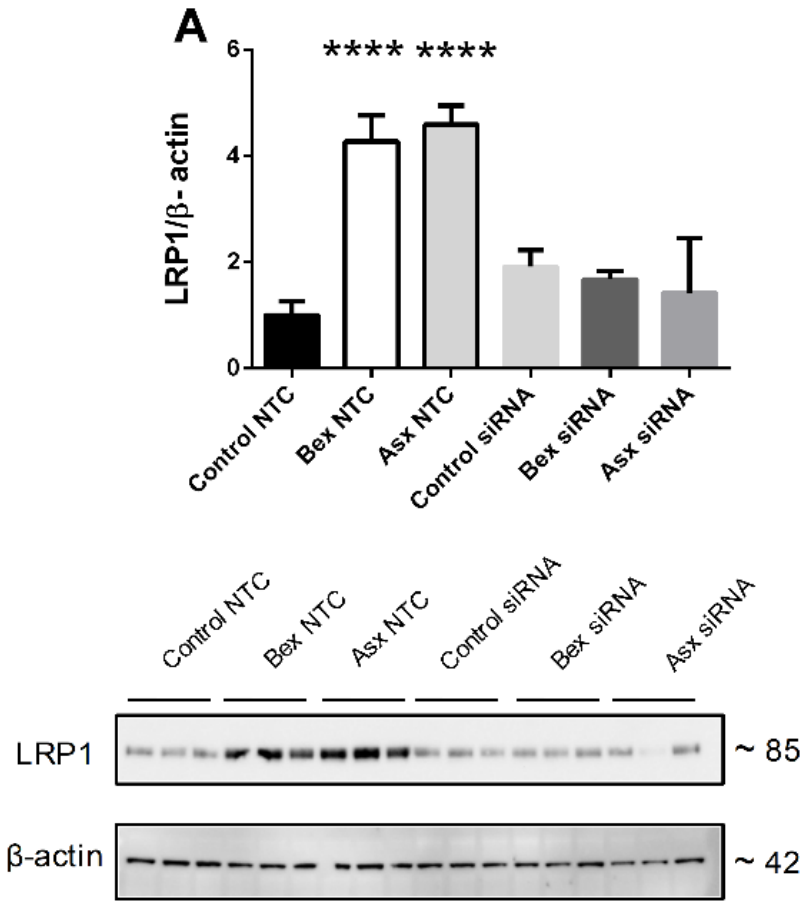
A
LRP1/β- actin
6
4
2
0
**** ****
Control NTC
Bex NTC
Asx NTC
Control siRNA
Bex siRNA
Asx siRNA
Control NTC
Bex NTC
Asx NTC
Control siRNA
Bex siRNA
Asx siRNA
LRP1
~ 85
β-actin
~ 42

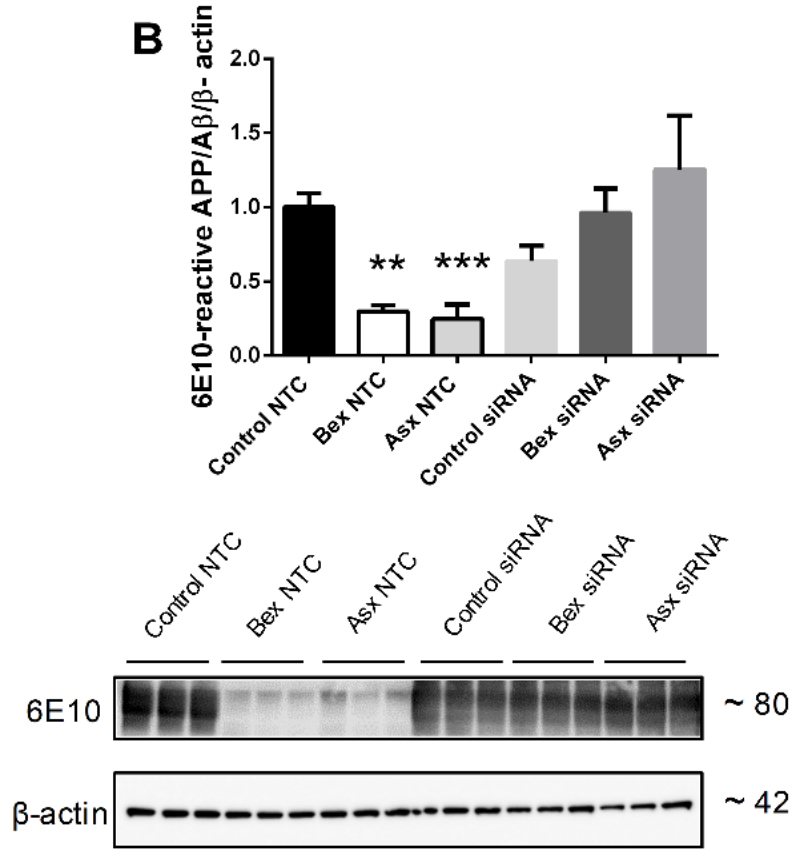
B
6E10-reactive APP/Aβ/β- actin
2.0
1.5
1.0
0.5
0.0
** ***
Control NTC
Bex NTC
Asx NTC
Control siRNA
Bex siRNA
Asx siRNA
Control NTC
Bex NTC
Asx NTC
Control siRNA
Bex siRNA
Asx siRNA
6E10
~ 80
β-actin
~ 42

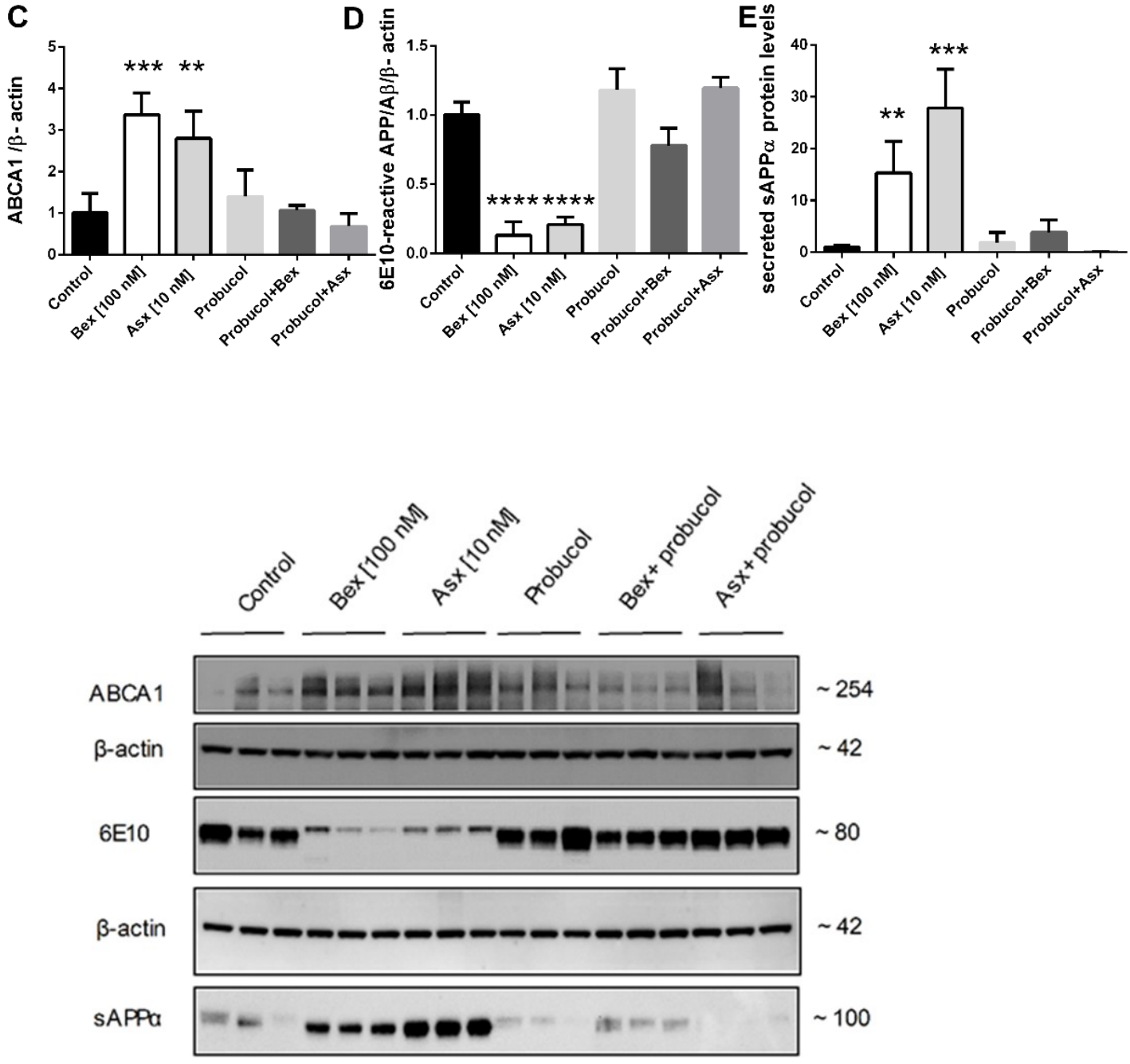

Figure 20: Silencing of LRP-1 or inhibition of ABCA1 activity reverses effects on APP processing in Asx-/Bex-treated pBCEC

(A) Primary pBCEC were cultured on 6-well plates and specific gene silencing was achieved by RNA interference using LRP-1 targeting siRNA, and NTC siRNA as control, for 48 h. After 24 h of silencing, cells were treated with Bex [100 nM] or Asx [10 nM] for 24 h. Proteins were extracted, separated by SDS-PAGE, and gene silencing efficiency was confirmed by immunoblot experiments using anti-LRP-1 as primary antibody. β-Actin was used as loading control (****p≤0.0001 vs controls). One representative blot out of 2 experiments is shown. **(B)**, Levels of intracellular ~80 kDa APP/Aβ species (normalized to

β-actin) was detected by immunoblot experiments using 6E10 as primary antibody. One representative blot out of 2 experiments is shown. The graphs represent densitometric evaluation of immunoreactive bands. (mean±SD; **p≤0.01; ***p≤0.001 vs controls). **(C-E)** pBCEC cultured on 6-well plates were pre-incubated with specific ABCA1 inhibitor probucol [10 μM] for 30 min and treated with control (0.5% ethanol), Bex [100 nM] or Asx [10 nM], Bex and probucol, or Asx and probucol, for 24 h. Proteins were extracted from cells (precipitated with TCA from supernatants), separated by SDS-PAGE, and levels of intracellular ~80 kDa APP/Aβ species (normalized to β-actin) and secreted sAPPα (normalized to Ponceau stained bands) were detected by immunoblot experiments using 6E10 as primary antibody. One representative blot out of 2 experiments is shown. The graphs represent densitometric evaluation of immunoreactive bands. (mean±SD; **p≤0.01; ***p≤0.001; ****p≤0.0001 vs controls). [Reproduced from Fanaee-Danesh E et al. with permission of Biochim Biophys Acta Mol Basis Dis (1)].

4.9 Effects of Bex and Asx on ROS levels and cell viability in pBCEC

Cultured pBCEC were also subjected to measurements of H_2DCFDA-reactive ROS levels after incubations in the absence (control; 0.5% ethanol) or presence of Bex [100 nM] or Asx [10 nM] for 24 h (1). Bex [100 nM] decreased ROS levels by 22±2.6% and Asx [10 nM] significantly decreased cellular ROS levels by even 61±34.8% **(Figure 21A)** (p=0.0045). On the other side, cell viability was also measured photometrically (WST1 assay) in response to Bex [100 nM] and Asx [10 nM] and no significant changes were observed. This indicates that reduction in ROS levels may contribute to maintain cell viability in pBCEC undergoing treatments with Asx and Bex when compared to control conditions **(Figure 21B)**.

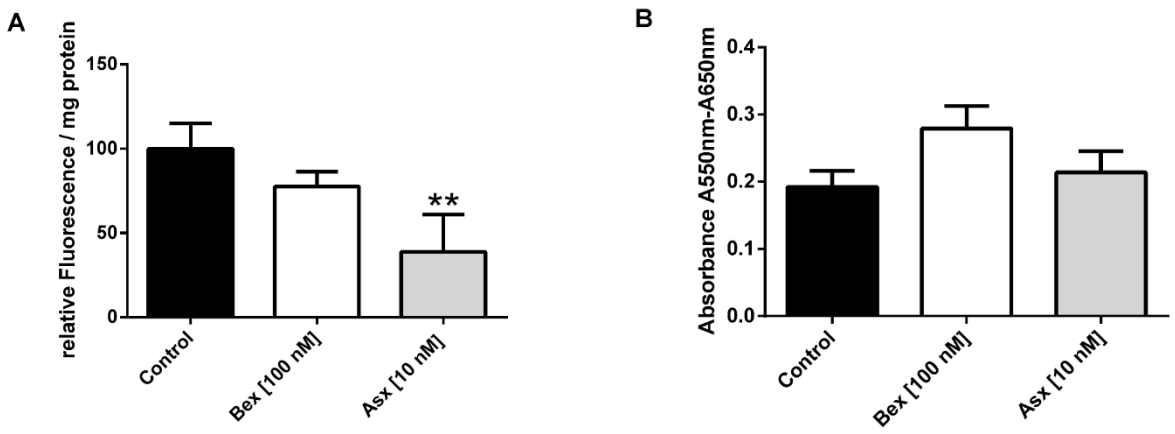

Figure 21: Bex and Asx suppress ROS levels and improve cell viability in pBCEC

Cells were cultured on 12-well plates, 10 µM H_2DCFDA dye was applied for 20 min at 37°C. Fluorescence was measured at excitation and emission wavelengths of 485 and 530 nm and normalized to cell protein contents. Data represent mean±SEM of 3 experiments performed in triplicates (**p≤0.01 versus control). **(B)** Cell viability test was performed by using Cell Proliferation Reagent WST-1 from Roche. Data represent mean±SEM of 3 experiments performed in triplicates. [Reproduced from Fanaee-Danesh E et al. with permission of Biochim Biophys Acta Mol Basis Dis (1)].

4.10 Plasma lipids and body weights of 3xTg AD mice

Adding to our *in vitro* results, the study of 3xTg AD mice is a vital part of this research to test the potential effects of Bex and Asx therapy as part of the applied research process. Bex treated mice showed elevated plasma levels of cholesterol **(Figure 22A,D)** and triglycerides **(Figure 22B,E)** in agreement with previous findings (Musolino et al., 2009) (250). Interestingly, no significant changes in plasma cholesterol or triglyceride levels were observed after treatment with Asx. Furthermore, in 3xTg AD mice subjected to Bex treatment, a significant weight loss **(Figure 22C, F)**, and hepatomegaly (data not shown) was observed, data which are again in line with previous findings (170). It is worth to note that neither side effects nor body weight changes were observed by Asx treatment (1).

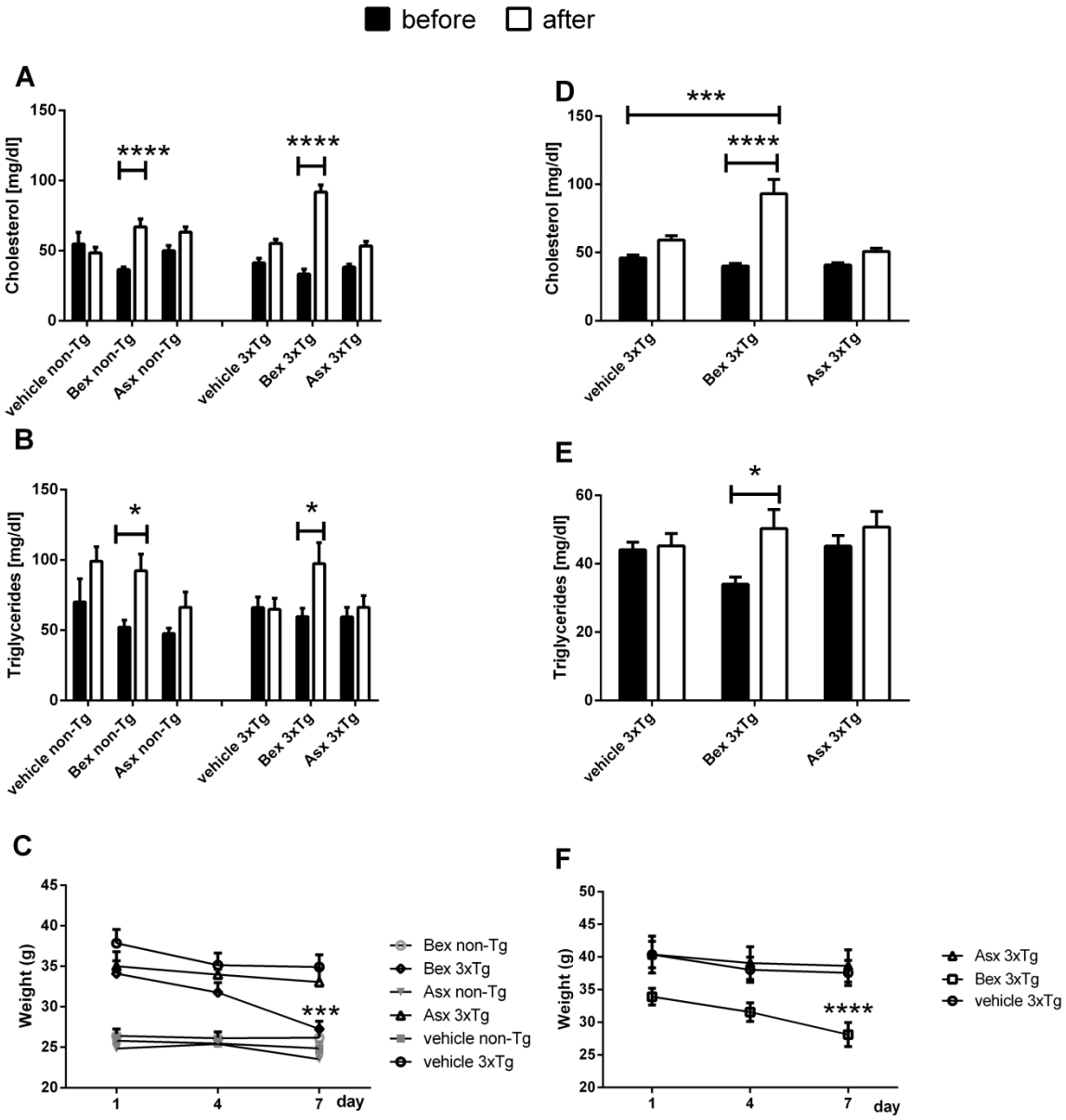

Figure 22: Effects of Bex and Asx on plasma lipids/body weights of 3xTg AD mice

(A-C) Female 3xTg AD mice (*study I*) were gavaged for 6 days with DMSO in corn oil as vehicle/control (n=10), Bex (n=9) or Asx (n=8) and non-Tg mice, vehicle (n=5), Bex (n=6) or Asx (n=7) and **(D-F)** female 3xTg AD mice (*study II*) were gavaged for 6 days with DMSO in corn oil as vehicle/control (n=8), Bex (n=6) or Asx (n=8). Plasma lipid parameters were determined enzymatically using the DiaSys kit. All data represent mean±SEM (*p≤0.05; ***p≤0.001; ****p≤0.0001 versus vehicle). [Reproduced from Fanaee-Danesh E et al. with permission of Biochim Biophys Acta Mol Basis Dis (1)].

4.11 Transcriptional profiles of cell-selective genes in isolated cerebral capillary endothelial cells relative to total mouse brain homogenates

Isolation of highly-purified endothelial cells is important to study the mechanisms of endothelial function. As other cells in the NVU are joined to endothelial cells, this isolation may not be optimal. Quantitative real-time PCR (qPCR) was carried out to validate the purity of isolated mBCEC. Messenger RNA expression of cell-selective markers such as cluster of differentiation 31 (CD31) for endothelial cells, aminopeptidase N (CD13) and beta-type platelet-derived growth factor receptor (PDGFRβ) for pericytes, glial fibrillary acidic protein (GFAP) for astrocytes, synaptophysin (SYP) for neurons, ionized calcium-binding adaptor molecule 1 (IBA1) for microglia, and smooth muscle actin (SMA) for smooth muscle cells **(Figure 23)**. The absence of pericytes in the isolated mBCEC fraction was confirmed by lack of CD13 or PDGFRβ mRNA. These results confirmed that the isolated mBCEC fraction was highly enriched in CD31 identifying endothelial cells (1).

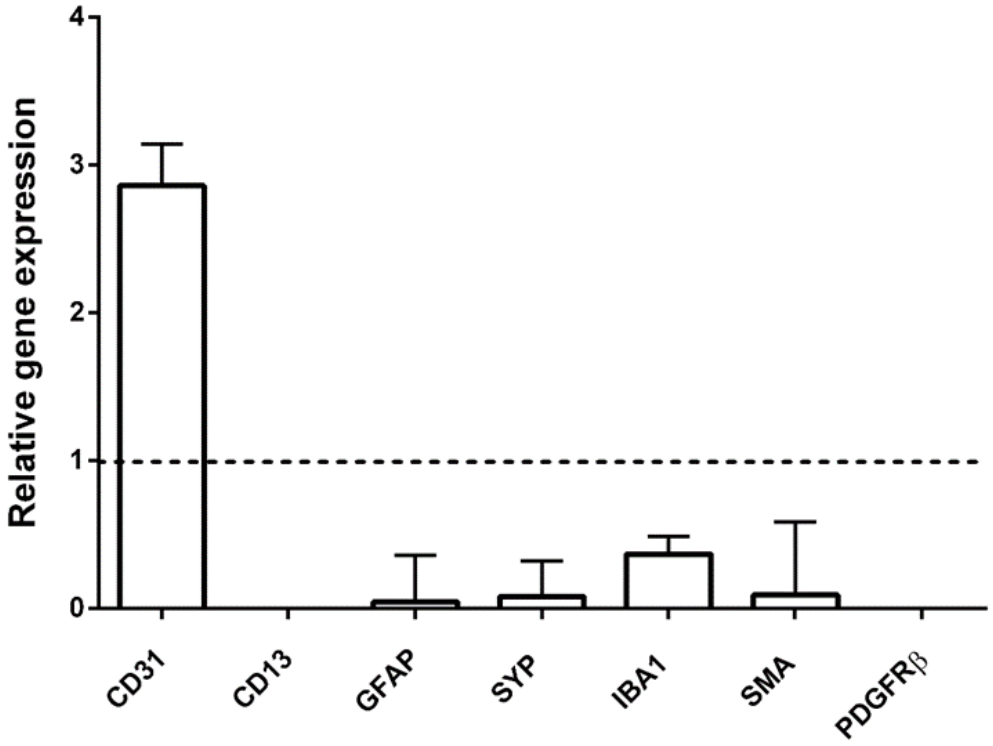

Figure 23: Transcriptional profiles of genes in mBCEC compared to total mouse brain homogenates

Three hemispheres from non-Tg animals were pooled to isolate mBCEC, and RNA was isolated and reverse-transcribed to cDNA. cluster of differentiation 31 (CD31), endothelial-specific marker; aminopeptidase N (CD13) and Beta-type platelet-derived growth factor receptor (PDGFRβ), pericyte markers; glial fibrillary acidic protein (GFAP), astrocyte marker; synaptophysin (SYP), neuronal marker, ionized calcium-binding adaptor molecule 1 (IBA1), microglial, and smooth muscle actin (SMA) markers were used. qPCR analyses were performed using the $^{\Delta\Delta}$Ct method and HPRT1 as housekeeping gene. Data are compared to relative gene expression of brain homogenates. All data represent mean±SEM from 3 to 4 pooled samples performed in triplicates. [Reproduced from Fanaee-Danesh E et al. with permission of Biochim Biophys Acta Mol Basis Dis (1)].

4.12 Bex but not Asx enhances *APOE* and *ABCA1* levels in mBCEC of 3xTg AD mice

In *study I,* both groups of animals, female 3xTg AD mice (32-49 weeks) and non-Tg mice (37-49 weeks) were gavaged for 6 days with either DMSO in corn oil (vehicle control), 100 mg/kg Bex, or 80 mg/kg Asx in DMSO and corn oil. Three hemispheres from different mice and from individual groups were pooled and mBCEC were isolated. Significantly elevated *APOE* mRNA expression levels were observed in mBCEC of all groups of 3xTg AD mice when compared to non-Tg mice: 3.8±0.44-fold for vehicle-treated 3xTg AD relative to non-Tg vehicle-treated mice; 4.8±0.54-fold for Bex-treated 3xTg AD versus Bex-treated non-Tg mice **(Figure 24A)**. Importantly, Bex treatment further increased *APOE* levels in 3xTg AD mice by 1.4±0.54-fold when compared to vehicle-treated 3xTg AD mice. Asx-treated 3xTg AD mice versus Asx-treated non-Tg mice showed an increase by 2.9±0.57-fold, however, Asx had no effect on *APOE* in mBCEC of treated versus untreated 3xTg AD mice (1).

Different from *APOE*, *ABCA1* mRNA expression levels in mBCEC did not significantly vary in vehicle-treated 3xTg AD mice as compared to vehicle-treated non-Tg mice **(Figure 24B)**. Isolated mBCEC of 3xTg AD mice treated with Bex revealed 2.2±0.33-fold increased *ABCA1* mRNA expression levels relative to Bex-treated non-Tg mice. In mBCEC from Bex-treated 3xTg AD mice, *ABCA1* mRNA expression levels were increased 1.7±0.33-fold when compared to vehicle-treated 3xTg AD mice **(Figure**

24B). Two-way ANOVA revealed a significant effect of treatment (p=0.0248). However, as for *APOE*, in mBCEC obtained from the Asx-treated group, no significant changes in *ABCA1* mRNA expression levels were observed when compared to that obtained from the vehicle-treated group **(Figure 24B)** (1).

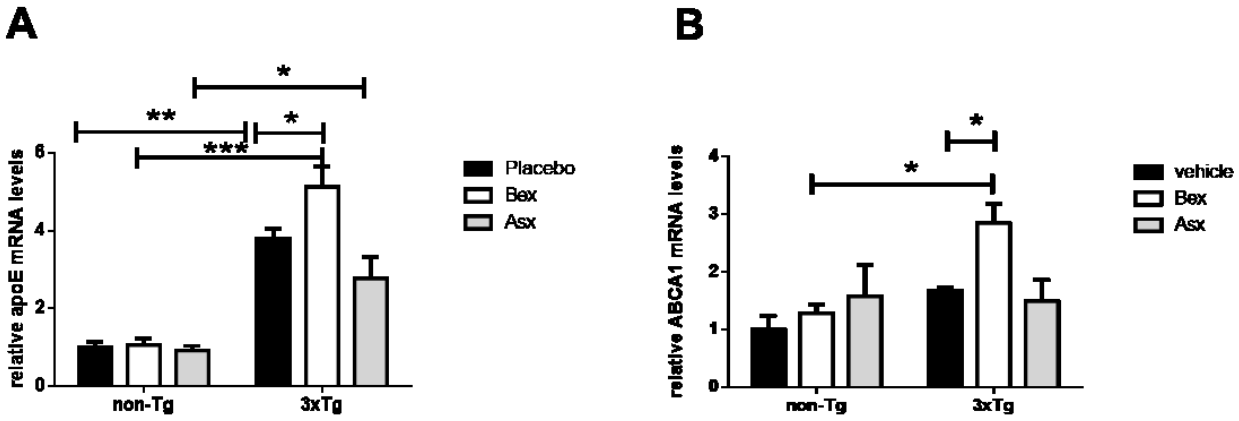

Figure 24: Bex increases *APOE* and *ABCA1* levels in mBCEC of 3xTg AD mice

(A-B) *study I:* Female 3xTg AD mice and C57BL/6 (non-Tg) mice were gavaged for 6 days vehicle (10% DMSO and corn oil) (n=10), Bex (n=9) and Asx (n=8) and non-Tg mice, vehicle (n=5), Bex (n=6) and Asx (n=7). Two to three hemispheres were pooled to isolate mBCEC RNA was isolated and reverse-transcribed to cDNA. QRT-PCR analysis was performed using the $^{\Delta\Delta}$Ct method and HPRT1 as housekeeping gene. Data were normalized to vehicle-treated non-Tg mice. All data represent mean±SEM from 3 to 4 samples, performed in triplicates (*p≤0.05; **p≤0.01; ***p≤0.001 vs controls). [Reproduced from Fanaee-Danesh E et al. with permission of Biochim Biophys Acta Mol Basis Dis (1)].

4.13 Bex and Asx enhance *LRP-1* and reduce *BACE1* levels in mBCEC of 3xTg AD mice

In mBCEC isolated from brains of mice of *study I* (32-49 weeks)*, BACE1* mRNA expression levels were up-regulated by 2.0±0.4-fold in mBCEC obtained from vehicle-treated 3xTg AD compared to those of vehicle-treated non-Tg mice **(Figure 25A)**. However, gavaging 3xTg AD mice with Bex or Asx reduced BACE1 mRNA expression levels in mBCEC significantly by 62±1.1% and 71±0.7% **(Figure 25A)**, when compared to mBCEC obtained from vehicle-treated 3xTg AD mice. Two-way ANOVA revealed a significant effect of treatments in 3xTg AD mice (p=0.0272). *BACE1* mRNA expression levels were not significantly altered by any treatment in mBCEC obtained from non-Tg mice **(Figure 25A)** (1).

Bex and Asx treatments substantially increased *LRP-1* mRNA levels by 3.5±0.31-fold 2.4±1.3-fold in mBCEC isolated from 3xTg AD mice. Two-way ANOVA revealed a significant effect of treatment (p=0.0072)**(Figure 25B)** (1).

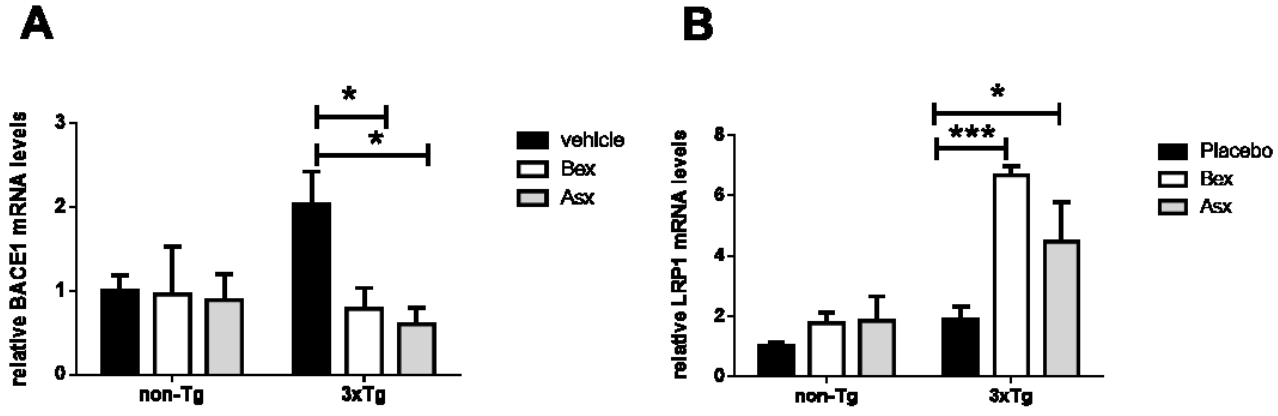

Figure 25: Bex and Asx increase *LRP-1* and decrease *BACE1* levels in mBCEC of 3xTg AD mice

(A-B) *Study I:* Female 3xTg AD mice and C57BL/6 (non-Tg) mice were gavaged for 6 days vehicle (10% DMSO and corn oil) (n=10), Bex (n=9) and Asx (n=8) and non-Tg mice, vehicle (n=5), Bex (n=6) and Asx (n=7). Two to three hemispheres were pooled to isolate mBCEC RNA was isolated and reverse-transcribed to cDNA. QRT-PCR analysis was performed using the $^{\Delta\Delta}$Ct method and HPRT1 as housekeeping gene. Data were normalized to vehicle-treated non-Tg mice. All data represent mean±SEM from 3 to 4 samples performed in triplicates (*p≤0.05; **p≤0.01; ***p≤0.001 vs controls). [Reproduced from Fanaee-Danesh E et al. with permission of Biochim Biophys Acta Mol Basis Dis (1)].

4.14 Effects of Bex and Asx on *APOE, ABCA1, BACE1,* and *LRP-1* levels in mBCEC of aged 3xTg AD mice

In *study II*, over 1-year-old female 3xTg AD mice (68-92 weeks) were gavaged for 6 days with DMSO in corn oil as vehicle/control, 100 mg/kg Bex, or 80 mg/kg Asx in DMSO and corn oil. For isolation of mBCEC, 3 hemispheres were pooled. Similar to the results obtained in *study I* (where younger animals were used), Bex treatment resulted in a 2.2±0.19-fold enhanced *ABCA1* mRNA expression in mBCEC compared to vehicle-treated mice **(Figure 26A)**. Two-way ANOVA revealed a significant effect of treatment (P=0.0001). No changes were observed in *ABCA1* mRNA levels in mBCEC isolated after administration of Asx **(Figure 26A)**. Furthermore, Bex treatment enhanced *APOE* mRNA levels in isolated mBCEC by 1.4±0.1-fold. Two-way ANOVA

revealed a significant effect of treatment (P=0.0024) while no significant effect was observed under Asx treatment conditions **(Figure 26B)** when compared to vehicle-treated 3xTg AD animals (1).

Interestingly, and similar to what we observed in study *I* in younger mice, a marked reduction in *BACE1* mRNA levels was found in mBCEC from aged 3xTg AD mice upon Bex treatment (-79±25.7%) or upon Asx treatment (-66±17.6%; **Figure 26C**) when compared to vehicle-treated animals. Two-way ANOVA revealed a significant effect of treatment (P=0.0004). In these group of mice an increase in LRP-1 mRNA Levels although not significantly was observed **(Figure 26D)** (1).

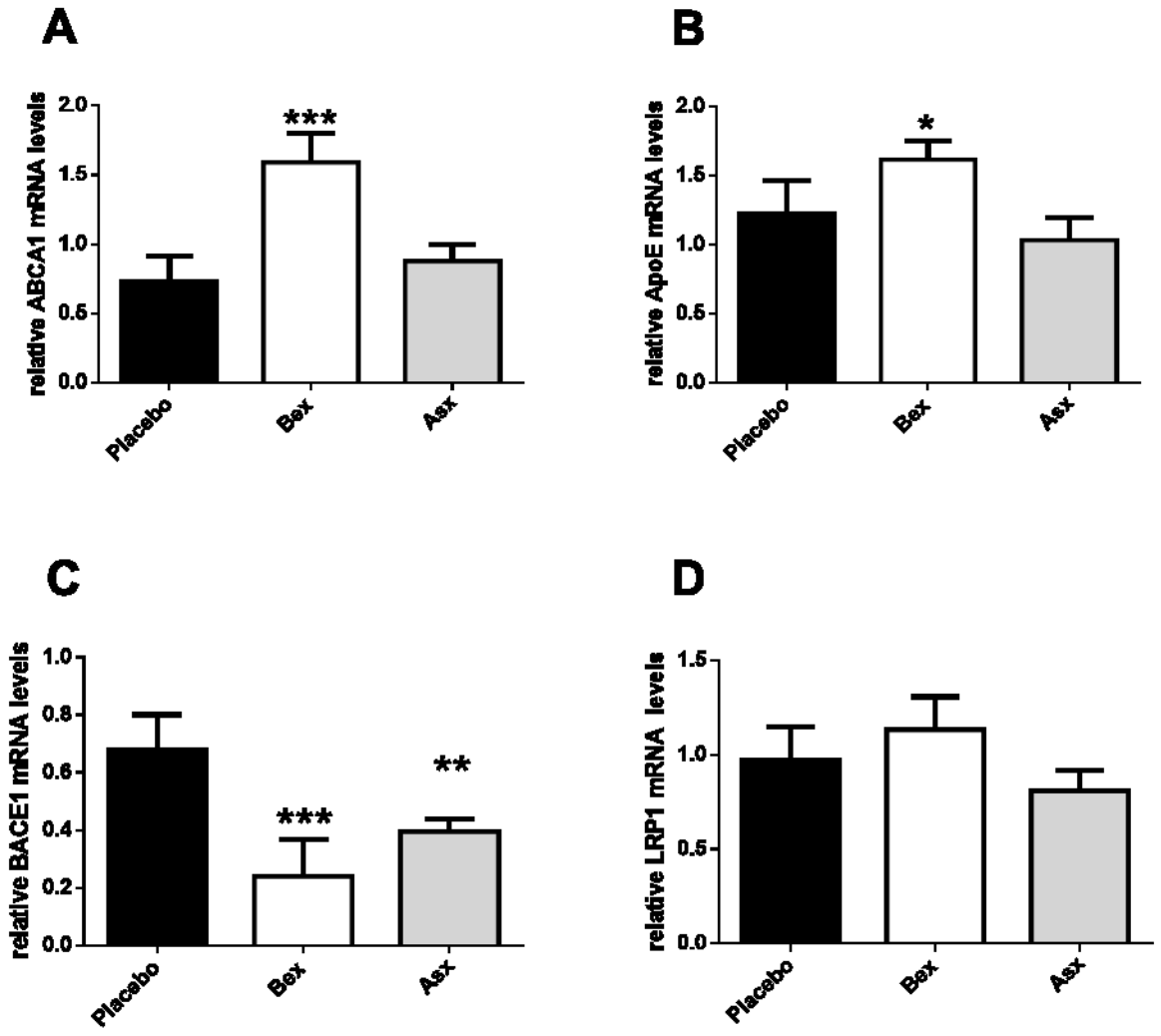

Figure 26: Bex enhances *ABCA1* and *APOE, Bex* and Asx decrease *BACE1* expression levels in mBCEC of 3xTg AD mice

(A-D) *Study II:* Female 3xTg AD mice (68-92 weeks, *study II*) were gavaged for 7 days with DMSO in corn oil as vehicle/control (N=8), 100 mg/kg Bex (N=6), or 80 mg/kg Asx (N=8) in DMSO and corn oil.

Two hemispheres were pooled to isolate mBCEC and RNA isolation was performed from mBCEC, reverse-transcribed to cDNA. qPCR analysis was performed using the $^{\Delta\Delta}$Ct method and HPRT1 as housekeeping gene. Data were normalized to vehicle non-Tg animals. All data represent mean±SEM from 3 to 4 samples performed in triplicates (*p≤0.05; **p<0.01; ***p<0.001 vs controls). [Reproduced from Fanaee-Danesh E et al. with permission of Biochim Biophys Acta Mol Basis Dis (1)].

4.15 Bex and Asx reduce Aβ oligomer levels in mBCEC of 3xTg AD mice

In *study I*, female 3xTg AD mice (32-49 weeks) and non-Tg mice (37-49 weeks) and in *study II*, aged female 3xTg AD mice (68-92 weeks) were gavaged for 6 days with either DMSO in corn oil (vehicle control), 100 mg/kg Bex or 80 mg/kg Asx in DMSO and corn oil (1). mBCEC were isolated from (2-3) pooled hemispheres from various mice of distinct groups.

In *study I*, mBCEC were homogenized and aliquots of protein lysates were loaded on 4-12% Bis-Tris gels for subsequent immunoblot experiments to detect expression of Aβ oligomers. Substantially, a particular immunoreactive ~56 kDa band (identified as murine Aβ oligomers (251) was detected in mBCEC protein lysates. Remarkably, Aβ oligomers were almost cleared in mBCEC from 3xTg AD mice when treated with either Bex (reduction by 93±30.3%) or Asx (reduction by 94±12.6%) **(Figure 27A)** as compared to vehicle-treated 3xTg AD mice. Two-way ANOVA demonstrated a significant effect of treatment ($p<0.0001$) (1).

Principally in *study II*, similar to *study I* a marked immunoreactive ~56 kDa band (indicative for Aβ oligomers) was also detected in mBCEC protein lysates. Aβ oligomers were almost cleared in mBCEC from 3xTg AD mice when treated with either Bex (reduction by 89±11.9%) or Asx (reduction by 90±20.3%) **(Figure 27B)** as compared to vehicle-treated 3xTg AD mice. Two-way ANOVA showed a significant effect of treatment ($p<0.0001$) (1).

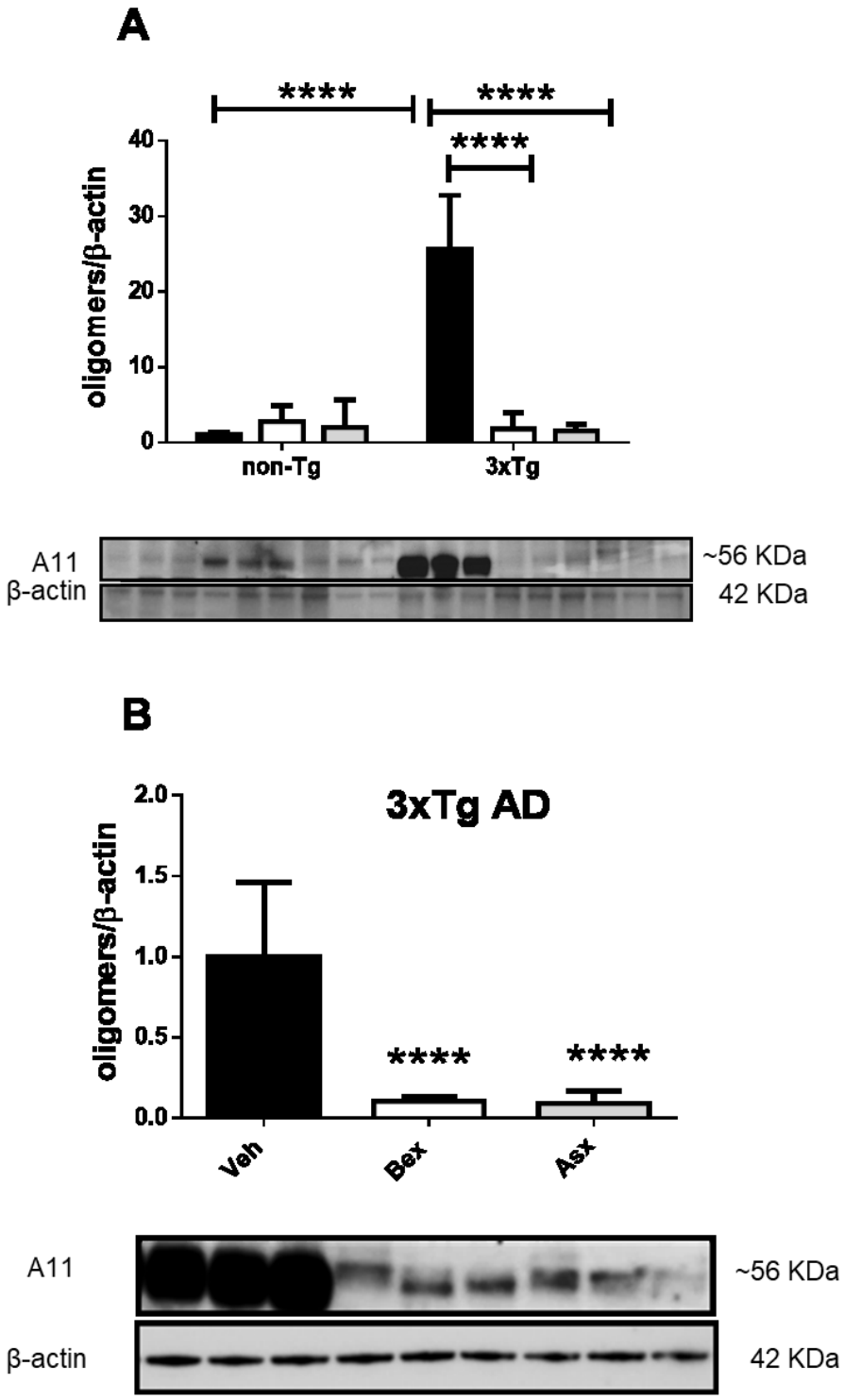

Figure 27: Bex and Asx decrease Aβ oligomer levels in mBCEC of 3xTg AD when compared to non-Tg mice

(A) *Study I:* Female 3xTg AD mice were gavaged for 6 days with DMSO in corn oil as vehicle/control (n=10), Bex (n=9), or Asx (n=8) in DMSO and corn oil and non-Tg mice, vehicle (n=5), Bex (n=6) and Asx (n=7). Two to three hemispheres were pooled to isolate mBCEC. Cellular proteins were extracted,

separated by SDS-PAGE and Aβ oligomers level were detected by immunoblot experiments using polyclonal anti-amyloid oligomer antibody A11 and normalized to β-actin levels. Data shown are mean±SEM of 3 pooled samples (****p≤0.0001 vs controls). **(B)** *study II:* Female 3xTg AD mice were gavaged for 6 days with DMSO in corn oil as vehicle/control (n=8), Bex (n=6), or Asx (n=8) in DMSO and corn oil. Two hemispheres were pooled to isolate mBCEC. Cellular proteins were extracted, separated by SDS-PAGE and Aβ oligomers level were detected by immunoblot experiments using polyclonal anti-amyloid oligomer antibody A11. Immunoreactive bands were normalized to β-actin. Data shown are mean±SEM of 3 to 4 pooled samples (****p≤0.0001 vs controls). [Reproduced from Fanaee-Danesh E et al. with permission of Biochim Biophys Acta Mol Basis Dis (1)].

4.16 Bex treatment reveals significant effects on *BACE1*, *ABCA1*, *APOE* and *LRP-1* expression in brain homogenates of 3xTg AD mice

In addition, mRNA expression levels in total brain lysates of Bex-treated animals showed a 18.0±6.63% reduction for BACE1 **(Figure 28A)** when compared to vehicle-treated 3xTg AD mice. One-way ANOVA revealed a significant effect of treatment in 3xTg AD mice (P=0.0360). Furthermore, a significant and pronounced increase (as observed in isolated mBCEC) was found in total brain homogenates of Bex-treated animals for *ABCA1* (2.4±0.56-fold) **(Figure 28B)**. One-way ANOVA revealed a significant effect of treatment in 3xTg AD mice (P=0.0052). *APOE* mRNA expression levels were elevated (1.6±0.29-fold) **(Figure 28C)**. Two-way ANOVA revealed a significant effect of treatment in 3xTg AD mice (P=0.0024). *LRP-1* mRNA expression levels were elevated by 1.4±0.21-fold **(Figure 28D)** when compared to vehicle-treated 3xTg AD mice. Two-way ANOVA revealed a significant effect of treatment in 3xTg AD mice (P=0.0054). In contrast, total brain homogenates of Asx-treated mice showed no significant changes on these mRNA expression levels mentioned above (1).

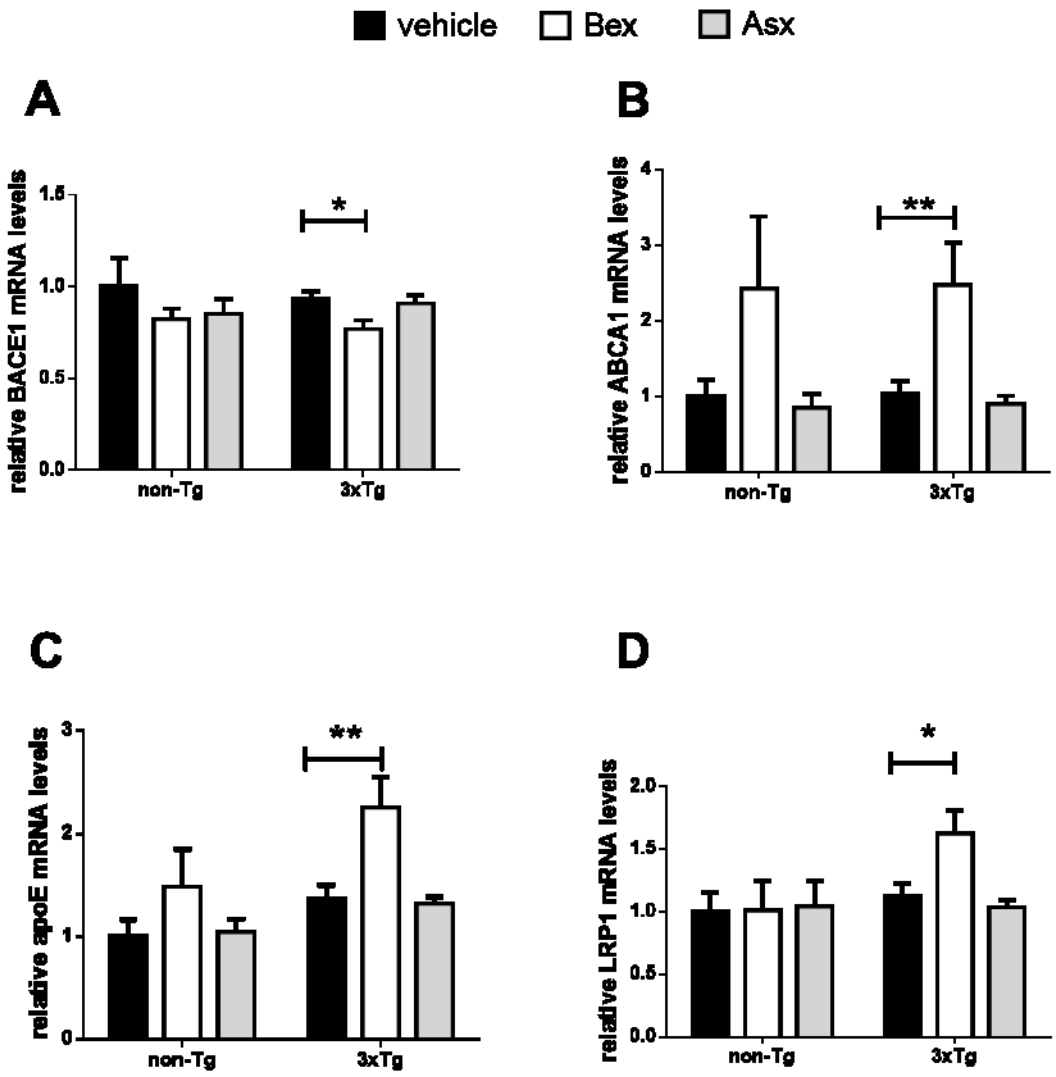

Figure 28: Bex increases *LRP-1, ABCA1*, *APOE* and decreases *BACE1* mRNA expression levels in brain homogenate of 3xTg AD mice

(A-D) *Study I:* Female 3xTg AD mice and C57BL/6 (non-Tg) mice were gavaged for 6 days vehicle (10% DMSO and corn oil) (n=10), Bex (n=9) and Asx (n=8) and non-Tg mice, vehicle (n=5), Bex (n=6) and Asx (n=7). Two to three hemispheres were pooled, RNA was isolated and reverse-transcribed to cDNA. QRT-PCR analysis was performed using the $^{\Delta\Delta}$Ct method and HPRT1 as housekeeping gene. Data were normalized to vehicle-treated non-Tg mice. All data represent mean±SEM from 3 to 4 samples performed in triplicates (*p≤0.05; **p≤0.01 vs controls). [Reproduced from Fanaee-Danesh E et al. with permission of Biochim Biophys Acta Mol Basis Dis (1)].

4.17 Profile of Aβ oligomerization in soluble (DEA) and insoluble (FA) fractions of mouse brain lysates

Immunoblotting experiments were performed for Aβ in the DEA (soluble) and FA (insoluble) fractions from mouse brain lysates, 6E10 was used as primary antibody which recognizes all APP/Aβ species, monomeric and oligomeric Aβ. As expected due to the presence of the human APP transgene, vehicle-treated 3xTg AD revealed higher intensity of monomeric and oligomeric Aβ bands when compared to vehicle-treated non-Tg mice in both fractions (1).

In DEA extracts, six distinct bands were observed, similar to previously described species by (252) **(Figure 29B)**; one band with ~110 kDa indicating APP and the other band with ~56 kDa representing Aβ oligomers (253), in addition to detected ~26 kDa band, all other bands such as trimers/CTF (~13 kDa), dimers (~8 kDa), and the monomeric band (~4 kDa) were displayed (1).

In Bex- and Asx-treated 3xTg AD mice (DEA fraction), a clear reduction in Aβ monomers and trimeric Aβ/CTFβ (~13 kDa) (253) was observed when compared to vehicle-treated 3xTg AD mice **(Figure 29B)**. Interestingly, in both Bex- and Asx-treated 3xTg AD mice, the ~56 putative oligomeric Aβ was also decreased when compared to vehicle-treated 3xTg AD mice **(Figure 29B)**. The ~56 kDa band has been previously characterized in brain soluble extracts from AD patients (254) and in brain tissues from APP transgenic mice (14) (1).

In the FA fraction, Bex- and Asx-treatment in 3xTg AD reduced the high molecular weight Aβ species (~30 and ~60 kDa) when compared to vehicle-treated 3xTg AD mice. In contrast, no significant changes were detected in the monomeric Aβ of FA/insoluble fractions **(Figure 29A)** (1).

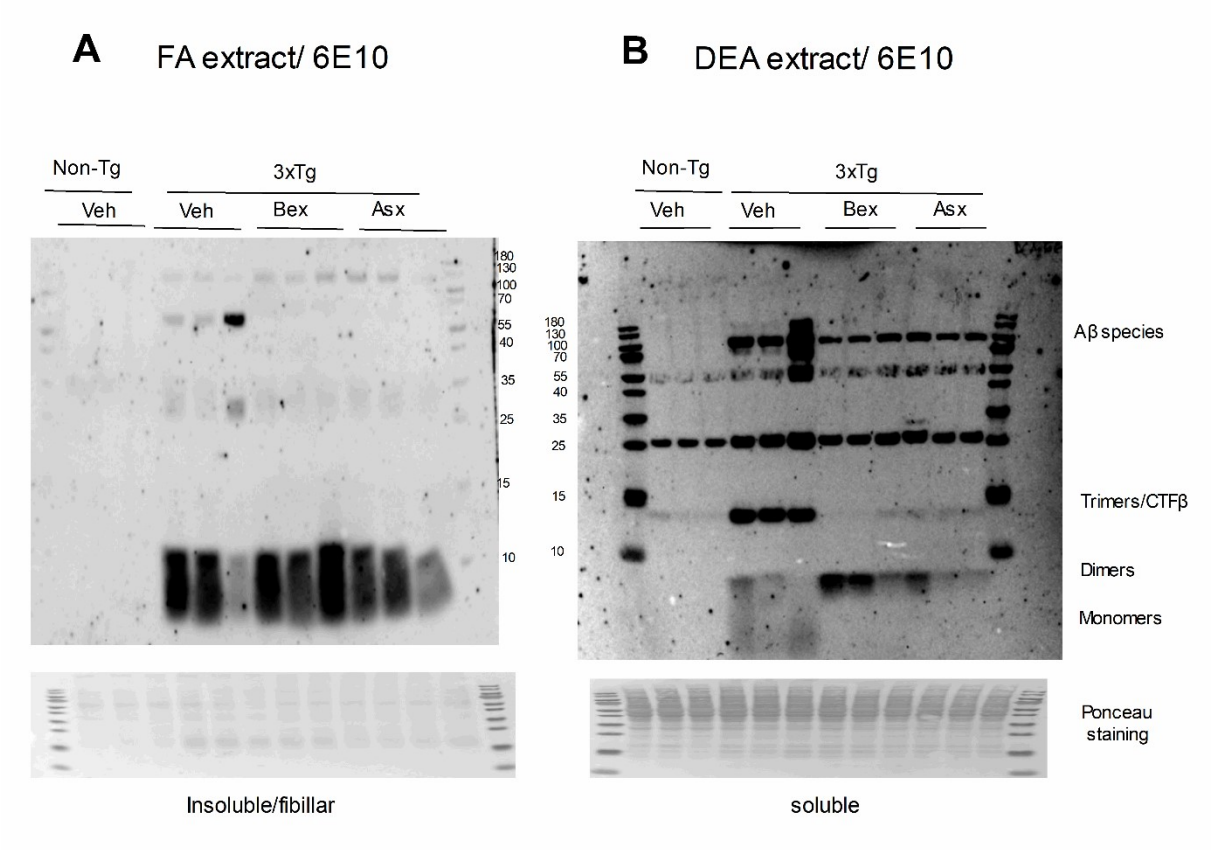

Figure 29: Bex and Asx treatment decrease Aβ species in soluble DEA and insoluble FA brain fractions of 3xTg AD mice

(A-B) Female 3xTg AD mice and C57BL/6 (non-Tg) mice were gavaged for 6 days vehicle (10% DMSO and corn oil) (n=10), Bex (n=9) and Asx (n=8) and non-Tg mice, vehicle (n=5), Bex (n=6) and Asx (n=7). One brain hemisphere of each animal was mechanically homogenized in tissue homogenization buffer and sequential extractions of both insoluble FA and soluble DEA fractions were performed as described in Materials and Methods. Proteins were separated by SDS-PAGE and Aβ species and monomers were detected by immunoblot experiments using 6E10 as primary antibody. Ponceau staining was used as loading control. [Reproduced from Fanaee-Danesh E et al. with permission of Biochim Biophys Acta Mol Basis Dis (1)].

4.18 Bex and Asx reduce Aβ burden in cerebral endothelium and brain parenchyma of 3xTg AD mice

Female 3xTg AD mice (68-92 weeks) in comparison to younger 3xTg AD mice develop normally more severe Aβ deposits, therefore immunofluorescence double staining on snap-frozen 18 µm sections of brains (cortex) derived from *study II* was performed for vWF (vWF is restrained to endothelial cells) and 6E10 (reactive to amino acid residues 1-16 of Aβ). Apparently, vWF and Aβcolocalized. A diffused form of Aβ burden in cerebrovascular cells **(Figure 30Ak)** was observed in Asx-treated mice while Bex-

treated mice showed a reduced number of Aβ epitopes **(Figure 30Ag)** when compared to vehicle-treated mice **(Figure 30Ac)**. In agreement with the results obtained from immunoblot experiments **(Figure 30A, B)**, reduced Aβ load was observed in cerebrovascular cells when treated with Bex and Asx **(Figure 30Ah, 31Al)**, respectively (when compared to vehicle controls) **(Figure 30Ad)** (1).

In addition, both, Aβ oligomer-specific antibody A11 and anti-β-Amyloid 6E10 antibody were applied on snap-frozen brain sections from female 3xTg AD mice (68-92 weeks). In Bex- **(Figure 30Bd, 31Be)** or Asx- **(Figure 30Bg, 31Bh)** treated mice, a marked reduction of immunofluorescence of Aβ/oligomers was detected when compared to vehicle-treated 3xTg AD mice **(Figure 30Ba, 31Bb)** (1).

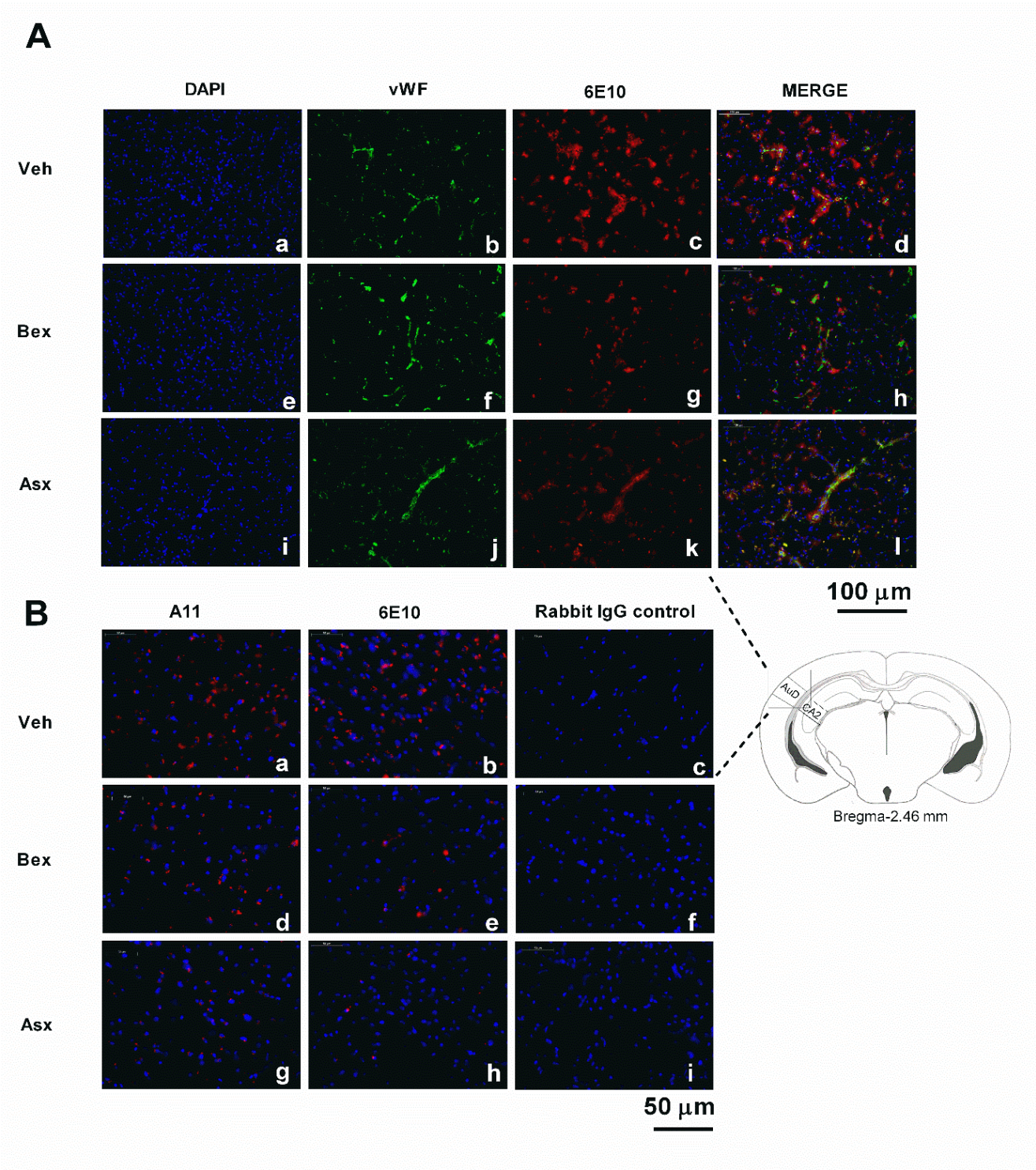

Figure 30: Bex and Asx reduce Aβ levels shown with specific staining in brain capillary endothelial cells and in brain parenchyma of aged 3xTg AD mice

(A) Immunofluorescence double staining was performed on snap-frozen 18 µm sections of mouse brains obtained from untreated and Bex- or Asx-treated female 3xTg AD mice by using anti-Aβ antibody (6E10) at 5.0 µg/ml (**c,g,k**) and rabbit anti-human-vWF at 0.16 µg/ml (**b,f,j**) for 1 h. Sections were washed with TBST and secondary antibodies, i.e. goat anti-rabbit Cy-3 (red, 1.88 µg/ml) and donkey anti-rabbit

Dylight 488 (green, 1.66 µg/ml) were applied for 30 min. Sections were rinsed with TBST and DAPI was added to the slides for 20 min as a nuclei counter stain (blue). Images are from auditory cortex dorsal part. Veh (vehicle). **(B)** Immunofluorescence staining was performed on snap-frozen mouse brain 18 µm sections by using polyclonal anti-amyloid oligomer antibody A11 (AB9234, 8 µg/ml) (**a,d,g**) and anti-Aβ antibody 6E10 (SIG-39320, 5 µg/ml) (**b,e,h**) for 1 h. Slides were washed with TBST and goat anti-rabbit Cy-3 (red, 1.88 µg/ml) was used as a secondary antibody (30 min). Sections were rinsed again with TBST and DAPI was added to the slides for 20 min as a nuclei counter stain (blue). Non-immune rabbit or mouse IgG was used as negative control (**c,f,i**). Images are from auditory cortex dorsal part. [Reproduced from Fanaee-Danesh E et al. with permission of Biochim Biophys Acta Mol Basis Dis (1)].

4.19 Bex reduces Aβ in APP/PS1 and APP/PS1/SREBP2 mice when compared to vehicle-treated animals

In addition to 3xTg AD mice, immunohistochemical staining was performed on sections of paraffin-embedded brains derived from transgenic APP/PS1 (APPswe/PS1ΔE9) (24-40 weeks) and APP/PS1/SREBP2 mice that overexpress the dominant-positive truncated form of the sterol regulatory element-binding protein 2 (SREBP2) (24-40 weeks). These animals exhibit mitochondrial cholesterol accumulation, enhanced oxidative damage and higher Aβ deposition (255). As the number of mice available for the different treatment regimens was limited, studies were performed only with Bex. A reduction of Aβ plaques in brains of APP/PS1 and APP/PS1/SREBP2 mice was evident in Bex-treated animals **(Figure 31C, E)** when compared to vehicle-treated animals **(Figure 31B, D)**.

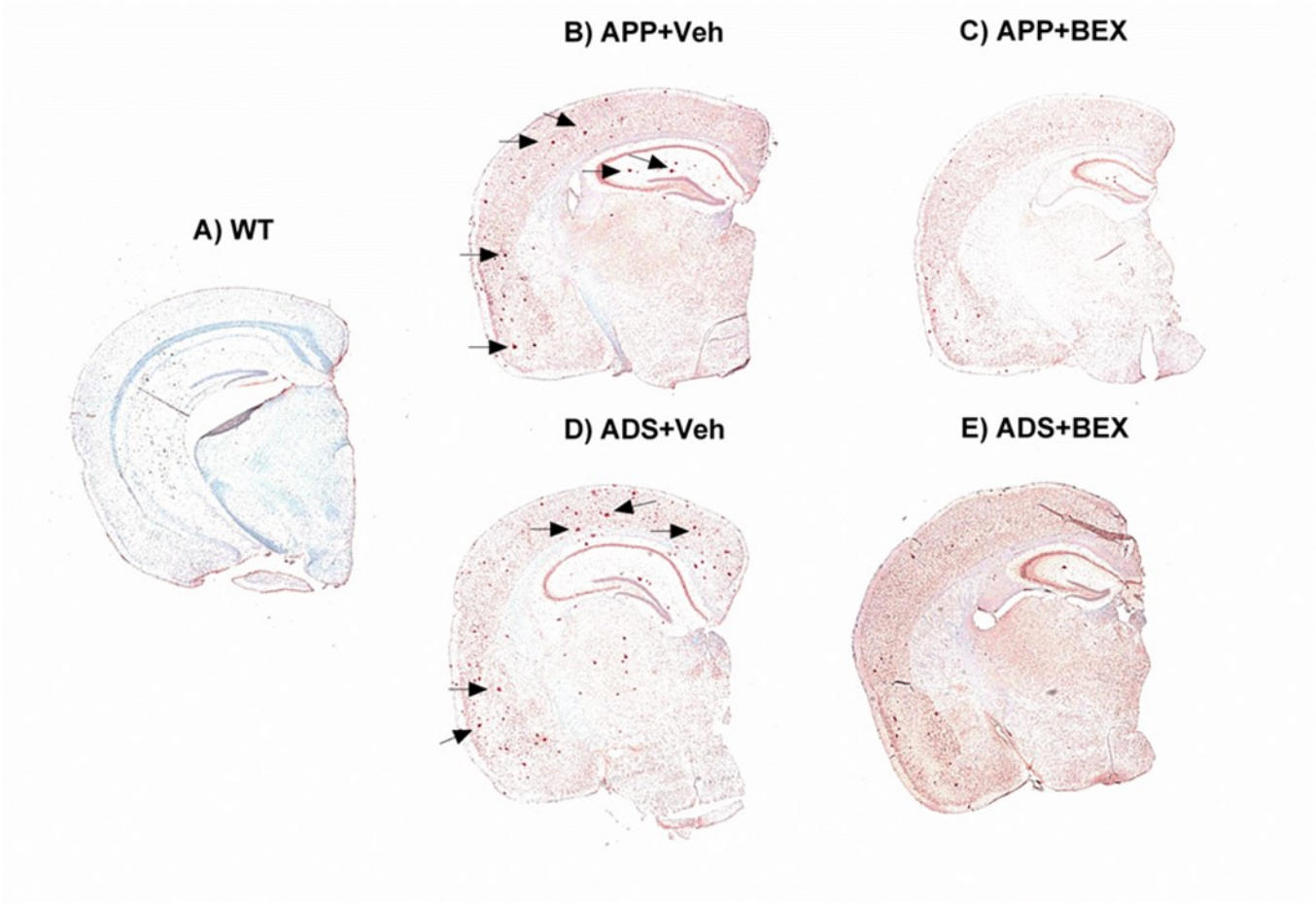

Figure 31: Bex reduces Aβ plaques in male transgenic APP/PS1 and APP/PS1/SREBP2 mice compared to vehicle-treated mice

(A) Male wild-type mice, **(B-C)** male transgenic APP/PS1 mice (APP) and **(D-E)** male (APP/PS1/SREBP2) (ADS) mice (N=3; 24-40 weeks) were gavaged daily for 7 days with ethanol as vehicle/control and 100 mg/kg Bex (in ethanol and corn oil). Immunohistochemistry was performed on paraffin-embedded 5 µm brain sections using anti-β-Amyloid 6E10 (5.0 µg/ml, 1 h) as primary antibody. Sections were washed with PBS for 5 min, primary antibody enhancer was used for 30 min and HRP polymer was applied for 20 min. Then the sections were incubated with 3-amino-9-ethylcarbazol for 10 min counterstained with Mayer's Hematoxylin and mounted with Kaiser's glycerol gelatin. Some of the plaques are indicated with arrows.

4.20 Nissl staining on brain sections of Bex and Asx treated 3xTg AD mice

Our *in vivo* studies obtained significant results in very short acute experimentation (6 days). The deposition of Aβ and changes in amyloid levels occur over prolonged periods of time and the rapid acute effects in the present study may raise the concern that the finding might be an artifact of cell death or other indirect causes

Short term effects of Bex are well established: upon oral administration to a mouse model of AD Bex cleared soluble Aβ within hours, and even Aβ plaque area was reduced by more than 50% within just 72 h (164). Short-term effects have also been reported for Asx, albeit in rats: Asx treatment (30 mg/kg) improved CA1 hippocampal neuronal density after a 7 day treatment in a rat global cerebral ischemia model (204), Asx (10-40 mg/kg) effectively improved cognitive function and reduced cerebral inflammation in diabetes mellitus in a rat model (Male Wistar rats) after 5 days.

In order to assess the potential of cell death occurring, we applied Nissl staining on 18 µm cryosections from snap-frozen mouse brain from vehicle-, Bex- and Asx-treated 3xTg AD mice and non-Tg mice. No significant morphological changes such as shrunken cell bodies or dark cytoplasm were observed after 6 d treatment with Bex or Asx **(Figure 32)**. In accordance with cytoprotective properties observed during the present thesis (e.g. section 4.9), this result confirmed that no significant cell death of cell bodies occurred with acute Asx and Bex treatments applied (1).

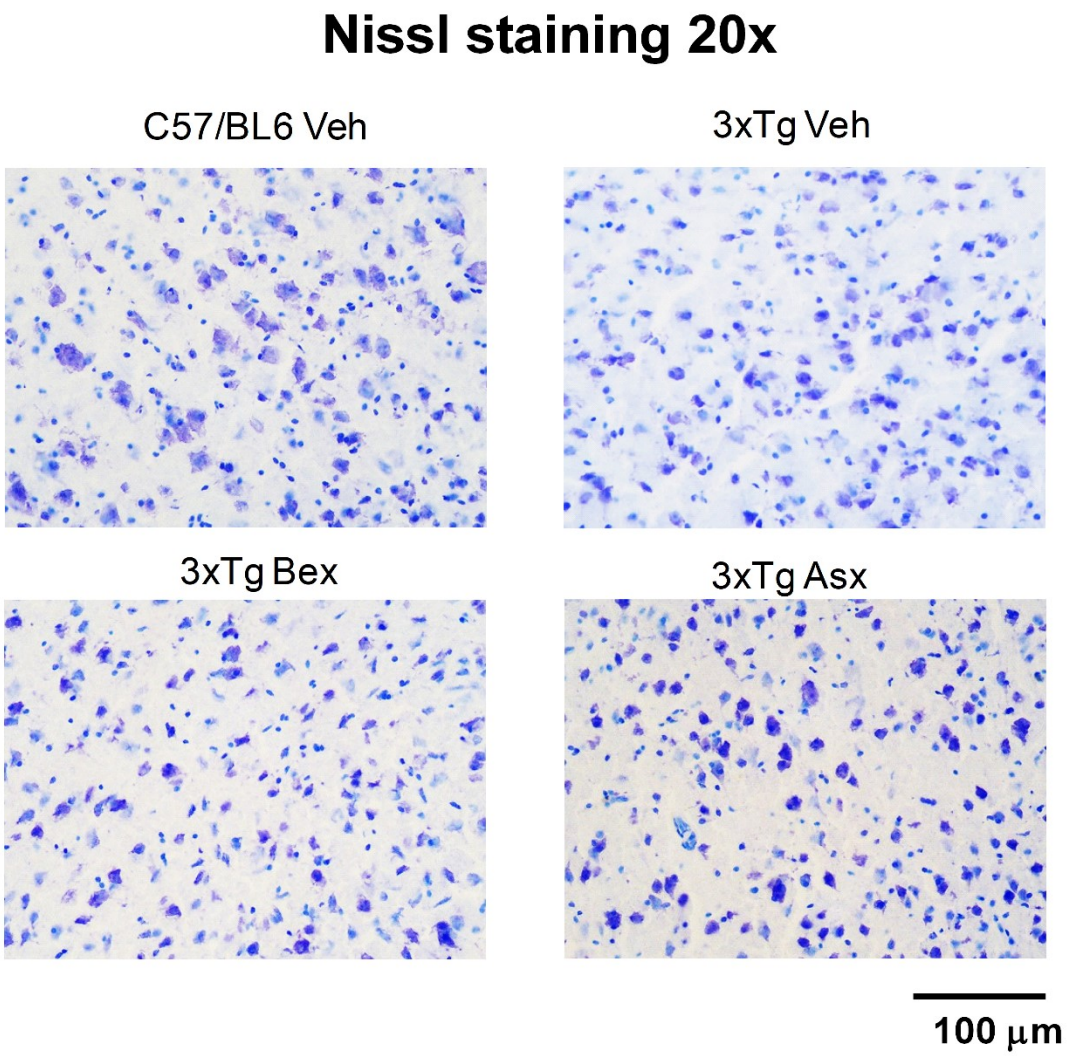

Figure 32: Bex and Asx have no effect on the morphology of neural tissue

Female 3xTg AD mice were gavaged for 6 days vehicle (10% DMSO and corn oil) (n=10), Bex (n=9), or Asx (n=8) and non-Tg (C57BL/6) mice with vehicle (n=5), Bex (n=6) and Asx (n=7). Snap-frozen mouse brain (hippocampus) sections were fixed with 4% PFA for 15 min and immunohistochemical staining was performed on mouse brain 18 µm sections using 0.1% thionine for 5 sec. Sections were washed with ddH_2O and mounted with permount. Scale bar=100 µm. [Reproduced from Fanaee-Danesh E et al. with permission of Biochim Biophys Acta Mol Basis Dis (1)].

5. Discussion

Parts of this chapter have been literally published in:
Fanaee-Danesh E, Gali CC, Tadic J, Zandl-Lang M, Carmen Kober A, Agujetas VR, et al. Astaxanthin exerts protective effects similar to bexarotene in Alzheimer's disease by modulating amyloid-beta and cholesterol homeostasis in blood-brain barrier endothelial cells. Biochim Biophys Acta Mol Basis Dis. 2019 Sep 1;1865(9):2224–45 (1).

The primary goal of this thesis project was to examine the effects of Asx, a PPARα agonist, and Bex, an RXR agonist, on APP processing and cleavage products (sAPPα, CTF), Aβ transfer across the BBB, and on pathways essential for maintaining cholesterol homeostasis in cerebrovascular endothelium the BBB.
Our major results can be summarized as follows:
First, both Bex and Asx exert extensive beneficial and similar effects on APP processing, in that generation of non-amyloidogenic cleavage products is increased and presence of amyloidogenic APP/Aβ species is reduced in BCEC.
Second, *BACE1, ABCA1* and *LRP-1* are the major targets that are up-regulated and activated by Bex or Asx treatment in BCEC (*in vitro* and partially *in vivo)* and were identified to bring about the beneficial effects of Bex and Asx on APP processing/Aβ clearance.
Third, a link between ameliorated cellular cholesterol homeostasis in BCEC with decreased Aβ load became apparent.

Of the two compounds investigated in the present thesis, Bex has been more extensively studied in relation to AD. Bex gavage has been found to lower Aβ load and/or cognitive impairment in mouse models of AD (164,237,253–255) due to its RXR activating properties (130). Corona and coworkers have shown that treatment with Bex (7 d, 100 mg/kg/day) reduced levels of soluble $A\beta_{1-40}$ and $A\beta_{1-42}$ in the hippocampus of ABCA1 wild type APP/PS1 mice but reduction of Aβ levels by Bex was not observed in ABCA1 KO mice. It is worthy to note that also deficits ameliorated by Bex treatment in APP/PS1 mice were ABCA1 depended. Interestingly, in their findings, no changes in insoluble levels of Aβ and plaque loads were detected by Bex treatment, and the

effect of Bex on microglial inflammatory genes was not based on ABCA1 genotype. These data specify the essential role of ABCA1 for Bex to clear hippocampal soluble Aβ and improve cognitive deficits. Yuan and coworkers reported that application of a Bex derivative (OAB-14) for 15 days or 3 months reduced 71% of Aβ in APP/PS1 mice, and this small molecule had no significant side effects regarding body weight or toxicity of the liver.

Asx as natural compound acts as singlet oxygen quencher, lipid peroxidation or oxidative stress inhibitor (259). It has been shown that 0.1 μM of Asx prevents the neurotoxicity of 30 μM of Aβ in rat PC12 cells (an artificial model for neuronal cells) (260). Other reports demonstrated that Asx plays a protective role against Aβ induced ROS as well as calcium dysregulation in primary neurons of hippocampus (261) and BBB disruption (198). However, to our knowledge, protective effects of Asx have not yet been explored *in vitro* or *in vivo* as an effectual modulator of BBB function in AD.

During initial experiments we studied whether Asx and Bex may direct APP processing enzymes, control amyloidogenic Aβ oligomers, and improve non-amyloidogenic APP product sAPPα in pBCEC, a cellular *in vitro* system corresponding to the BBB and known to stimulate APP/Aβ processing and transport (108,109). Asx or Bex treatment dose-dependently elevated mRNA expression levels of *APP,* α secretase *ADAM10* and increased sAPPα protein level were marked in pBCEC (1).

Concurrently, a prominent 6E10-reactive intracellular ~80 kDa APP/Aβ species was almost cleared in pBCEC with the higher doses of Asx/Bex applied. As the antibody clone 6E10 reacts with the processed isoforms of Aβ as well as with various forms of APP, another immunoblotting was additionally performed with anti-C-terminal APP antibody to approve lack of cross-reactivity with anti APP antibody (data not shown). However, the particular nature of the APP processing product remains to be proven in future experiments, maybe by using APP KO mouse brain lysate as a negative control (1).
Moreover, a reduction in β-secretase *BACE1* on mRNA expression and activity levels, along with declined Aβ oligomers in pBCEC were observed (1). In general it appears that Asx and Bex conduct APP processing in pBCEC towards the non-amyloidogenic pathway (1).

It is interesting to note that, in elderly AD patients, ADAM10 levels were found to be lowered when compared to elderly non-AD subjects (259). Promoting the non-amyloidogenic direction or inhibiting the formation of Aβ peptide through stimulating α-secretase ADAM10 as optional therapeutic treatments has been investigated (263). Lowering cholesterol levels might increase α-secretase activity (264). In this connection, outcomes in cell culture systems and/or animal models, have explored that excess cholesterol may promote amyloidogenesis by neuronal cells, on the other side hypercholesterolemia is linked with higher Aβ deposition in the brain (265). Long-term (7 months) cholesterol-rich regimen increased plasma cholesterol and the cholesterol content in neurons in rabbits. In parallel, the level of BACE and Aβ $_{1\text{-}42}$ itself was found to be increased. Cholesterol-BACE1 colocalization has been reported in the hippocampal neurons (CA1 area) of cholesterol-treated animals (266). It is further important to note that lipid rafts play a major role in regulating Aβ production. APP inside raft clusters is cleaved by BACE1 to generate Aβ, whereas APP outside the clusters is cleaved by α-secretase (267). Therefore, APP in cholesterol-rich lipid rafts will be cleaved preferentially by BACE1 due to the high colocalization affinity of cholesterol and BACE1. Importantly, cholesterol dietary regimen was demonstrated to unstabilize the semi-permeability of the BBB (268). Thus, it seems that cholesterol levels somehow interact with β-amyloidogenesis and cytotoxic effects of Aβ, as proteolytic processing of APP mainly takes place in cholesterol-rich lipid rafts localized at cellular membranes (269).

We here report that cellular cholesterol homeostasis is modified in pBCEC after applying Bex or Asx (described under section 4.3). Moreover, we reveal that mRNA and protein expression levels of ABCA1 are enhanced in response to Bex or Asx in pBCEC in a dose and time-dependent course (1). Since LXRs (as do PPARs) heterodimerize with RXR to become active, RXR activation promotes transcription of LXR and PPAR target genes (1). We reported in advance that besides LXR agonists (24(S)OH-cholesterol, TO901317) (80), PPARα agonists (bezafibrate, fenofibrate) PPARgamma (troglitazone, pioglitazone) (so-called regulators of cholesterol mobilization) elevated expression of ABCA1 and apoA-I in pBCEC as well (110). Therefore, a possible interpretation for enhanced ABCA1 and apoA-I/apoE expression by Asx and/or Bex is that both compounds represent potent PPARα or RXR agonists. In this context, it needs to be mentioned that cells in the brain regulate cholesterol

homeostasis differently. Thus, astrocytes act through apoE and lipoproteins, neurons metabolize cholesterol to 24(S)-hydroxycholesterol. ABCA1 is required for cholesterol efflux primarily from astrocytes (270). In Human endothelial cells of the placental barrier, it has been already shown (by our laboratory) that inhibition of ABCA1 led to decreased cholesterol efflux to apoA-I which indicates the essential role of ABCA1 for cholesterol efflux in endothelial cells (271).

The higher doses of Bex [100 nM] and Asx [10 nM] were applied in the absence and presence of RXR or PPARα antagonists to investigate time-course implications on ABCA1 expression and cholesterol efflux from pBCEC (1). Asx and Bex enhanced apoA-I- and HDL_3-mediated [^{3}H]-cholesterol efflux from pBCEC, in accordance with up-regulation of ABCA1 and ABCG1, respectively (1). The two nuclear receptor antagonists partially reversed up-regulation of ABCA1 by Bex or Asx treatments, which was also reflected by decreased cellular cholesterol release (1). Thus, RXR and PPARα appear to have essential regulatory roles in cholesterol homeostasis in pBCEC consistent with previous findings by our group (110) (1).

ApoA-I (the major apolipoprotein in its lipid-free form mediating cellular cholesterol efflux via ABCA1) mRNA expression and secretion of protein was elevated after treatment with Bex in pBCEC. ApoE is another partner apolipoprotein for ABCA1 and most abundant apolipoprotein within the brain, however not expressed in pBCEC. In contrast, apoA-I is synthesized and secreted from pBCEC (80). On another note, apoE is expressed in mBCEC but not apoA-I (unpublished observations by our laboratory).

Moreover, we observed that Bex gavaging 100 mg/kg/day for 6 d significantly elevated *APOE* and *ABCA1* expression levels in mBCEC, while enhanced mRNA expression levels of *ABCA1* by Asx was observed only in pBCEC but not in mBCEC isolated from Asx-gavaged mice (1). This issue in particular needs further investigation. We believe that higher dosis or long-term treatment with Asx may increase ABCA1 and possibly apoE expression levels in mBCEC and total brain. ApoE plays a major role as cholesterol carrier in the brain since it (i) stimulates lipid trafficking, (ii) can link to receptors on the cell-surface to pass lipids, and (iii) may also attach to Aβ contributing to controlling its clearance (171,238,269,270).

In pBCEC, we demonstrated an essential role of active ABCA1 to impact APP processing and Aβ content, since blocking ABCA1 by probucol almost entirely canceled the effects of Bex and Asx by enhancing 6E10-reactive APP/Aβ species in pBCEC and decreasing the non-amyloidogenic sAPPα cellular release. In good agreement with our findings (with Bex), it has been stated that the potential of Bex to clear hippocampal soluble Aβ and to improve cognitive deficits in APP/PS1 mice depends on ABCA1 and ABCA1-induced lipidation of apoE (239) (1).

On the other side, stimulated cellular cholesterol efflux by the apoA-I- or apoE/ABCA1-mediated pathway has also been proven to modify secreted Aβ levels (238). Thus, elevated ABCA1 expression reduced Aβ levels in an AD mouse model (71), and lack of ABCA1 caused further Aβ deposition (241). Of further relevance for the present thesis, it has been reported that treatment with Bex enhanced ABCA1 expression and induced cholesterol efflux in an *in vitro* model of human BCEC (240). Regarding Asx effects, cholesterol efflux from macrophages has been reported earlier by others to be promoted by Asx application at 10-100 µM for 24 h (271). Previous findings have shown that Asx (6 and 12 mg/day for 12 weeks) as dietary supplementation increases serum levels of HDL-cholesterol in humans (272,273), and increased cellular cholesterol efflux was in agreement with this observation (1).
It is also known that Aβ aggregation into fibrils can be prevented by the presence of HDL-like particles (274). In the present thesis, Asx and Bex (i) improved cholesterol release and (ii) diminished cholesterol biosynthesis and cholesterol esterification from [^{14}C]-acetate in pBCEC. Overall, both drugs act clearly as regulators of cellular cholesterol and Aβ homeostasis; moreover, both drugs direct cholesterol efflux by modulating expression of ABCA1 and by decreasing cholesterol ester content and cholesterol biosynthesis in pBCEC. The present findings further demonstrate that declined *de novo* cholesterol synthesis by both compounds promotes the non-amyloidogenic pathway in pBCEC due to their ability for altering of total cellular cholesterol pools (1).

We determined the effects of both Asx and Bex on *in vitro* uptake and transport of $A\beta_{1-40}$ through polarized endothelial cells of cerebrovascular origin, we here verify that Asx and Bex facilitate transcytosis of [^{125}I]-$A\beta_{1-40}$ from the ‘brain’ to the ‘plasma’ side. Notably, we found *LRP-1* mRNA expression levels at the BBB, that is required in the uptake, transport, and clearance (89) of Aβ, significantly elevated by Asx and Bex

treatment in pBCEC. LRP-1 contributes to the pathogenesis of the AD (86) particularly, LRP-1 of brain endothelial cells has been considerably explored as a potential target for the treatment of AD (278). Monomeric $A\beta_{1-40}$ can attach to specific domains of LRP-1 (90); on the other side oligomeric or aggregated Aβ is also a weak ligand for LRP-1 as well (90,276). Above all, the critical point of cerebrovascular LRP-1 for Aβ removal from the brain endothelial cells has been lately validated via tamoxifen-inducible deletion of *LRP-1* in the 5xFAD mouse model of AD; LRP1 knockout leads subsequently to reduced plasma Aβ levels but enhanced soluble Aβ in the brain (89). In the present thesis, we declare that LRP-1 accelerates brain Aβ removal and may reduce amyloid content in pBCEC *in vitro*. Our findings further reveal that LRP-1 is required for a reduction in potentially amyloidogenic Aβ species mediated by Bex and Asx, as the silencing of LRP-1 did not modulate Aβ load intracellularly in pBCEC (1). Forebrain neuron-specific LRP-$1^{-/-}$ mice were used by Tachibana and coworkers (170) to show that the beneficial effects of Bex for synaptic integrity depend on neuronal LRP-1, it is worth mentioning that in both nLRP-$1^{-/-}$ and wild-type mice, ABCA1 and apoE levels in the brain were also enhanced by Bex. Neuroinflammation was abolished by Asx through stimulating M2 microglia polarization in BV2 cells stimulated with lipopolysaccharide (280) which was dependent on LRP-1, manifesting a potential anti-inflammatory property of Asx (1).
The *in vivo* studies of the present thesis approved that Bex treatment enhances both *ABCA1* and *apoE* expression levels, and Bex and Asx increased *LRP-1* in mBCEC of 3xTg AD mice (1).

Based on our *in vitro* results obtained from experiments conducted using pBCEC, application of both drugs reduced *BACE1* expression in mBCEC. Remarkably, applying designed BACE1 peptide inhibitors lowered cerebral Aβ levels in mice (281) and BACE inhibitors have been suggested as potential persuasive therapeutics to lower Aβ levels (282). In BACE1 conditional knockout mice, Aβ deposition was reversed and cognitive function was improved (29). Interestingly, a direct though low binding potency of Bex to BACE1 was disclosed (280). It has further been revealed that enhanced cellular cholesterol levels (in Niemann-Pick disease, type C1-deficient cells) may direct amyloidogenic APP processing by modulating the endocytic trafficking of APP and BACE1 (281) and mistrafficked APP and BACE1 was corrected by cholesterol reduction. Thus, lowering cellular cholesterol mediated by Asx or Bex as described in the present thesis might reduce the colocalization of BACE1 with

cholesterol in lipid rafts so APP can be cleaved outside the cluster by α-secretase so reducing Aβ production (1).

We further studied the APP/Aβ content in both brain soluble and insoluble Aβ fractions of 3xTg AD mice and non-Tg mice by immunoblotting. A marked clearance/reduction of monomeric and trimeric/CTFβ and less notable reduction in putative oligomers were observed mostly in soluble Aβ fractions obtained from brains of Bex- and Asx-treated 3xTg AD mice (when compared to vehicle-treated 3xTg AD). In the insoluble fractions, monomeric Aβ was not significantly reduced. Our findings on Bex effects, in general, are in agreement with those by Corona and coworkers (239), indicating lower soluble $A\beta_{1-40}$ and $A\beta_{1-42}$ levels in the hippocampus of Bex-treated ABCA1 wild-type mice which was not observed in ABCA1 knock-out APP/PS1 mice. It is worth to note that insoluble levels of Aβ and plaque burden were also unaltered by Bex in that study (1). Histological staining of cortical sections revealed neither morphological changes nor shrunken cell bodies or dark cytoplasm in Bex- and Asx-treated 3xTg AD mice, which indicates intact neuronal integrity was maintained (Fig. 26) (1).

However, as opposed to Asx, Bex treatment caused adverse side effects such as hepatomegaly and significant weight loss as also reported by (170). Bex administration has been proposed to be re-evaluated since it may modify serum lipid that may elevate the risk of stroke and heart attack (282). As opposed to Bex, Asx can be a possible therapeutic choice for an alternative drug owing to its safety and numerous health-promoting effects (1).

In conclusion **(Figure 33)**, we propose that Asx and Bex increase the removal of Aβ from the brain by elevating transcription of LRP-1 and ABCA1 in BCEC of 3xTg AD mice. Bex and Asx affect not only the clearance but also the production of Aβ, as both drugs favor non-amyloidogenic processing of APP by reducing both BACE1 (mRNA levels and enzyme activity) and lowering Aβ/oligomers in mBCEC and in the brain. Asx and Bex lower both cholesterol biosynthesis and esterification, in contrast, stimulate cholesterol efflux by increasing ABCA1 and apoA-I/E levels. ABCA1 has an essential role in ameliorating BCEC APP/Aβ homeostasis, as inhibition of ABCA1 holds Aβ burden in the cells and suppresses secretion of beneficial, non-amyloidogenic sAPPα. Asx and Bex facilitate the non-amyloidogenic pathway of APP processing, defined by elevated *ADAM10* and sAPPα levels. On the other side, amyloidogenic APP

processing is suppressed by reduced BACE1 activity. As a consequence, less Aβ is produced by BCEC. At the same time, enhanced LRP-1 levels at the BBB presumably participate in Aβ clearance by accelerating uptake of Aβ and transcytosis across at the BBB, subsequently, alleviating Aβ/oligomers in the cerebrovasculature as well as in the brain (1).

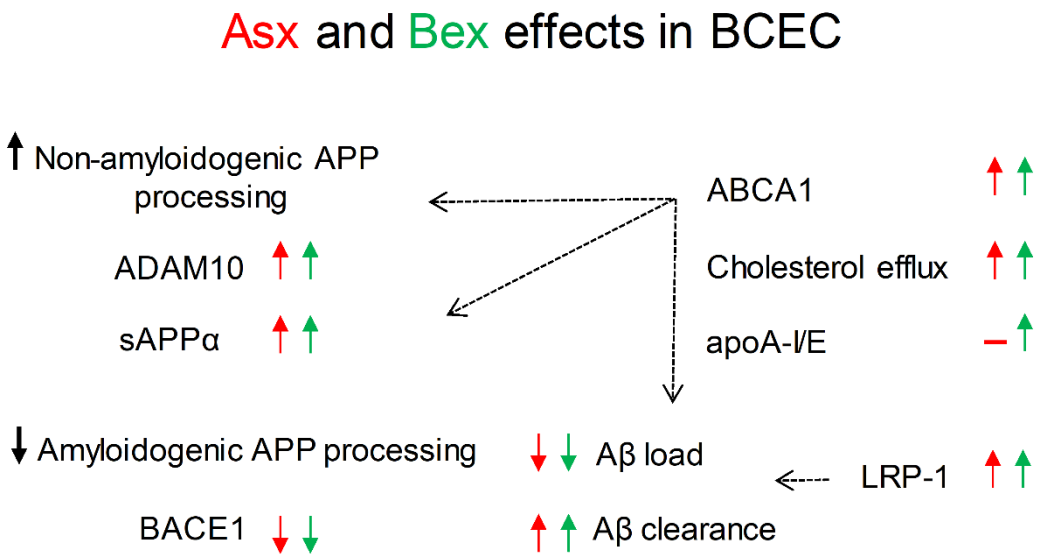

Figure 33: Bex and Asx have beneficial effects in brain capillary endothelial cells

Asx. (red) and Bex (green) reduce cholesterol biosynthesis and esterification but promote cholesterol efflux by elevating ABCA1 and apoA-I/E levels. ABCA1 plays a crucial role in improving BCEC APP/Aβ homeostasis, as inhibition of ABCA1 retains Aβ load in the cells and decreases secretion of beneficial, non-amyloidogenic sAPPα. Asx and Bex promote the non-amyloidogenic route of APP processing, represented by elevated ADAM10 and sAPPα levels. In parallel, amyloidogenic APP processing is diminished by reduced BACE1 activity. Consequently, less Aβ is produced by BCEC. In parallel, LRP-1 levels at the BBB are increased likely contributing to enhanced Aβ clearance by accelerating Aβ uptake and transcytosis across at the BBB, in turn reducing Aβ/oligomers in the cerebrovasculature and in the brain. [Reproduced from Fanaee-Danesh E et al. with permission of Biochim Biophys Acta Mol Basis Dis (1)].

6. References

1. Fanaee-Danesh E, Gali CC, Tadic J, Zandl-Lang M, Carmen Kober A, Agujetas VR, et al. Astaxanthin exerts protective effects similar to bexarotene in Alzheimer's disease by modulating amyloid-beta and cholesterol homeostasis in blood-brain barrier endothelial cells. Biochim Biophys Acta Mol Basis Dis. 2019 Sep 1;1865(9):2224–45.

2. MacDuffie KE, Atkins AS, Flegal KE, Clark CM, Reuter-Lorenz PA. Memory distortion in Alzheimer's disease: deficient monitoring of short- and long-term memory. Neuropsychology. 2012 Jul;26(4):509–16.

3. Corrada MM, Brookmeyer R, Paganini-Hill A, Berlau D, Kawas CH. Dementia incidence continues to increase with age in the oldest old: the 90+ study. Ann Neurol. 2010 Jan;67(1):114–21.

4. Isik AT. Late onset Alzheimer's disease in older people. Clin Interv Aging. 2010 Oct 11;5:307–11.

5. Joas E, Bäckman K, Gustafson D, Ostling S, Waern M, Guo X, et al. Blood pressure trajectories from midlife to late life in relation to dementia in women followed for 37 years. Hypertens Dallas Tex 1979. 2012 Apr;59(4):796–801.

6. Tolppanen A-M, Solomon A, Soininen H, Kivipelto M. Midlife vascular risk factors and Alzheimer's disease: evidence from epidemiological studies. J Alzheimers Dis JAD. 2012;32(3):531–40.

7. Johansson L, Guo X, Waern M, Ostling S, Gustafson D, Bengtsson C, et al. Midlife psychological stress and risk of dementia: a 35-year longitudinal population study. Brain J Neurol. 2010 Aug;133(Pt 8):2217–24.

8. Mehlig K, Skoog I, Waern M, Miao Jonasson J, Lapidus L, Björkelund C, et al. Physical activity, weight status, diabetes and dementia: a 34-year follow-up of the population study of women in Gothenburg. Neuroepidemiology. 2014;42(4):252–9.

9. Scarmeas N, Stern Y. Imaging studies and APOE genotype in persons at risk for Alzheimer's disease. Curr Psychiatry Rep. 2006 Feb;8(1):11–7.

10. Grundke-Iqbal I, Iqbal K, Tung YC, Quinlan M, Wisniewski HM, Binder LI. Abnormal phosphorylation of the microtubule-associated protein tau (tau) in Alzheimer cytoskeletal pathology. Proc Natl Acad Sci U S A. 1986 Jul;83(13):4913–7.

11. Anand R, Gill KD, Mahdi AA. Therapeutics of Alzheimer's disease: Past, present and future. Neuropharmacology. 2014 Jan;76 Pt A:27–50.

12. Glenner GG, Wong CW. Alzheimer's disease: initial report of the purification and characterization of a novel cerebrovascular amyloid protein. Biochem Biophys Res Commun. 1984 May 16;120(3):885–90.

13. Bitan G, Kirkitadze MD, Lomakin A, Vollers SS, Benedek GB, Teplow DB. Amyloid beta -protein (Abeta) assembly: Abeta 40 and Abeta 42 oligomerize through distinct pathways. Proc Natl Acad Sci U S A. 2003 Jan 7;100(1):330–5.

14. Lesné S, Koh MT, Kotilinek L, Kayed R, Glabe CG, Yang A, et al. A specific amyloid-beta protein assembly in the brain impairs memory. Nature. 2006 Mar 16;440(7082):352–7.

15. Wang H-W, Pasternak JF, Kuo H, Ristic H, Lambert MP, Chromy B, et al. Soluble oligomers of beta amyloid (1-42) inhibit long-term potentiation but not long-term depression in rat dentate gyrus. Brain Res. 2002 Jan 11;924(2):133–40.

16. Yanagisawa K. Role of gangliosides in Alzheimer's disease. Biochim Biophys Acta. 2007 Aug;1768(8):1943–51.

17. Yamamoto N, Matsubara E, Maeda S, Minagawa H, Takashima A, Maruyama W, et al. A ganglioside-induced toxic soluble Abeta assembly. Its enhanced formation from Abeta bearing the Arctic mutation. J Biol Chem. 2007 Jan 26;282(4):2646–55.

18. De Felice FG, Velasco PT, Lambert MP, Viola K, Fernandez SJ, Ferreira ST, et al. Abeta oligomers induce neuronal oxidative stress through an N-methyl-D-aspartate receptor-dependent mechanism that is blocked by the Alzheimer drug memantine. J Biol Chem. 2007 Apr 13;282(15):11590–601.

19. Sherrington R, Froelich S, Sorbi S, Campion D, Chi H, Rogaeva EA, et al. Alzheimer's disease associated with mutations in presenilin 2 is rare and variably penetrant. Hum Mol Genet. 1996 Jul;5(7):985–8.

20. Bayer TA, Cappai R, Masters CL, Beyreuther K, Multhaup G. It all sticks together--the APP-related family of proteins and Alzheimer's disease. Mol Psychiatry. 1999 Nov;4(6):524–8.

21. Saitoh T, Sundsmo M, Roch JM, Kimura N, Cole G, Schubert D, et al. Secreted form of amyloid beta protein precursor is involved in the growth regulation of fibroblasts. Cell. 1989 Aug 25;58(4):615–22.

22. Barger SW, Fiscus RR, Ruth P, Hofmann F, Mattson MP. Role of cyclic GMP in the regulation of neuronal calcium and survival by secreted forms of beta-amyloid precursor. J Neurochem. 1995 May;64(5):2087–96.

23. Furukawa K, Barger SW, Blalock EM, Mattson MP. Activation of K+ channels and suppression of neuronal activity by secreted beta-amyloid-precursor protein. Nature. 1996 Jan 4;379(6560):74–8.

24. Sannerud R, Declerck I, Peric A, Raemaekers T, Menendez G, Zhou L, et al. ADP ribosylation factor 6 (ARF6) controls amyloid precursor protein (APP) processing by mediating the endosomal sorting of BACE1. Proc Natl Acad Sci U S A. 2011 Aug 23;108(34):E559-568.

25. Kalvodova L, Kahya N, Schwille P, Ehehalt R, Verkade P, Drechsel D, et al. Lipids as modulators of proteolytic activity of BACE: involvement of cholesterol, glycosphingolipids, and anionic phospholipids in vitro. J Biol Chem. 2005 Nov 4;280(44):36815–23.

26. Zhao J, Fu Y, Yasvoina M, Shao P, Hitt B, O'Connor T, et al. Beta-site amyloid precursor protein cleaving enzyme 1 levels become elevated in neurons around amyloid plaques: implications for Alzheimer's disease pathogenesis. J Neurosci Off J Soc Neurosci. 2007 Apr 4;27(14):3639–49.

27. Crunkhorn S. Alzheimer disease: BACE1 inhibitor reduces β-amyloid production in humans. Nat Rev Drug Discov. 2016 Dec 29;16(1):18.

28. Peters F, Salihoglu H, Rodrigues E, Herzog E, Blume T, Filser S, et al. BACE1 inhibition more effectively suppresses initiation than progression of β-amyloid pathology. Acta Neuropathol (Berl). 2018 Jan 11;

29. Hu X, Das B, Hou H, He W, Yan R. BACE1 deletion in the adult mouse reverses preformed amyloid deposition and improves cognitive functions. J Exp Med. 2018 Feb 14;

30. Vassar R. BACE1: the beta-secretase enzyme in Alzheimer's disease. J Mol Neurosci MN. 2004;23(1–2):105–14.

31. Yan R. Stepping closer to treating Alzheimer's disease patients with BACE1 inhibitor drugs. Transl Neurodegener. 2016;5:13.

32. Lauritzen I, Pardossi-Piquard R, Bauer C, Brigham E, Abraham J-D, Ranaldi S, et al. The β-secretase-derived C-terminal fragment of βAPP, C99, but not Aβ, is a key contributor to early intraneuronal lesions in triple-transgenic mouse hippocampus. J Neurosci Off J Soc Neurosci. 2012 Nov 14;32(46):16243–11655a.

33. Kim S, Sato Y, Mohan PS, Peterhoff C, Pensalfini A, Rigoglioso A, et al. Evidence that the rab5 effector APPL1 mediates APP-βCTF-induced dysfunction of endosomes in Down syndrome and Alzheimer's disease. Mol Psychiatry. 2016 May;21(5):707–16.

34. Panahi A, Bandara A, Pantelopulos GA, Dominguez L, Straub JE. Specific Binding of Cholesterol to C99 Domain of Amyloid Precursor Protein Depends Critically on Charge State of Protein. J Phys Chem Lett. 2016 Sep 15;7(18):3535–41.

35. Chasseigneaux S, Dinc L, Rose C, Chabret C, Coulpier F, Topilko P, et al. Secreted amyloid precursor protein β and secreted amyloid precursor protein α induce axon outgrowth in vitro through Egr1 signaling pathway. PloS One. 2011 Jan 27;6(1):e16301.

36. Nikolaev A, McLaughlin T, O'Leary DDM, Tessier-Lavigne M. APP binds DR6 to trigger axon pruning and neuron death via distinct caspases. Nature. 2009 Feb 19;457(7232):981–9.

37. Wang W, Mutka A-L, Zmrzljak UP, Rozman D, Tanila H, Gylling H, et al. Amyloid precursor protein α- and β-cleaved ectodomains exert opposing control of cholesterol homeostasis via SREBP2. FASEB J Off Publ Fed Am Soc Exp Biol. 2014 Feb;28(2):849–60.

38. Sisodia SS, St George-Hyslop PH. gamma-Secretase, Notch, Abeta and Alzheimer's disease: where do the presenilins fit in? Nat Rev Neurosci. 2002 Apr;3(4):281–90.

39. Sakono M, Zako T. Amyloid oligomers: formation and toxicity of Abeta oligomers. FEBS J. 2010 Mar;277(6):1348–58.

40. Li T, Wen H, Brayton C, Laird FM, Ma G, Peng S, et al. Moderate reduction of gamma-secretase attenuates amyloid burden and limits mechanism-based liabilities. J Neurosci Off J Soc Neurosci. 2007 Oct 3;27(40):10849–59.

41. Vingtdeux V, Sergeant N, Buée L. Potential contribution of exosomes to the prion-like propagation of lesions in Alzheimer's disease. Front Physiol. 2012;3:229.

42. Biffi A, Greenberg SM. Cerebral amyloid angiopathy: a systematic review. J Clin Neurol Seoul Korea. 2011 Mar;7(1):1–9.

43. Prokop S, Stenzel W, Goebel HH, Heppner FL. [Amyloidoses in neuropathology]. Pathol. 2009 May;30(3):193–6.

44. Smith EE, Greenberg SM. Beta-amyloid, blood vessels, and brain function. Stroke. 2009 Jul;40(7):2601–6.

45. Yamada M. Cerebral amyloid angiopathy: emerging concepts. J Stroke. 2015 Jan;17(1):17–30.

46. Stopa EG, Butala P, Salloway S, Johanson CE, Gonzalez L, Tavares R, et al. Cerebral cortical arteriolar angiopathy, vascular beta-amyloid, smooth muscle actin, Braak stage, and APOE genotype. Stroke. 2008 Mar;39(3):814–21.

47. Sudlow C, Martínez González NA, Kim J, Clark C. Does apolipoprotein E genotype influence the risk of ischemic stroke, intracerebral hemorrhage, or subarachnoid hemorrhage? Systematic review and meta-analyses of 31 studies among 5961 cases and 17,965 controls. Stroke. 2006 Feb;37(2):364–70.

48. Holtzman DM. Role of apoe/Abeta interactions in the pathogenesis of Alzheimer's disease and cerebral amyloid angiopathy. J Mol Neurosci MN. 2001 Oct;17(2):147–55.

49. Vonsattel JP, Myers RH, Hedley-Whyte ET, Ropper AH, Bird ED, Richardson EP. Cerebral amyloid angiopathy without and with cerebral hemorrhages: a comparative histological study. Ann Neurol. 1991 Nov;30(5):637–49.

50. Luppe S, Betmouni S, Scolding N, Wilkins A. Cerebral amyloid angiopathy related vasculitis: successful treatment with azathioprine. J Neurol. 2010 Dec;257(12):2103–5.

51. Biffi A, Halpin A, Towfighi A, Gilson A, Busl K, Rost N, et al. Aspirin and recurrent intracerebral hemorrhage in cerebral amyloid angiopathy. Neurology. 2010 Aug 24;75(8):693–8.

52. Kniesel U, Wolburg H. Tight junctions of the blood-brain barrier. Cell Mol Neurobiol. 2000 Feb;20(1):57–76.

53. Bergers G, Song S. The role of pericytes in blood-vessel formation and maintenance. Neuro-Oncol. 2005 Oct;7(4):452–64.

54. Feustel SM, Meissner M, Liesenfeld O. Toxoplasma gondii and the blood-brain barrier. Virulence. 2012 Apr;3(2):182–92.

55. Pajouhesh H, Lenz GR. Medicinal chemical properties of successful central nervous system drugs. NeuroRx J Am Soc Exp Neurother. 2005 Oct;2(4):541–53.

56. Jaeger LB, Dohgu S, Hwang MC, Farr SA, Murphy MP, Fleegal-DeMotta MA, et al. Testing the neurovascular hypothesis of Alzheimer's disease: LRP-1 antisense reduces blood-brain barrier clearance, increases brain levels of amyloid-beta protein, and impairs cognition. J Alzheimers Dis JAD. 2009;17(3):553–70.

57. Tohidpour A, Morgun AV, Boitsova EB, Malinovskaya NA, Martynova GP, Khilazheva ED, et al. Neuroinflammation and Infection: Molecular Mechanisms Associated with Dysfunction of Neurovascular Unit. Front Cell Infect Microbiol. 2017;7:276.

58. de Wit NM, Kooij G, de Vries HE. In Vitro and Ex Vivo Model Systems to Measure ABC Transporter Activity at the Blood-Brain Barrier. Curr Pharm Des. 2016;22(38):5768–73.

59. Uchida Y, Ohtsuki S, Katsukura Y, Ikeda C, Suzuki T, Kamiie J, et al. Quantitative targeted absolute proteomics of human blood-brain barrier transporters and receptors. J Neurochem. 2011 Apr;117(2):333–45.

60. Pardridge WM. Drug transport across the blood-brain barrier. J Cereb Blood Flow Metab Off J Int Soc Cereb Blood Flow Metab. 2012 Nov;32(11):1959–72.

61. Glavinas H, Krajcsi P, Cserepes J, Sarkadi B. The role of ABC transporters in drug resistance, metabolism and toxicity. Curr Drug Deliv. 2004 Jan;1(1):27–42.

62. Albrecht C, Viturro E. The ABCA subfamily--gene and protein structures, functions and associated hereditary diseases. Pflugers Arch. 2007 Feb;453(5):581–9.

63. Locher KP. Review. Structure and mechanism of ATP-binding cassette transporters. Philos Trans R Soc Lond B Biol Sci. 2009 Jan 27;364(1514):239–45.

64. Vasiliou V, Vasiliou K, Nebert DW. Human ATP-binding cassette (ABC) transporter family. Hum Genomics. 2009 Apr;3(3):281–90.

65. Montanari F, Ecker GF. Prediction of drug-ABC-transporter interaction--Recent advances and future challenges. Adv Drug Deliv Rev. 2015 Jun 23;86:17–26.

66. Lefèvre F, Boutry M. Towards Identification of the Substrates of ATP-Binding Cassette Transporters. Plant Physiol. 2018;178(1):18–39.

67. Uehara Y, Saku K. High-density lipoprotein and atherosclerosis: Roles of lipid transporters. World J Cardiol. 2014 Oct 26;6(10):1049–59.

68. Sahoo S, Aurich MK, Jonsson JJ, Thiele I. Membrane transporters in a human genome-scale metabolic knowledgebase and their implications for disease. Front Physiol. 2014;5:91.

69. Tall AR. Cholesterol efflux pathways and other potential mechanisms involved in the athero-protective effect of high density lipoproteins. J Intern Med. 2008 Mar;263(3):256–73.

70. Yin K, Liao D, Tang C. ATP-binding membrane cassette transporter A1 (ABCA1): a possible link between inflammation and reverse cholesterol transport. Mol Med Camb Mass. 2010 Oct;16(9–10):438–49.

71. Wahrle SE, Jiang H, Parsadanian M, Kim J, Li A, Knoten A, et al. Overexpression of ABCA1 reduces amyloid deposition in the PDAPP mouse model of Alzheimer disease. J Clin Invest. 2008 Feb;118(2):671–82.

72. Kim WS, Weickert CS, Garner B. Role of ATP-binding cassette transporters in brain lipid transport and neurological disease. J Neurochem. 2008 Mar;104(5):1145–66.

73. Kober AC, Manavalan APC, Tam-Amersdorfer C, Holmér A, Saeed A, Fanaee-Danesh E, et al. Implications of cerebrovascular ATP-binding cassette transporter G1 (ABCG1) and apolipoprotein M in cholesterol transport at the blood-brain barrier. Biochim Biophys Acta. 2017;1862(6):573–88.

74. Oldfield S, Lowry C, Ruddick J, Lightman S. ABCG4: a novel human white family ABC-transporter expressed in the brain and eye. Biochim Biophys Acta. 2002 Aug 19;1591(1–3):175–9.

75. Wang J, Sun F, Zhang D, Ma Y, Xu F, Belani JD, et al. Sterol transfer by ABCG5 and ABCG8: in vitro assay and reconstitution. J Biol Chem. 2006 Sep 22;281(38):27894–904.

76. Adorni MP, Zimetti F, Billheimer JT, Wang N, Rader DJ, Phillips MC, et al. The roles of different pathways in the release of cholesterol from macrophages. J Lipid Res. 2007 Nov;48(11):2453–62.

77. Larrede S, Quinn CM, Jessup W, Frisdal E, Olivier M, Hsieh V, et al. Stimulation of cholesterol efflux by LXR agonists in cholesterol-loaded human macrophages is ABCA1-dependent but ABCG1-independent. Arterioscler Thromb Vasc Biol. 2009 Nov;29(11):1930–6.

78. Chirackal Manavalan AP, Kober A, Metso J, Lang I, Becker T, Hasslitzer K, et al. Phospholipid transfer protein is expressed in cerebrovascular endothelial

cells and involved in high density lipoprotein biogenesis and remodeling at the blood-brain barrier. J Biol Chem. 2014 Feb 21;289(8):4683–98.

79. Kratzer I, Wernig K, Panzenboeck U, Bernhart E, Reicher H, Wronski R, et al. Apolipoprotein A-I coating of protamine-oligonucleotide nanoparticles increases particle uptake and transcytosis in an in vitro model of the blood-brain barrier. J Control Release Off J Control Release Soc. 2007 Feb 26;117(3):301–11.

80. Panzenboeck U, Balazs Z, Sovic A, Hrzenjak A, Levak-Frank S, Wintersperger A, et al. ABCA1 and scavenger receptor class B, type I, are modulators of reverse sterol transport at an in vitro blood-brain barrier constituted of porcine brain capillary endothelial cells. J Biol Chem. 2002 Nov 8;277(45):42781–9.

81. Rader DJ. Molecular regulation of HDL metabolism and function: implications for novel therapies. J Clin Invest. 2006 Dec;116(12):3090–100.

82. Lillis AP, Van Duyn LB, Murphy-Ullrich JE, Strickland DK. LDL receptor-related protein 1: unique tissue-specific functions revealed by selective gene knockout studies. Physiol Rev. 2008 Jul;88(3):887–918.

83. Sakamoto K, Shinohara T, Adachi Y, Asami T, Ohtaki T. A novel LRP1-binding peptide L57 that crosses the blood brain barrier. Biochem Biophys Rep. 2017 Dec;12:135–9.

84. Zhang J, Liu Q. Cholesterol metabolism and homeostasis in the brain. Protein Cell. 2015 Apr;6(4):254–64.

85. Boucher P, Gotthardt M, Li W-P, Anderson RGW, Herz J. LRP: role in vascular wall integrity and protection from atherosclerosis. Science. 2003 Apr 11;300(5617):329–32.

86. Shinohara M, Tachibana M, Kanekiyo T, Bu G. Role of LRP1 in the pathogenesis of Alzheimer's disease: evidence from clinical and preclinical studies. J Lipid Res. 2017 Jul;58(7):1267–81.

87. Urmoneit B, Prikulis I, Wihl G, D'Urso D, Frank R, Heeren J, et al. Cerebrovascular smooth muscle cells internalize Alzheimer amyloid beta protein via a lipoprotein pathway: implications for cerebral amyloid angiopathy. Lab Investig J Tech Methods Pathol. 1997 Aug;77(2):157–66.

88. Deane R, Bell RD, Sagare A, Zlokovic BV. Clearance of amyloid-beta peptide across the blood-brain barrier: implication for therapies in Alzheimer's disease. CNS Neurol Disord Drug Targets. 2009 Mar;8(1):16–30.

89. Storck SE, Meister S, Nahrath J, Meißner JN, Schubert N, Di Spiezio A, et al. Endothelial LRP1 transports amyloid-β(1-42) across the blood-brain barrier. J Clin Invest. 2016 Jan;126(1):123–36.

90. Deane R, Wu Z, Sagare A, Davis J, Du Yan S, Hamm K, et al. LRP/amyloid beta-peptide interaction mediates differential brain efflux of Abeta isoforms. Neuron. 2004 Aug 5;43(3):333–44.

91. Yamada K, Hashimoto T, Yabuki C, Nagae Y, Tachikawa M, Strickland DK, et al. The low density lipoprotein receptor-related protein 1 mediates uptake of amyloid beta peptides in an in vitro model of the blood-brain barrier cells. J Biol Chem. 2008 Dec 12;283(50):34554–62.

92. Kanekiyo T, Zhang J, Liu Q, Liu C-C, Zhang L, Bu G. Heparan sulphate proteoglycan and the low-density lipoprotein receptor-related protein 1 constitute major pathways for neuronal amyloid-beta uptake. J Neurosci Off J Soc Neurosci. 2011 Feb 2;31(5):1644–51.

93. Muratoglu SC, Mikhailenko I, Newton C, Migliorini M, Strickland DK. Low density lipoprotein receptor-related protein 1 (LRP1) forms a signaling complex with platelet-derived growth factor receptor-beta in endosomes and regulates activation of the MAPK pathway. J Biol Chem. 2010 May 7;285(19):14308–17.

94. Maier W, Bednorz M, Meister S, Roebroek A, Weggen S, Schmitt U, et al. LRP1 is critical for the surface distribution and internalization of the NR2B NMDA receptor subtype. Mol Neurodegener. 2013 Jul 17;8:25.

95. von Einem B, Schwanzar D, Rehn F, Beyer A-S, Weber P, Wagner M, et al. The role of low-density receptor-related protein 1 (LRP1) as a competitive substrate of the amyloid precursor protein (APP) for BACE1. Exp Neurol. 2010 Sep;225(1):85–93.

96. Liu Q, Zhang J, Tran H, Verbeek MM, Reiss K, Estus S, et al. LRP1 shedding in human brain: roles of ADAM10 and ADAM17. Mol Neurodegener. 2009 Apr 16;4:17.

97. Kinoshita A, Shah T, Tangredi MM, Strickland DK, Hyman BT. The intracellular domain of the low density lipoprotein receptor-related protein modulates transactivation mediated by amyloid precursor protein and Fe65. J Biol Chem. 2003 Oct 17;278(42):41182–8.

98. Sagare A, Deane R, Bell RD, Johnson B, Hamm K, Pendu R, et al. Clearance of amyloid-beta by circulating lipoprotein receptors. Nat Med. 2007 Sep;13(9):1029–31.

99. Bu G. The roles of receptor-associated protein (RAP) as a molecular chaperone for members of the LDL receptor family. Int Rev Cytol. 2001;209:79–116.

100. Ulery PG, Beers J, Mikhailenko I, Tanzi RE, Rebeck GW, Hyman BT, et al. Modulation of beta-amyloid precursor protein processing by the low density lipoprotein receptor-related protein (LRP). Evidence that LRP contributes to the pathogenesis of Alzheimer's disease. J Biol Chem. 2000 Mar 10;275(10):7410–5.

101. Pappolla MA, Bryant-Thomas TK, Herbert D, Pacheco J, Fabra Garcia M, Manjon M, et al. Mild hypercholesterolemia is an early risk factor for the development of Alzheimer amyloid pathology. Neurology. 2003 Jul 22;61(2):199–205.

102. Wollmer MA, Streffer JR, Lütjohann D, Tsolaki M, Iakovidou V, Hegi T, et al. ABCA1 modulates CSF cholesterol levels and influences the age at onset of Alzheimer's disease. Neurobiol Aging. 2003 Jun;24(3):421–6.

103. Björkhem I, Meaney S. Brain cholesterol: long secret life behind a barrier. Arterioscler Thromb Vasc Biol. 2004 May;24(5):806–15.

104. Mahley RW. Central Nervous System LipoproteinsHighlights: ApoE and Regulation of Cholesterol Metabolism. Arterioscler Thromb Vasc Biol. 2016 Jul;36(7):1305–15.

105. Koldamova R, Fitz NF, Lefterov I. ATP-binding cassette transporter A1: from metabolism to neurodegeneration. Neurobiol Dis. 2014 Dec;72 Pt A:13–21.

106. Piedrahita JA, Zhang SH, Hagaman JR, Oliver PM, Maeda N. Generation of mice carrying a mutant apolipoprotein E gene inactivated by gene targeting in embryonic stem cells. Proc Natl Acad Sci U S A. 1992 May 15;89(10):4471–5.

107. Lane-Donovan C, Herz J. ApoE, ApoE Receptors, and the Synapse in Alzheimer's Disease. Trends Endocrinol Metab TEM. 2017;28(4):273–84.

108. Schweinzer C, Kober A, Lang I, Etschmaier K, Scholler M, Kresse A, et al. Processing of endogenous AβPP in blood-brain barrier endothelial cells is modulated by liver-X receptor agonists and altered cellular cholesterol homeostasis. J Alzheimers Dis JAD. 2011;27(2):341–60.

109. Zandl-Lang M, Fanaee-Danesh E, Sun Y, Albrecher NM, Gali CC, Čančar I, et al. Regulatory effects of simvastatin and apoJ on APP processing and amyloid-β clearance in blood-brain barrier endothelial cells. Biochim Biophys Acta Mol Cell Biol Lipids. 2018 Jan;1863(1):40–60.

110. Panzenboeck U, Kratzer I, Sovic A, Wintersperger A, Bernhart E, Hammer A, et al. Regulatory effects of synthetic liver X receptor- and peroxisome-proliferator activated receptor agonists on sterol transport pathways in polarized cerebrovascular endothelial cells. Int J Biochem Cell Biol. 2006;38(8):1314–29.

111. Koch S, Donarski N, Goetze K, Kreckel M, Stuerenburg HJ, Buhmann C, et al. Characterization of four lipoprotein classes in human cerebrospinal fluid. J Lipid Res. 2001 Jul;42(7):1143–51.

112. Murray PJ. Understanding and exploiting the endogenous interleukin-10/STAT3-mediated anti-inflammatory response. Curr Opin Pharmacol. 2006 Aug;6(4):379–86.

113. Stukas S, Robert J, Lee M, Kulic I, Carr M, Tourigny K, et al. Intravenously injected human apolipoprotein A-I rapidly enters the central nervous system via the choroid plexus. J Am Heart Assoc. 2014 Nov 12;3(6):e001156.

114. Roheim PS, Carey M, Forte T, Vega GL. Apolipoproteins in human cerebrospinal fluid. Proc Natl Acad Sci U S A. 1979 Sep;76(9):4646–9.

115. Quazi F, Molday RS. Lipid transport by mammalian ABC proteins. Essays Biochem. 2011 Sep 7;50(1):265–90.

116. Sorci-Thomas MG, Bhat S, Thomas MJ. Activation of lecithin:cholesterol acyltransferase by HDL ApoA-I central helices. Clin Lipidol. 2009 Feb;4(1):113–24.

117. Zhao G-J, Yin K, Fu Y-C, Tang C-K. The interaction of ApoA-I and ABCA1 triggers signal transduction pathways to mediate efflux of cellular lipids. Mol Med Camb Mass. 2012 Mar 27;18:149–58.

118. Tang C, Vaughan AM, Oram JF. Janus kinase 2 modulates the apolipoprotein interactions with ABCA1 required for removing cellular cholesterol. J Biol Chem. 2004 Feb 27;279(9):7622–8.

119. Wang N, Silver DL, Costet P, Tall AR. Specific binding of ApoA-I, enhanced cholesterol efflux, and altered plasma membrane morphology in cells expressing ABC1. J Biol Chem. 2000 Oct 20;275(42):33053–8.

120. Takahashi Y, Smith JD. Cholesterol efflux to apolipoprotein AI involves endocytosis and resecretion in a calcium-dependent pathway. Proc Natl Acad Sci U S A. 1999 Sep 28;96(20):11358–63.

121. Saito K, Seishima M, Heyes MP, Song H, Fujigaki S, Maeda S, et al. Marked increases in concentrations of apolipoprotein in the cerebrospinal fluid of poliovirus-infected macaques: relations between apolipoprotein concentrations and severity of brain injury. Biochem J. 1997 Jan 1;321 (Pt 1):145–9.

122. Wisniewski T, Golabek AA, Kida E, Wisniewski KE, Frangione B. Conformational mimicry in Alzheimer's disease. Role of apolipoproteins in amyloidogenesis. Am J Pathol. 1995 Aug;147(2):238–44.

123. Saczynski JS, White L, Peila RL, Rodriguez BL, Launer LJ. The relation between apolipoprotein A-I and dementia: the Honolulu-Asia aging study. Am J Epidemiol. 2007 May 1;165(9):985–92.

124. Golabek A, Marques MA, Lalowski M, Wisniewski T. Amyloid beta binding proteins in vitro and in normal human cerebrospinal fluid. Neurosci Lett. 1995 May 19;191(1–2):79–82.

125. Koldamova RP, Lefterov IM, Lefterova MI, Lazo JS. Apolipoprotein A-I directly interacts with amyloid precursor protein and inhibits A beta aggregation and toxicity. Biochemistry. 2001 Mar 27;40(12):3553–60.

126. Lefterov I, Fitz NF, Cronican AA, Fogg A, Lefterov P, Kodali R, et al. Apolipoprotein A-I deficiency increases cerebral amyloid angiopathy and cognitive deficits in APP/PS1DeltaE9 mice. J Biol Chem. 2010 Nov 19;285(47):36945–57.

127. Kontush A, Chapman MJ. HDL: close to our memories? Arterioscler Thromb Vasc Biol. 2008 Aug;28(8):1418–20.

128. Kim J, Yoon H, Basak J, Kim J. Apolipoprotein E in synaptic plasticity and Alzheimer's disease: potential cellular and molecular mechanisms. Mol Cells. 2014 Nov;37(11):767–76.

129. Lane-Donovan C, Philips GT, Herz J. More than cholesterol transporters: lipoprotein receptors in CNS function and neurodegeneration. Neuron. 2014 Aug 20;83(4):771–87.

130. Mounier A, Georgiev D, Nam KN, Fitz NF, Castranio EL, Wolfe CM, et al. Bexarotene-Activated Retinoid X Receptors Regulate Neuronal Differentiation and Dendritic Complexity. J Neurosci. 2015 Aug 26;35(34):11862–76.

131. Main BS, Villapol S, Sloley SS, Barton DJ, Parsadanian M, Agbaegbu C, et al. Apolipoprotein E4 impairs spontaneous blood brain barrier repair following traumatic brain injury. Mol Neurodegener. 2018 Apr 4;13(1):17.

132. Lahoz C, Schaefer EJ, Cupples LA, Wilson PW, Levy D, Osgood D, et al. Apolipoprotein E genotype and cardiovascular disease in the Framingham Heart Study. Atherosclerosis. 2001 Feb 15;154(3):529–37.

133. Holtzman DM, Bales KR, Tenkova T, Fagan AM, Parsadanian M, Sartorius LJ, et al. Apolipoprotein E isoform-dependent amyloid deposition and neuritic degeneration in a mouse model of Alzheimer's disease. Proc Natl Acad Sci U S A. 2000 Mar 14;97(6):2892–7.

134. Mahley RW, Huang Y. Apolipoprotein (apo) E4 and Alzheimer's disease: unique conformational and biophysical properties of apoE4 can modulate neuropathology. Acta Neurol Scand Suppl. 2006;185:8–14.

135. Hirsch-Reinshagen V, Zhou S, Burgess BL, Bernier L, McIsaac SA, Chan JY, et al. Deficiency of ABCA1 impairs apolipoprotein E metabolism in brain. J Biol Chem. 2004 Sep 24;279(39):41197–207.

136. Michikawa M, Fan QW, Isobe I, Yanagisawa K. Apolipoprotein E exhibits isoform-specific promotion of lipid efflux from astrocytes and neurons in culture. J Neurochem. 2000 Mar;74(3):1008–16.

137. Minagawa H, Gong J-S, Jung C-G, Watanabe A, Lund-Katz S, Phillips MC, et al. Mechanism underlying apolipoprotein E (ApoE) isoform-dependent lipid efflux from neural cells in culture. J Neurosci Res. 2009 Aug 15;87(11):2498–508.

138. Wu L, Zhao L. ApoE2 and Alzheimer's disease: time to take a closer look. Neural Regen Res. 2016 Mar;11(3):412–3.

139. Gomez-Isla T, West HL, Rebeck GW, Harr SD, Growdon JH, Locascio JJ, et al. Clinical and pathological correlates of apolipoprotein E epsilon 4 in Alzheimer's disease. Ann Neurol. 1996 Jan;39(1):62–70.

140. Gibson GE, Haroutunian V, Zhang H, Park LC, Shi Q, Lesser M, et al. Mitochondrial damage in Alzheimer's disease varies with apolipoprotein E genotype. Ann Neurol. 2000 Sep;48(3):297–303.

141. Dodart J-C, Marr RA, Koistinaho M, Gregersen BM, Malkani S, Verma IM, et al. Gene delivery of human apolipoprotein E alters brain Abeta burden in a mouse

model of Alzheimer's disease. Proc Natl Acad Sci U S A. 2005 Jan 25;102(4):1211–6.

142. Altmann A, Tian L, Henderson VW, Greicius MD, Alzheimer's Disease Neuroimaging Initiative Investigators. Sex modifies the APOE-related risk of developing Alzheimer disease. Ann Neurol. 2014 Apr;75(4):563–73.

143. Reed B, Villeneuve S, Mack W, DeCarli C, Chui HC, Jagust W. Associations between serum cholesterol levels and cerebral amyloidosis. JAMA Neurol. 2014 Feb;71(2):195–200.

144. Panchal M, Loeper J, Cossec J-C, Perruchini C, Lazar A, Pompon D, et al. Enrichment of cholesterol in microdissected Alzheimer's disease senile plaques as assessed by mass spectrometry. J Lipid Res. 2010 Mar;51(3):598–605.

145. Xiong H, Callaghan D, Jones A, Walker DG, Lue L-F, Beach TG, et al. Cholesterol retention in Alzheimer's brain is responsible for high beta- and gamma-secretase activities and Abeta production. Neurobiol Dis. 2008 Mar;29(3):422–37.

146. Simons M, Keller P, De Strooper B, Beyreuther K, Dotti CG, Simons K. Cholesterol depletion inhibits the generation of beta-amyloid in hippocampal neurons. Proc Natl Acad Sci U S A. 1998 May 26;95(11):6460–4.

147. Abramov AY, Ionov M, Pavlov E, Duchen MR. Membrane cholesterol content plays a key role in the neurotoxicity of β-amyloid: implications for Alzheimer's disease. Aging Cell. 2011 Aug;10(4):595–603.

148. Kurata T, Kawai H, Miyazaki K, Kozuki M, Morimoto N, Ohta Y, et al. Statins have therapeutic potential for the treatment of Alzheimer's disease, likely via protection of the neurovascular unit in the AD brain. J Neurol Sci. 2012 Nov 15;322(1–2):59–63.

149. Fassbender K, Simons M, Bergmann C, Stroick M, Lutjohann D, Keller P, et al. Simvastatin strongly reduces levels of Alzheimer's disease beta -amyloid peptides Abeta 42 and Abeta 40 in vitro and in vivo. Proc Natl Acad Sci U S A. 2001 May 8;98(10):5856–61.

150. Park I-H, Hwang EM, Hong HS, Boo JH, Oh SS, Lee J, et al. Lovastatin enhances Abeta production and senile plaque deposition in female Tg2576 mice. Neurobiol Aging. 2003 Sep;24(5):637–43.

151. Grimm MOW, Mett J, Grimm HS, Hartmann T. APP Function and Lipids: A Bidirectional Link. Front Mol Neurosci. 2017;10:63.

152. Lefterov I, Fitz NF, Cronican A, Lefterov P, Staufenbiel M, Koldamova R. Memory deficits in APP23/Abca1+/- mice correlate with the level of Aβ oligomers. ASN Neuro. 2009 Apr 30;1(2).

153. Elali A, Rivest S. The role of ABCB1 and ABCA1 in beta-amyloid clearance at the neurovascular unit in Alzheimer's disease. Front Physiol. 2013;4:45.

154. Heck MC, Wagner CE, Shahani PH, MacNeill M, Grozic A, Darwaiz T, et al. Modeling, Synthesis, and Biological Evaluation of Potential Retinoid X Receptor (RXR)-Selective Agonists: Analogues of 4-[1-(3,5,5,8,8-Pentamethyl-5,6,7,8-tetrahydro-2-naphthyl)ethynyl]benzoic Acid (Bexarotene) and 6-(Ethyl(5,5,8,8-tetrahydronaphthalen-2-yl)amino)nicotinic Acid (NEt-TMN). J Med Chem. 2016 Oct 13;59(19):8924–40.

155. Tanita K, Fujimura T, Sato Y, Hidaka T, Furudate S, Kambayashi Y, et al. Successful Treatment of Primary Cutaneous Peripheral T-Cell Lymphoma Presenting Acquired Ichthyosis with Oral Bexarotene Monotherapy. Case Rep Oncol. 2017 Apr;10(1):328–32.

156. Dragnev KH, Petty WJ, Shah SJ, Lewis LD, Black CC, Memoli V, et al. A proof-of-principle clinical trial of bexarotene in patients with non-small cell lung cancer. Clin Cancer Res Off J Am Assoc Cancer Res. 2007 Mar 15;13(6):1794–800.

157. Esteva FJ, Glaspy J, Baidas S, Laufman L, Hutchins L, Dickler M, et al. Multicenter phase II study of oral bexarotene for patients with metastatic breast cancer. J Clin Oncol Off J Am Soc Clin Oncol. 2003 Mar 15;21(6):999–1006.

158. Riancho J, Ruiz-Soto M, Berciano MT, Berciano J, Lafarga M. Neuroprotective Effect of Bexarotene in the SOD1(G93A) Mouse Model of Amyotrophic Lateral Sclerosis. Front Cell Neurosci. 2015;9:250.

159. McFarland K, Spalding TA, Hubbard D, Ma J-N, Olsson R, Burstein ES. Low dose bexarotene treatment rescues dopamine neurons and restores behavioral function in models of Parkinson's disease. ACS Chem Neurosci. 2013 Nov 20;4(11):1430–8.

160. Natrajan MS, Komori M, Kosa P, Johnson KR, Wu T, Franklin RJM, et al. Pioglitazone regulates myelin phagocytosis and multiple sclerosis monocytes. Ann Clin Transl Neurol. 2015;2(12):1071–84.

161. Bomben V, Holth J, Reed J, Cramer P, Landreth G, Noebels J. Bexarotene reduces network excitability in models of Alzheimer's disease and epilepsy. Neurobiol Aging. 2014 Sep;35(9):2091–5.

162. Zhu J, Ning R-B, Lin X-Y, Chai D-J, Xu C-S, Xie H, et al. Retinoid X receptor agonists inhibit hypertension-induced myocardial hypertrophy by modulating LKB1/AMPK/p70S6K signaling pathway. Am J Hypertens. 2014 Aug;27(8):1112–24.

163. Certo M, Endo Y, Ohta K, Sakurada S, Bagetta G, Amantea D. Activation of RXR/PPARγ underlies neuroprotection by bexarotene in ischemic stroke. Pharmacol Res. 2015 Dec;102:298–307.

164. Cramer PE, Cirrito JR, Wesson DW, Lee CYD, Karlo JC, Zinn AE, et al. ApoE-directed therapeutics rapidly clear β-amyloid and reverse deficits in AD mouse models. Science. 2012 Mar 23;335(6075):1503–6.

165. LaClair KD, Manaye KF, Lee DL, Allard JS, Savonenko AV, Troncoso JC, et al. Treatment with bexarotene, a compound that increases apolipoprotein-E, provides no cognitive benefit in mutant APP/PS1 mice. Mol Neurodegener. 2013 Jun 13;8:18.

166. Price AR, Xu G, Siemienski ZB, Smithson LA, Borchelt DR, Golde TE, et al. Comment on “ApoE-directed therapeutics rapidly clear β-amyloid and reverse deficits in AD mouse models.” Science. 2013 May 24;340(6135):924-d.

167. Tesseur I, Lo AC, Roberfroid A, Dietvorst S, Van Broeck B, Borgers M, et al. Comment on “ApoE-directed therapeutics rapidly clear β-amyloid and reverse deficits in AD mouse models.” Science. 2013 May 24;340(6135):924-e.

168. Mariani MM, Malm T, Lamb R, Jay TR, Neilson L, Casali B, et al. Neuronally-directed effects of RXR activation in a mouse model of Alzheimer’s disease. Sci Rep. 2017 Feb 16;7:42270.

169. Repa JJ, Turley SD, Lobaccaro JA, Medina J, Li L, Lustig K, et al. Regulation of absorption and ABC1-mediated efflux of cholesterol by RXR heterodimers. Science. 2000 Sep 1;289(5484):1524–9.

170. Tachibana M, Shinohara M, Yamazaki Y, Liu C-C, Rogers J, Bu G, et al. Rescuing effects of RXR agonist bexarotene on aging-related synapse loss depend on neuronal LRP1. Exp Neurol. 2016 Mar;277:1–9.

171. Tai LM, Koster KP, Luo J, Lee SH, Wang Y, Collins NC, et al. Amyloid-β pathology and APOE genotype modulate retinoid X receptor agonist activity in vivo. J Biol Chem. 2014 Oct 31;289(44):30538–55.

172. Savage JC, Jay T, Goduni E, Quigley C, Mariani MM, Malm T, et al. Nuclear receptors license phagocytosis by trem2+ myeloid cells in mouse models of Alzheimer’s disease. J Neurosci Off J Soc Neurosci. 2015 Apr 22;35(16):6532–43.

173. Yuan C, Guo X, Zhou Q, Du F, Jiang W, Zhou X, et al. OAB-14, a bexarotene derivative, improves Alzheimer’s disease-related pathologies and cognitive impairments by increasing β-amyloid clearance in APP/PS1 mice. Biochim Biophys Acta BBA - Mol Basis Dis [Internet]. 2018 Oct [cited 2018 Nov 6]; Available from: https://linkinghub.elsevier.com/retrieve/pii/S0925443918304319

174. Huuskonen MT, Loppi S, Dhungana H, Keksa-Goldsteine V, Lemarchant S, Korhonen P, et al. Bexarotene targets autophagy and is protective against thromboembolic stroke in aged mice with tauopathy. Sci Rep. 2016 14;6:33176.

175. Dickey AS, Sanchez DN, Arreola M, Sampat KR, Fan W, Arbez N, et al. PPARδ activation by bexarotene promotes neuroprotection by restoring bioenergetic and quality control homeostasis. Sci Transl Med. 2017 Dec 6;9(419).

176. Faul MM, Ratz AM, Sullivan KA, Trankle WG, Winneroski LL. Synthesis of Novel Retinoid X Receptor-Selective Retinoids. J Org Chem. 2001 Aug;66(17):5772–82.

177. Barros MP, Marin DP, Bolin AP, de Cássia Santos Macedo R, Campoio TR, Fineto C, et al. Combined astaxanthin and fish oil supplementation improves glutathione-based redox balance in rat plasma and neutrophils. Chem Biol Interact. 2012 Apr 15;197(1):58–67.

178. Tyagi S, Gupta P, Saini AS, Kaushal C, Sharma S. The peroxisome proliferator-activated receptor: A family of nuclear receptors role in various diseases. J Adv Pharm Technol Res. 2011 Oct;2(4):236–40.

179. Wang Y-X. PPARs: diverse regulators in energy metabolism and metabolic diseases. Cell Res. 2010 Feb;20(2):124–37.

180. Mulholland DJ, Dedhar S, Coetzee GA, Nelson CC. Interaction of nuclear receptors with the Wnt/beta-catenin/Tcf signaling axis: Wnt you like to know? Endocr Rev. 2005 Dec;26(7):898–915.

181. D Orio B, Fracassi A, Cerù MP, Moreno S. Targeting PPARalpha In Alzheimer`s Disease. Curr Alzheimer Res. 2017 04;

182. Kalinin S, Richardson JC, Feinstein DL. A PPARdelta agonist reduces amyloid burden and brain inflammation in a transgenic mouse model of Alzheimer's disease. Curr Alzheimer Res. 2009 Oct;6(5):431–7.

183. Hoque MT, Robillard KR, Bendayan R. Regulation of breast cancer resistant protein by peroxisome proliferator-activated receptor α in human brain microvessel endothelial cells. Mol Pharmacol. 2012 Apr;81(4):598–609.

184. Mysiorek C, Culot M, Dehouck L, Derudas B, Staels B, Bordet R, et al. Peroxisome-proliferator-activated receptor-alpha activation protects brain capillary endothelial cells from oxygen-glucose deprivation-induced hyperpermeability in the blood-brain barrier. Curr Neurovasc Res. 2009 Aug;6(3):181–93.

185. Warden A, Truitt J, Merriman M, Ponomareva O, Jameson K, Ferguson LB, et al. Localization of PPAR isotypes in the adult mouse and human brain. Sci Rep. 2016 10;6:27618.

186. Chakravarthy MV, Zhu Y, López M, Yin L, Wozniak DF, Coleman T, et al. Brain fatty acid synthase activates PPARα to maintain energy homeostasis. J Clin Invest. 2007 Sep 4;117(9):2539–52.

187. Roy A, Jana M, Kundu M, Corbett GT, Rangaswamy SB, Mishra RK, et al. HMG-CoA Reductase Inhibitors Bind to PPARα to Upregulate Neurotrophin Expression in the Brain and Improve Memory in Mice. Cell Metab. 2015 Aug;22(2):253–65.

188. Fidaleo M, Fanelli F, Ceru MP, Moreno S. Neuroprotective properties of peroxisome proliferator-activated receptor alpha (PPARα) and its lipid ligands. Curr Med Chem. 2014;21(24):2803–21.

189. Corbett GT, Gonzalez FJ, Pahan K. Activation of peroxisome proliferator-activated receptor α stimulates ADAM10-mediated proteolysis of APP. Proc Natl Acad Sci. 2015 Jul 7;112(27):8445–50.

190. Jia Y, Kim J-Y, Jun H-J, Kim S-J, Lee J-H, Hoang MH, et al. The natural carotenoid astaxanthin, a PPAR-α agonist and PPAR-γ antagonist, reduces hepatic lipid accumulation by rewiring the transcriptome in lipid-loaded hepatocytes. Mol Nutr Food Res. 2012 Jun;56(6):878–88.

191. Biswal S. Oxidative stress and astaxanthin: The novel supernutrient carotenoid. Int J Health Allied Sci. 2014;3(3):147.

192. McNulty HP, Byun J, Lockwood SF, Jacob RF, Mason RP. Differential effects of carotenoids on lipid peroxidation due to membrane interactions: X-ray diffraction analysis. Biochim Biophys Acta. 2007 Jan;1768(1):167–74.

193. Wu W, Wang X, Xiang Q, Meng X, Peng Y, Du N, et al. Astaxanthin alleviates brain aging in rats by attenuating oxidative stress and increasing BDNF levels. Food Funct. 2014 Jan;5(1):158–66.

194. Grimmig B, Kim S-H, Nash K, Bickford PC, Douglas Shytle R. Neuroprotective mechanisms of astaxanthin: a potential therapeutic role in preserving cognitive function in age and neurodegeneration. GeroScience. 2017;39(1):19–32.

195. Yook JS, Okamoto M, Rakwal R, Shibato J, Lee MC, Matsui T, et al. Astaxanthin supplementation enhances adult hippocampal neurogenesis and spatial memory in mice. Mol Nutr Food Res. 2016 Mar;60(3):589–99.

196. Kim YJ, Kim YA, Yokozawa T. Protection against oxidative stress, inflammation, and apoptosis of high-glucose-exposed proximal tubular epithelial cells by astaxanthin. J Agric Food Chem. 2009 Oct 14;57(19):8793–7.

197. Ambati RR, Phang SM, Ravi S, Aswathanarayana RG. Astaxanthin: sources, extraction, stability, biological activities and its commercial applications--a review. Mar Drugs. 2014 Jan 7;12(1):128–52.

198. Zhang X-S, Zhang X, Wu Q, Li W, Wang C-X, Xie G-B, et al. Astaxanthin offers neuroprotection and reduces neuroinflammation in experimental subarachnoid hemorrhage. J Surg Res. 2014 Nov;192(1):206–13.

199. Yamagishi R, Aihara M. Neuroprotective effect of astaxanthin against rat retinal ganglion cell death under various stresses that induce apoptosis and necrosis. Mol Vis. 2014;20:1796–805.

200. Zhang X-S, Zhang X, Wu Q, Li W, Zhang Q-R, Wang C-X, et al. Astaxanthin alleviates early brain injury following subarachnoid hemorrhage in rats: possible involvement of Akt/bad signaling. Mar Drugs. 2014 Jul 28;12(8):4291–310.

201. Al-Amin MM, Reza HM, Saadi HM, Mahmud W, Ibrahim AA, Alam MM, et al. Astaxanthin ameliorates aluminum chloride-induced spatial memory impairment and neuronal oxidative stress in mice. Eur J Pharmacol. 2016 Apr 15;777:60–9.

202. Zhang X, Pan L, Wei X, Gao H, Liu J. Impact of astaxanthin-enriched algal powder of Haematococcus pluvialis on memory improvement in BALB/c mice. Environ Geochem Health. 2007 Dec;29(6):483–9.

203. Katagiri M, Satoh A, Tsuji S, Shirasawa T. Effects of astaxanthin-rich Haematococcus pluvialis extract on cognitive function: a randomised, double-blind, placebo-controlled study. J Clin Biochem Nutr. 2012;51(2):102–7.

204. Lee D-H, Lee YJ, Kwon KH. Neuroprotective Effects of Astaxanthin in Oxygen-Glucose Deprivation in SH-SY5Y Cells and Global Cerebral Ischemia in Rat. J Clin Biochem Nutr. 2010 Sep;47(2):121–9.

205. Xu L, Zhu J, Yin W, Ding X. Astaxanthin improves cognitive deficits from oxidative stress, nitric oxide synthase and inflammation through upregulation of PI3K/Akt in diabetes rat. Int J Clin Exp Pathol. 2015;8(6):6083–94.

206. Martina Zandl-Lang. Interactions of simvastatin and apoJ with APP processing and amyloid-β clearance in blood-brain barrier endothelial cells [Internet]. Medizinische Universität Graz; 2017. Available from: https://permalink.obvsg.at/AC15013879

207. Yidan Sun. The Impact of Gestational Diabetes Mellitus on Regulating Cholesterol Homeostasis in Human Fetoplacental Endothelium [Internet]. Medizinische Universität Graz; 2018. Available from: https://permalink.obvsg.at/AC15192752

208. Franke H, Galla H, Beuckmann CT. Primary cultures of brain microvessel endothelial cells: a valid and flexible model to study drug transport through the blood-brain barrier in vitro. Brain Res Brain Res Protoc. 2000 Jul;5(3):248–56.

209. Laemmli UK. Cleavage of structural proteins during the assembly of the head of bacteriophage T4. Nature. 1970 Aug 15;227(5259):680–5.

210. Haid A, Suissa M. Immunochemical identification of membrane proteins after sodium dodecyl sulfate-polyacrylamide gel electrophoresis. Methods Enzymol. 1983;96:192–205.

211. Schefe JH, Lehmann KE, Buschmann IR, Unger T, Funke-Kaiser H. Quantitative real-time RT-PCR data analysis: current concepts and the novel “gene expression’s CT difference” formula. J Mol Med Berl Ger. 2006 Nov;84(11):901–10.

212. Livak KJ, Schmittgen TD. Analysis of relative gene expression data using real-time quantitative PCR and the 2(-Delta Delta C(T)) Method. Methods San Diego Calif. 2001 Dec;25(4):402–8.

213. Sattler W, Mohr D, Stocker R. Rapid isolation of lipoproteins and assessment of their peroxidation by high-performance liquid chromatography postcolumn chemiluminescence. Methods Enzymol. 1994;233:469–89.

214. Bergt C, Oettl K, Keller W, Andreae F, Leis HJ, Malle E, et al. Reagent or myeloperoxidase-generated hypochlorite affects discrete regions in lipid-free

and lipid-associated human apolipoprotein A-I. Biochem J. 2000 Mar 1;346 Pt 2:345–54.

215. Kozina A, Opresnik S, Wong MSK, Hallström S, Graier WF, Malli R, et al. Oleoyl-lysophosphatidylcholine limits endothelial nitric oxide bioavailability by induction of reactive oxygen species. PloS One. 2014;9(11):e113443.

216. Oddo S, Caccamo A, Shepherd JD, Murphy MP, Golde TE, Kayed R, et al. Triple-transgenic model of Alzheimer's disease with plaques and tangles: intracellular Abeta and synaptic dysfunction. Neuron. 2003 Jul 31;39(3):409–21.

217. Barnes LL, Wilson RS, Bienias JL, Schneider JA, Evans DA, Bennett DA. Sex differences in the clinical manifestations of Alzheimer disease pathology. Arch Gen Psychiatry. 2005 Jun;62(6):685–91.

218. Carroll JC, Rosario ER, Kreimer S, Villamagna A, Gentzschein E, Stanczyk FZ, et al. Sex differences in β-amyloid accumulation in 3xTg-AD mice: Role of neonatal sex steroid hormone exposure. Brain Res. 2010 Dec;1366:233–45.

219. Bowman PD, Betz AL, Ar D, Wolinsky JS, Penney JB, Shivers RR, et al. Primary culture of capillary endothelium from rat brain. In Vitro. 1981 Apr;17(4):353–62.

220. Casali BT, Landreth GE. Aβ Extraction from Murine Brain Homogenates. Bio-Protoc. 2016 Apr 20;6(8).

221. Ciallella JR, Rangnekar VV, McGillis JP. Heat shock alters Alzheimer's beta amyloid precursor protein expression in human endothelial cells. J Neurosci Res. 1994 Apr 15;37(6):769–76.

222. Muche A, Arendt T, Schliebs R. Oxidative stress affects processing of amyloid precursor protein in vascular endothelial cells. PloS One. 2017;12(6):e0178127.

223. Austin SA, Sens MA, Combs CK. Amyloid precursor protein mediates a tyrosine kinase-dependent activation response in endothelial cells. J Neurosci Off J Soc Neurosci. 2009 Nov 18;29(46):14451–62.

224. Canobbio I, Visconte C, Momi S, Guidetti GF, Zarà M, Canino J, et al. Platelet amyloid precursor protein is a modulator of venous thromboembolism in mice. Blood. 2017 27;130(4):527–36.

225. Mattson MP. Cellular actions of beta-amyloid precursor protein and its soluble and fibrillogenic derivatives. Physiol Rev. 1997 Oct;77(4):1081–132.

226. Obregon D, Hou H, Deng J, Giunta B, Tian J, Darlington D, et al. Soluble amyloid precursor protein-α modulates β-secretase activity and amyloid-β generation. Nat Commun. 2012 Apr 10;3:777.

227. Racchi M, Baetta R, Salvietti N, Ianna P, Franceschini G, Paoletti R, et al. Secretory processing of amyloid precursor protein is inhibited by increase in cellular cholesterol content. Biochem J. 1997 Mar 15;322 (Pt 3):893–8.

228. Kuhn P-H, Wang H, Dislich B, Colombo A, Zeitschel U, Ellwart JW, et al. ADAM10 is the physiologically relevant, constitutive alpha-secretase of the amyloid precursor protein in primary neurons. EMBO J. 2010 Sep 1;29(17):3020–32.

229. Das B, Yan R. Role of BACE1 in Alzheimer's synaptic function. Transl Neurodegener. 2017;6:23.

230. Wildsmith KR, Holley M, Savage JC, Skerrett R, Landreth GE. Evidence for impaired amyloid β clearance in Alzheimer's disease. Alzheimers Res Ther. 2013;5(4):33.

231. Fitz NF, Cronican A, Pham T, Fogg A, Fauq AH, Chapman R, et al. Liver X receptor agonist treatment ameliorates amyloid pathology and memory deficits caused by high-fat diet in APP23 mice. J Neurosci Off J Soc Neurosci. 2010 May 19;30(20):6862–72.

232. Mandrekar-Colucci S, Karlo JC, Landreth GE. Mechanisms underlying the rapid peroxisome proliferator-activated receptor-γ-mediated amyloid clearance and reversal of cognitive deficits in a murine model of Alzheimer's disease. J Neurosci Off J Soc Neurosci. 2012 Jul 25;32(30):10117–28.

233. Banka CL, Black AS, Curtiss LK. Localization of an apolipoprotein A-I epitope critical for lipoprotein-mediated cholesterol efflux from monocytic cells. J Biol Chem. 1994 Apr 8;269(14):10288–97.

234. Barkia A, Puchois P, Ghalim N, Torpier G, Barbaras R, Ailhaud G, et al. Differential role of apolipoprotein AI-containing particles in cholesterol efflux from adipose cells. Atherosclerosis. 1991 Apr;87(2–3):135–46.

235. Stein O, Dabach Y, Hollander G, Ben-Naim M, Halperin G, Breslow JL, et al. Delayed loss of cholesterol from a localized lipoprotein depot in apolipoprotein A-I-deficient mice. Proc Natl Acad Sci U S A. 1997 Sep 2;94(18):9820–4.

236. Shao B, Tang C, Sinha A, Mayer PS, Davenport GD, Brot N, et al. Humans with atherosclerosis have impaired ABCA1 cholesterol efflux and enhanced high-density lipoprotein oxidation by myeloperoxidase. Circ Res. 2014 May 23;114(11):1733–42.

237. Reynolds CA, Hong M-G, Eriksson UK, Blennow K, Bennet AM, Johansson B, et al. A survey of ABCA1 sequence variation confirms association with dementia. Hum Mutat. 2009 Sep;30(9):1348–54.

238. Koldamova R, Staufenbiel M, Lefterov I. Lack of ABCA1 considerably decreases brain ApoE level and increases amyloid deposition in APP23 mice. J Biol Chem. 2005 Dec 30;280(52):43224–35.

239. Corona AW, Kodoma N, Casali BT, Landreth GE. ABCA1 is Necessary for Bexarotene-Mediated Clearance of Soluble Amyloid Beta from the Hippocampus of APP/PS1 Mice. J Neuroimmune Pharmacol Off J Soc NeuroImmune Pharmacol. 2016 Mar;11(1):61–72.

240. Kim WS, Rahmanto AS, Kamili A, Rye K-A, Guillemin GJ, Gelissen IC, et al. Role of ABCG1 and ABCA1 in regulation of neuronal cholesterol efflux to apolipoprotein E discs and suppression of amyloid-beta peptide generation. J Biol Chem. 2007 Feb 2;282(5):2851–61.

241. Wahrle SE, Jiang H, Parsadanian M, Hartman RE, Bales KR, Paul SM, et al. Deletion of Abca1 increases Abeta deposition in the PDAPP transgenic mouse model of Alzheimer disease. J Biol Chem. 2005 Dec 30;280(52):43236–42.

242. Kuntz M, Candela P, Saint-Pol J, Lamartinière Y, Boucau M-C, Sevin E, et al. Bexarotene Promotes Cholesterol Efflux and Restricts Apical-to-Basolateral Transport of Amyloid-β Peptides in an In Vitro Model of the Human Blood-Brain Barrier. J Alzheimers Dis JAD. 2015;48(3):849–62.

243. Martín MG, Pfrieger F, Dotti CG. Cholesterol in brain disease: sometimes determinant and frequently implicated. EMBO Rep. 2014 Oct;15(10):1036–52.

244. Simpson JE, Ince PG, Minett T, Matthews FE, Heath PR, Shaw PJ, et al. Neuronal DNA damage response-associated dysregulation of signalling pathways and cholesterol metabolism at the earliest stages of Alzheimer-type pathology. Neuropathol Appl Neurobiol. 2016 Feb;42(2):167–79.

245. Donahue JE, Flaherty SL, Johanson CE, Duncan JA, Silverberg GD, Miller MC, et al. RAGE, LRP-1, and amyloid-beta protein in Alzheimer's disease. Acta Neuropathol (Berl). 2006 Oct;112(4):405–15.

246. Shibata M, Yamada S, Kumar SR, Calero M, Bading J, Frangione B, et al. Clearance of Alzheimer's amyloid-ss(1-40) peptide from brain by LDL receptor-related protein-1 at the blood-brain barrier. J Clin Invest. 2000 Dec;106(12):1489–99.

247. Au DT, Strickland DK, Muratoglu SC. The LDL Receptor-Related Protein 1: At the Crossroads of Lipoprotein Metabolism and Insulin Signaling. J Diabetes Res. 2017;2017:8356537.

248. Croy JE, Brandon T, Komives EA. Two apolipoprotein E mimetic peptides, ApoE(130-149) and ApoE(141-155)2, bind to LRP1. Biochemistry. 2004 Jun 15;43(23):7328–35.

249. Wu C-A, Tsujita M, Hayashi M, Yokoyama S. Probucol inactivates ABCA1 in the plasma membrane with respect to its mediation of apolipoprotein binding and high density lipoprotein assembly and to its proteolytic degradation. J Biol Chem. 2004 Jul 16;279(29):30168–74.

250. Musolino A, Panebianco M, Zendri E, Santini M, Di Nuzzo S, Ardizzoni A. Hypertriglyceridaemia with bexarotene in cutaneous T cell lymphoma: the role of omega-3 fatty acids. Br J Haematol. 2009 Apr;145(1):84–6.

251. Lesné SE, Sherman MA, Grant M, Kuskowski M, Schneider JA, Bennett DA, et al. Brain amyloid-β oligomers in ageing and Alzheimer's disease. Brain J Neurol. 2013 May;136(Pt 5):1383–98.

252. Manczak M, Calkins MJ, Reddy PH. Impaired mitochondrial dynamics and abnormal interaction of amyloid beta with mitochondrial protein Drp1 in neurons from patients with Alzheimer's disease: implications for neuronal damage. Hum Mol Genet. 2011 Jul 1;20(13):2495–509.

253. Leinenga G, Götz J. Scanning ultrasound removes amyloid-β and restores memory in an Alzheimer's disease mouse model. Sci Transl Med. 2015 Mar 11;7(278):278ra33.

254. Gong Y, Chang L, Viola KL, Lacor PN, Lambert MP, Finch CE, et al. Alzheimer's disease-affected brain: presence of oligomeric A beta ligands (ADDLs) suggests a molecular basis for reversible memory loss. Proc Natl Acad Sci U S A. 2003 Sep 2;100(18):10417–22.

255. Barbero-Camps E, Fernández A, Martínez L, Fernández-Checa JC, Colell A. APP/PS1 mice overexpressing SREBP-2 exhibit combined Aβ accumulation and tau pathology underlying Alzheimer's disease. Hum Mol Genet. 2013 Sep 1;22(17):3460–76.

256. Casali BT, Reed-Geaghan EG, Landreth GE. Nuclear receptor agonist-driven modification of inflammation and amyloid pathology enhances and sustains cognitive improvements in a mouse model of Alzheimer's disease. J Neuroinflammation. 2018 Feb 15;15(1):43.

257. Fitz NF, Cronican AA, Lefterov I, Koldamova R. Comment on "ApoE-directed therapeutics rapidly clear β-amyloid and reverse deficits in AD mouse models." Science. 2013 May 24;340(6135):924–c.

258. Veeraraghavalu K, Zhang C, Miller S, Hefendehl JK, Rajapaksha TW, Ulrich J, et al. Comment on "ApoE-directed therapeutics rapidly clear β-amyloid and reverse deficits in AD mouse models." Science. 2013 May 24;340(6135):924-f.

259. Galasso C, Orefice I, Pellone P, Cirino P, Miele R, Ianora A, et al. On the Neuroprotective Role of Astaxanthin: New Perspectives? Mar Drugs. 2018 Jul 24;16(8).

260. Chang C-H, Chen C-Y, Chiou J-Y, Peng RY, Peng C-H. Astaxanthine secured apoptotic death of PC12 cells induced by beta-amyloid peptide 25-35: its molecular action targets. J Med Food. 2010 Jun;13(3):548–56.

261. Lobos P, Bruna B, Cordova A, Barattini P, Galáz JL, Adasme T, et al. Astaxanthin Protects Primary Hippocampal Neurons against Noxious Effects of Aβ-Oligomers. Neural Plast. 2016;2016:3456783.

262. Manzine PR, de França Bram JM, Barham EJ, do Vale F de AC, Selistre-de-Araújo HS, Cominetti MR, et al. ADAM10 as a biomarker for Alzheimer's disease: a study with Brazilian elderly. Dement Geriatr Cogn Disord. 2013;35(1–2):58–66.

263. Wang Y-Q, Qu D-H, Wang K. Therapeutic approaches to Alzheimer's disease through stimulating of non-amyloidogenic processing of amyloid precursor protein. Eur Rev Med Pharmacol Sci. 2016 Jun;20(11):2389–403.

264. Kojro E, Gimpl G, Lammich S, Marz W, Fahrenholz F. Low cholesterol stimulates the nonamyloidogenic pathway by its effect on the alpha -secretase ADAM 10. Proc Natl Acad Sci U S A. 2001 May 8;98(10):5815–20.

265. Ricciarelli R, Canepa E, Marengo B, Marinari UM, Poli G, Pronzato MA, et al. Cholesterol and Alzheimer's disease: a still poorly understood correlation. IUBMB Life. 2012 Dec;64(12):931–5.

266. Ghribi O, Larsen B, Schrag M, Herman MM. High cholesterol content in neurons increases BACE, beta-amyloid, and phosphorylated tau levels in rabbit hippocampus. Exp Neurol. 2006 Aug;200(2):460–7.

267. Ehehalt R, Keller P, Haass C, Thiele C, Simons K. Amyloidogenic processing of the Alzheimer beta-amyloid precursor protein depends on lipid rafts. J Cell Biol. 2003 Jan 6;160(1):113–23.

268. Ehrlich D, Pirchl M, Humpel C. Effects of long-term moderate ethanol and cholesterol on cognition, cholinergic neurons, inflammation, and vascular impairment in rats. Neuroscience. 2012 Mar 15;205:154–66.

269. Vetrivel KS, Thinakaran G. Membrane rafts in Alzheimer's disease beta-amyloid production. Biochim Biophys Acta. 2010 Aug;1801(8):860–7.

270. Chen J, Zhang X, Kusumo H, Costa LG, Guizzetti M. Cholesterol efflux is differentially regulated in neurons and astrocytes: implications for brain cholesterol homeostasis. Biochim Biophys Acta. 2013 Feb;1831(2):263–75.

271. Stefulj J, Panzenboeck U, Becker T, Hirschmugl B, Schweinzer C, Lang I, et al. Human endothelial cells of the placental barrier efficiently deliver cholesterol to the fetal circulation via ABCA1 and ABCG1. Circ Res. 2009 Mar 13;104(5):600–8.

272. de Chaves EP, Narayanaswami V. Apolipoprotein E and cholesterol in aging and disease in the brain. Future Lipidol. 2008 Oct;3(5):505–30.

273. Tamamizu-Kato S, Cohen JK, Drake CB, Kosaraju MG, Drury J, Narayanaswami V. Interaction with amyloid beta peptide compromises the lipid binding function of apolipoprotein E. Biochemistry. 2008 May 6;47(18):5225–34.

274. Iizuka M, Ayaori M, Uto-Kondo H, Yakushiji E, Takiguchi S, Nakaya K, et al. Astaxanthin enhances ATP-binding cassette transporter A1/G1 expressions and cholesterol efflux from macrophages. J Nutr Sci Vitaminol (Tokyo). 2012;58(2):96–104.

275. Kidd P. Astaxanthin, cell membrane nutrient with diverse clinical benefits and anti-aging potential. Altern Med Rev J Clin Ther. 2011 Dec;16(4):355–64.

276. Yoshida H, Yanai H, Ito K, Tomono Y, Koikeda T, Tsukahara H, et al. Administration of natural astaxanthin increases serum HDL-cholesterol and adiponectin in subjects with mild hyperlipidemia. Atherosclerosis. 2010 Apr;209(2):520–3.

277. Olesen OF, Dagø L. High density lipoprotein inhibits assembly of amyloid beta-peptides into fibrils. Biochem Biophys Res Commun. 2000 Apr 2;270(1):62–6.

278. Storck SE, Pietrzik CU. Endothelial LRP1 - A Potential Target for the Treatment of Alzheimer's Disease : Theme: Drug Discovery, Development and Delivery in Alzheimer's Disease Guest Editor: Davide Brambilla. Pharm Res. 2017 Sep 25;

279. Li Y, Cheng D, Cheng R, Zhu X, Wan T, Liu J, et al. Mechanisms of U87 astrocytoma cell uptake and trafficking of monomeric versus protofibril Alzheimer's disease amyloid-β proteins. PloS One. 2014;9(6):e99939.

280. Wen X, Xiao L, Zhong Z, Wang L, Li Z, Pan X, et al. Astaxanthin acts via LRP-1 to inhibit inflammation and reverse lipopolysaccharide-induced M1/M2 polarization of microglial cells. Oncotarget. 2017 Sep 19;8(41):69370–85.

281. Ruderisch N, Schlatter D, Kuglstatter A, Guba W, Huber S, Cusulin C, et al. Potent and Selective BACE-1 Peptide Inhibitors Lower Brain Aβ Levels Mediated by Brain Shuttle Transport. EBioMedicine. 2017 Oct;24:76–92.

282. Zhao X-J, Gong D-M, Jiang Y-R, Guo D, Zhu Y, Deng Y-C. Multipotent AChE and BACE-1 inhibitors for the treatment of Alzheimer's disease: Design, synthesis and bio-analysis of 7-amino-1,4-dihydro-2H-isoquilin-3-one derivates. Eur J Med Chem. 2017 Sep 29;138:738–47.

283. Pham HDQ, Thai NQ, Bednarikova Z, Linh HQ, Gazova Z, Li MS. Bexarotene cannot reduce amyloid beta plaques through inhibition of production of amyloid beta peptides: in silico and in vitro study. Phys Chem Chem Phys PCCP. 2018 Sep 26;20(37):24329–38.

284. Malnar M, Kosicek M, Lisica A, Posavec M, Krolo A, Njavro J, et al. Cholesterol-depletion corrects APP and BACE1 misstrafficking in NPC1-deficient cells. Biochim Biophys Acta. 2012 Aug;1822(8):1270–83.

285. Cummings JL, Zhong K, Kinney JW, Heaney C, Moll-Tudla J, Joshi A, et al. Double-blind, placebo-controlled, proof-of-concept trial of bexarotene Xin moderate Alzheimer's disease. Alzheimers Res Ther. 2016 Jan 29;8:4.